EFFECTS OF KAOLIN CALCINED AT DIFFERENT TEMPERATURES ON THE PROPERTIES OF RIVER SAND AND QUARRY DUST CONCRETE

BY

IBE, KIZITO CHIDOZIE (B. ENG)
REG. NO 20184143618

A THESIS SUBMITTED TO THE POSTGRADUATE SCHOOL,
FEDERAL UNIVERSITY OF TECHNOLOGY, OWERRI

IN PARTIAL FULFILLMENT OF THE REQUIREMENTS FOR
THE AWARD OF MASTER OF ENGINEERING (M.ENG) DEGREE
IN CIVIL ENGINEERING (STRUCTURES)

APRIL, 2024

CERTIFICATION

This research thesis "Effects of kaolin calcined at different temperatures on river sand and quarry dust concrete" by Ibe, Kizito Chidozie (Reg. No. 20184143618) is certified as a satisfactory research thesis in partial fulfillment of the requirements for the award of Master of Engineering (M.Eng) Degree in Structural Engineering in the department of Civil Engineering, Federal University of Technology, Owerri.

Engr. Prof. J.C. Ezeh
Supervisor

16/04/2024
Date

Engr. Dr. C.T.G. Awodiji
Co-Supervisor

16/04/2024
Date.

Engr. Dr. O. M. Ibearugbulem
Head of Department.

16/04/2024
Date

Engr. Prof. R. Uche
Dean, School of Engineering and Engineering Technology.

08/05/24
Date

Prof. B.O. Esonu
Dean, School of Postgraduate Studies.

Date

Engr. Prof. J.O. Afolayan
External Examiner.

16/4/2024
Date

DEDICATION

This research report is dedicated to God Almighty for his mercies in my life.

ACKNOWLEDGEMENTS

I am grateful to my supervisor, Engr. Prof. J.C. Ezeh for the role he has played on the course of developing this work. He always encouraged me and my colleagues to work hard so as to complete the work in goof time. His encouragement, advice and guide have actually paid off. May you be always favoured in this your field of career. My special thanks goes to my second supervisor, Engr. Dr. C.T.G. Awodiji, for her priceless and unquantifiable contribution towards the realization of this research. She provided me all the necessary support w and followed up the research at every stage of the work. May God grant you multiple blessings.

I am grateful to Prof. D.O. Onwuka and Rev. Prof. L. O. Ettu, for their spiritual and academic contributions in my life and towards my postgraduate program. I am also thankful to Engr. Prof. B. U. Dike, Engr. Prof. J. C. Osuagwu, Engr. Dr. U. C. Anya, Engr. Dr. O.M. Ibearugbulem, Engr. Dr. Mrs. C. Okere, Engr. Dr. H. U. Nwoke, Engr. Dr. L. Anyaogu, Engr. Dr. F. C. Njoku and Engr. Dr. Mrs. J. I. Arimanwa, for their huge support toward this work. To the entire staff and of Civil Engineering Department, Federal University of Technology, Owerri (FUTO) ably headed by Engr. Dr. O.M. Ibearugbulem, I want to say thank you for all of your various contributions to the success of this work. My thanks also goes to Prof. B.O. Esonu, the Dean of Post Graduate School for the necessary support throughout this research work.

God will bless the management of Michael Okpara University of Agriculture Umudike, Abia State for employing me and making it conducive for me to carry out this research. My profound gratitude goes to the entire staff and management of Civil Engineering Department, Michael Okpara University of Agriculture, Umudike, Abia State for their contribution towards this programme.

I am very much indebted to my dear parents, Mr. and Mrs. S.I. Ibe, my siblings, Mr. Ibe Kenneth and Mrs. Assumpta Aladum. I want to appreciate my friends, Adanma Udenze, Ude Joan Chiamaka and Engr. Chukwudi Prince, for their love, care and support. May God bless the fruit of your labours in life, Amen. Finally, I am very grateful to the Most High God for making this dream a reality.

TABLE OF CONTENTS

LIST OF TABLES

LIST OF FIGURES

LIST OF PLATES

ABSTRACT

The study explored the mechanical and durability properties of concrete blended with kaolin from Umuariaga, Ikwuano Local Government Area, Abia State, Nigeria. The kaolin was calcined at 650^0C, 750^0C, and 850^0C accordingly to obtain metakaolin (MK). Two sets of binary concrete were investigated. The first set was composed of Portland cement, metakaolin, river sand (RS) and crushed granite. While, the second sample was made of a similar composition except that quarry dust (QD) was used in place of river sand. MK was utilized to replace Portland cement at percentages ranging from 0% to 50% at 5% intervals. Mix ratio of 1: 1.68: 2.32 (i.e. cement: river sand: crushed granite) and 1:1.42:2.04 (i.e. cement: quarry dust: crushed granite) at 0.4 water-cement ratio targeting 30 MPa compressive strength value were experimented. The compressive strength, young modulus of elasticity and water absorption property of the various concrete cube samples of size 150×150×150 mm^3 were tested after curing by immersing in water for 7 and 28 days. The multiple regression analysis (MRA) of the experimental data was conducted using historical design (HD) of the response surface methodology (RSM). This was implemented using the Design expert software version 13. Generally, the results show that the effect of the different calcination temperatures for producing the metakaolin did affect the slump and strength properties of the concrete. However, as the percentage of metakaolin increased, the slump values lessened for both RS and QD concrete. At 0%MK for all three temperatures, the maximum slumps for RS and QD concrete were found to be 112 mm and 98 mm, respectively. Minimum values were noted at 50% inclusion of MK. It was found that, for both types of concrete, the compressive strength values at 750^0C were slightly higher than the other two temperatures. After 28 days, the binary concrete containing river sand exhibited the highest compressive strength at 15%MK for 650^0C, 20%MK for 750^0C, and 20%MK for 850^0C, with corresponding values of 38.92 N/mm^2, 42.05 N/mm^2, and 40.98 N/mm^2. While the quarry dust concrete had 36.48 N/mm^2, 38.02 N/mm^2, and 36.30 N/mm^2 for 650^0C, 750^0C, and 850^0C respectively, all at 20%MK. The Young modulus for the river sand had 33.55 GPa at 15%MK, 34.88 GPa at 20%MK, 34.30 GPa at 20%MK while the young modulus for quarry dust had 32.45GPa at 20%MK, 33.16 GPa at 20%MK, 32.64GPa at 20%MK for 650^0C, 750^0C, and 850^0C respectively. The Water absorption for river sand had 1.22% at 20%MK, 1.10% at 20%MK, 1.22% at 20%MK while the water absorption for quarry dust had 1.46% at 20%MK, 1.33% at 20%MK, 1.45% at 20%MK for 650^0C, 750^0C, and 850^0C respectively. The multiple regression analysis gave a 2-factor interaction (2FI) model for the best binary concrete achieved at 750 ^{0}C with R-squared values of 0.9182, 0.9451, and 0.9566 for compressive strength, young modulus and water absorption respectively with river sand. While with the quarry dust, the R-squared values of 0.9618, 0.9756, 0.9953 for compressive strength, young modulus and water absorption respectively was achieved. The investigation showed that metakaolin gotten from Umuariaga, Abia State in Nigeria improved the mechanical and durability properties of the tested concrete from 5%MK -20%MK replacement level.

Key Words

Metakaolin; Binary concrete; Compressive strength; Young modulus; Water absorption; Response surface methodology.

CHAPTER ONE

INTRODUCTION

1.1 Background information

The construction industry is one of the world's fastest growing industry. This is as a result of increase in the world's population. This industry provides the planning, design and construction of infrastructures such as buildings, dams, bridges, highways, and structural amenities. Most of these infrastructures are made of concrete. Concrete, second to water in global use, is a durable and reliable material in the construction industry (Abdul, Aleem and Arumairaj, 2012). It is a composite material with significant constituents such as coarse aggregate, fine aggregate, , water, and cement, with a global production rate of 4.4 billion metric tons in 2020 (Lim, Jung, Lee, Jang, Oh, and Shin, 2020). In developing countries, the most used binder in the production of concrete is ordinary Portland cement (OPC), whose production is the second highest source of carbon dioxide after automobiles and requires a high quantity of energy during manufacturing (Srinivasan et al., 2010). The cement is synthesized by heating limestone (calcium carbonate) with other materials (such as clay) to a temperature of 1,450 °C in a kiln which is known as the calcination process. The molecule of carbondixodide is liberated from calcium carbonate in order to form quick lime. The quicklime therefore mix with other materials to create the calcium silicate and other cementitious composites.

An estimated 125 litres of fossil fuel and 118 kWH of electricity are consumed in producing one ton of cement (Bondar, 2013). Cement production requires the burning of fuel, which results in a significant release of a large amount of carbon dioxide (CO_2). Patricija, Aleksandrs, and Valdemars (2013), noted that cement does not only consume energy during its production, but it

is also accountable for a substantial part of manufactured CO_2 emission, which leads to environmental pollution and global warming. The global warming impacts includes destruction on the envitonment, outbreak of respiratory related diseases , kidney diseases, and other deadly human illnesses (Vazinram and Khodaparast, 2009).

Nowadays, the consruction industry faces the issues of preserving the environment. Portland cement production adds 6% to 8% of CO_2, greenhouse gas emission (Bignozzi, Manzi, Natali, Rickard and Riessen, 2014). In 2018, mineral waste in the European Union (EU) was 63% of the entire waste generated while the building industries were responsible for about 33% of the waste produced by economic events (i.e. 821 million tonnes in 2018). The amount of other harmful solid waste has been Europe's major problem in the last few years. The increased disquiet about waste removal and its impact on the land has led to renewed studies on new procedures or possibilities for reusing these materials (Hardjito, Wallah and Sumajouw, 2014).

The manufacturing of 1 ton of cement consumes about 1 to 1⅓ tons of earth resources like limestone. At the same time, an equivalent quantity of CO_2 and other greenhouse gases are released into the atmosphere (Srinivasan et al., 2010). According to Jindal and Kamal (2015), globally the current Portland cement production in tons , exceeds 2.6 billion tons yearly and increases at a 5% rate each year. This generate nearly 7% of atmospheric carbon dioxide (CO_2), which adds mainly to global warming. Priya and Partheeban (2013), reported that CO_2 constitutes up to 65% of global warming.

Therefore, the increase in cement utilization and production has generated an unbalanced ecological system due to the rise in the release of CO_2 and other greenhouse gases (Malhotra, 2002). There is a need for researchers in Nigeria to join world researchers in reducing the

problems created by using Portland cement. As a result, researchers from major countires that consumes cement such as China, India, Brazil, Turkey, and Russia have tried reducing Portland cement utilization in their construction industry (International Energy Agency, 2010). To lessen the effects of producing Portland cement, part of the cement is partially replaced with supplementary cementing materials such as fly ash, ground granulated blast furnace slag, rice husk ash, metakaolin, etc. (Franklin, 2009).

To ensure environmental sustainability, which is the seventh (7^{th}) goal of the United Nations Millennium Development Goals, agreed upon by 191 UN member states and in line with the Sustainable Development Goals (SDG) decided in 2015 by 195 nations, efforts have been made to develop environmentally friendly materials for the construction industries which will help in reducing the greenhouse gas emissions.For greater economic advancement, materials that are used to partially replace cement such as metakaolin, fly ash, blast furnace slag and rice husk ash helps to increases the cementitious product of a hydrated cement should be studied and utilized to reduce the damages caused by cement production on the environment. (Davidovits, 2013).

The dangers of fire outbreaks rises with the arrangement of modern cities. Modern surroundings are crammed with objects made from highly combustible materials, which are possible ignition causes. Globally, structures constructed with concrete are exposed to a high risk of fire daily, which can lead to human and material damages (Morsy, Shebi and Rashad, 2010). High temperature negatively affects concrete because it causes the decomposition of hardened cement paste and aggregate, decreasing the stiffness of concrete and increasing irrecoverable deformation (Morsy et al., 2010). According to Jani and Hogland (2014), the concrete fire resistance could be enhanced when pozzolanic materials such as rice husk ash, fly ash, saw dust ash, metakaolin (MK), waste glass powder (WGP) etc., are used partially to replace cement.

Currently, the unmaintainable method of using river sand for concrete production has led to its reduction and great negative effects on the environment. Stakeholders in the building sector are seeking other sources of fine aggregate materials (by-products or recycled) to substitute river sand in the production of concrete. Crushed granite (Quarry) dust is the by-product from the crushing process of granite. After drying, the tiny dust poses a tremendous hazard to the ecosystem by contaminating the soil and water (Febin, Abhirami, Vineetha, Manisha, Ramkrishnan, Sathyan and Mini 2019). According to Mir (2015), the mechanical characteristics and elastic modulus of concrete were improved by using quarry dust as a sand substitute material. By substituting quarry dust at a 60:40 ratio for fine aggregates, the compressive strength was increased. To ensure sustainable development, concrete can be made using quarry dust as fine aggregate with high-quality components, the right amount of superplasticizers, efficient mixing techniques, and correct curing (Devi and Kannan, 2011). According to Chitlange and Pajgade (2010), when quarry dust completely replaced natural sand, the strength of plain concrete gradually increased. Ephraim, Akobo, Ukpata, and Akeke (2012) reported using quarry dust and lateral sand in their work as a partial replacement for fine aggregates for making concrete. The flexural and split tensile strengths therefore increased.

Metakaolin (MK) ($Al_2O_3.2SiO_2$) is a resultant product of calcined kaolin at 600 ºC to 900 ºC. Kaolin is a layered silicate structure in which the layers are bounded to each other by Van Der Weal's forces. Heating of the kaolin in air at about 600 ºC, causes structural changes which damages the layered structure due to dehydration and forms a transient phase known as metakaolin

(Jyothi and Chaitanya, 2015). The irregular molecular arrangement of the metakaolin in a thermodynamic condition results to the excitation molecular during cementitious reaction, thus it

can be utilized for high performance concrete. Metakaolin has been shown to have strong fire resistance when blended with cement in concrete up to 4000C, improving strength and concrete durability through the acceleration of ordinary Portland cement (OPC) hydration and the pozzolanic reaction with calcium hydroxide ($Ca(OH)_2$) (Morsy, Rasheed and El-nouhy, 2009; Rashad, 2013). One of the key factors taken into account in the design of buildings is human safety in the event of a fire. Before employing any building material in structural parts, it is crucial to fully understand how it will behave at high temperatures.

A researcher (analyze) can model an outcome (the response variable) as a function of one or more explanatory factors (or predictors) using regression, one of the strong and adaptable techniques used for data analysis. Regression forms the basis of many critical statistical models. The method permits the estimation of prediction error for model evaluation and selection, which are major concepts in getting models that best fit a given data set (Schneider, Hommel and Blettner, 2010). According to Akinoso, Aboaba, and Olajide (2011), response surface methodology is a collection of statistical and mathematical methodologies used for problem modeling and analysis in which a response is influenced by a number of variables. The tool is utilized in quantifying the relationship between the input parameters and the desired responses (Busari, Dahunsi, Akinmusuru, Loto and Ajayi, 2019). As a result, according to Kathleen et al. (2004), the response surface methodology entails an experimental strategy for investigating the independent variables and statistically developing a model from the relationship between the response and the process factors. In this study, the response surface methodology (RSM) was used to develop a regression model that predicted the properties of the hardened MK blended concrete.

1.2 Problem Statement

Due to Nigeria's large population, there is a significant demand for buildings and other infrastructure facilities, which has resulted in an increase in the usage of Portland cement and concrete as building materials. In addition to contributing to a rise in ecological imbalance, the manufacture of Portland limestone cement releases greenhouse gases such as carbon dioxide (CO_2) into the atmosphere. As a result, there has been an increase in global warming, environmental harm, and respiratory illnesses like asthma and lung cancer as well as other human disorders (Davidovits, 2013).

Cement use depletes raw materials (limestone) and pollutes the environment. Ordinary Portland Cement (OPC) production necessitates the burning of huge amounts of fuel and the breakdown of limestone, which results in significant CO_2 emissions (Kong and Sanjayan, 2008). Depending on the production method used, one ton of CO_2 is created for every ton of OPC manufactured (Davidovits, 2004). According to Malhotra (2002), cement plants may emit up to 1.5 billion tons of CO_2 yearly. The high energy consumption needed during Portland cement production has reduced the number of investors in its manufacture due to high operational cost. Consequently, the few investors in this line of business usually hike the cement price, discouraging low-income citizens from owning their own homes.

Quarry dust is a waste generated during the quarrying of rocks and results to pollution of air within the environment. However, quarry dust have been reported to possess strength required in cementitious material which improves workability (Sundaralingam, Peiris, Anburuvel, Sathiparan, 2022). Replacement of aggregate in construction with quarry dust would reduce the

cost of construction, provide ways of utilizing the waste natural material as well as reduce the rate of pollution within the environment.

In order to achieve sustainability in the construction industry, metakaolin have been adopted in construction process. However, the required mix design and estimation of the mechanical strength of the concrete becomes complex due to the non-homogenous nature of the concrete and the non-linear relationship between the strength and the mixture proportions. Hence, it becomes imperative to develop regression models for the estimation of the mechanical properties of the sustainable ternary blends with adequate accuracy. This will encourage the development of sustainable concretes that are less expensive and without time consuming trial batches. Therefore, this study examined the effects of kaolin calcined at different temperatures, on the properties of river sand and quarry dust concrete respectively.

1.3 Aim and Objectives of the Study

The aim of this study is to determine the effects of kaolin calcined at different temperatures, on the properties of river sand and quarry dust concrete. The objectives are;

i. To determine the chemical composition of metakaolin at different calcination temperatures of 650°C, 750 °C, and 850 °C and characterize the other materials used in the research.
ii. To determine the compressive strength, young modulus of elasticity, and water absorption of cement-metakaolin blended concrete produced at different metakaolin calcination temperatures.

iii. To develop multivariate regression models using response surface methodolology for predicting the compressive strength, young modulus of elasticity, and water absorption of the cement-metakaolin blended concrete produced with the best metakaolin calcination temperature.

iv. To compare the experimental results and the model predicted values of the cement-metakaolin blended concrete.

v. To check for the adequacy of the models to predict the compressive strength, young modulus of elasticity, and water absorption of the cement-metakaolin blended concrete produced with the best metakaolin calcination temperature.

1.4 Justification of the study

In achieving the environmental and infrastructure sustainability goal of the United Nations Millennium Development Goals, there is an urgent need to create innovative materials that have a less environmental impact, reduce the respiratory diseases caused by materials that emit greenhouse gases, and creates an environment for social and economic growth of Nations (Mukherjee and Vesmawala, 2013). Therefore, the use of calcined kaolin in concrete production will help to:

a. Reduce calcination temperature thereby reducing the operational cost for manufacturing cement. This will definitely reduce the cost of purchasing cement from the market.
b. More low and average income earners will be able to afford to build and own their homes

c. The inclusion of the calcined kaolin in the cement production process will help to reduce the quantity of clinker needed to make the cement. Consequently, CO_2 emission will drop resulting in less environmental pollution

d. The use of quarry dust in place of river sand as fine aggregate will help to curb the negative effect of air pollution associated with dumping the quarry dust in dump sites

e. Adopting the multivariate regression models for predicting the compressive strength, elastic modulus and water absorbing properties of the concrete under study, will make the process of mix design very fast and less labour demanding.

1.5 Scope of the study

This research focuses on the use of kaolin, calcined at 650^0C, 750^0C and 850^0C respectively, as a partial substitute for Portland cement in producing 7 days and 28 days old concrete samples. The properties of the concrete studies were limited to the compressive strength, elastic modulus and water absorption only. The river sand and quarry dust were adopted as fine aggregate for the concrete manufacture accordingly. The historical design of the response surface methodology (RSM) was used to carry out the multiple regression analysis in order to develop multivariate regression models for predicting the properties of the concrete. This was achieved using the design expert software version 13.

CHAPTER TWO

LITERATURE REVIEW

2.1 Cement

Cement is a powder that is mostly made of calcined lime and clay. Calcined lime yields calcium oxide, whereas clay produces silica, alumina, and iron oxide (Etim, 2021). Rock quarries are blasted by drilling and setting off explosives to remove the raw ingredients for cement (Powers and Brownyard, 2009). After that, these shattered stones are transported to the factory where they are stored in separate silos. After that, chutes deliver each one of them separately to crushes, where they are reduced in size to roughly half an inch chunks (Lea, 2018). After a process known as homogenization, the proportions of crushed clay, limestone, and any additional materials required are combined according to the type of cement being made. The mixture is then ground in a vertical steel mill under pressure from three conical rollers that roll over a rotating milling table.

Furthermore, there are horizontal mills that have a side where steel balls are used to crush the material. After another homogenization, the raw material is calcined at 1400°C in revolving kilns to produce clinker, which is a small, dark-gray nodule with a diameter of 3-5 cm. The clinker, which is extracted from the kiln's bottom end while it is still hot, is ground into a very fine powder after being combined with a small quantity of gypsum and limestone (Schneider, Romer, Tschudin, and Bolio, 2011). This process creates cement.

The aforementioned oxides combine to produce more complex compounds during the calcination process in the kiln at high temperatures (Elimbi, Tchkoute, and Njopwouo, 2011).For instance, a

reaction between $CaCO_3$, $Al_3(SiO_3)_2$, and Fe_2O_3 would give a complex mixture of alite, $(CaO)_3 SiO_2$ (C_3S); belite, $(CaO)_2 SiO_2$ (C_2S); tricalcium aluminate, $Ca_3(Al_2O_3)$ (C_3A); and ferrite phase tetracalcium aluminoferrite, $Ca_4Al_2O_3Fe_2O_3$ (C_4AF) with the evolution of CO_2 gas in the Portland cement clinker (Ali et al., 2011). Sodium (Na), Potassium (K), and sulphur (S) are present in natural clay, but there may also be a large number of additional small components. Cement's elemental makeup is examined in the chemical analysis (e.g., Ca, Si, Al, Mg, Fe, Na, K, and S). The composition is then estimated using their oxide sand, which is often represented as a weight percentage of oxides. For the sake of simplicity, if the clinker contains the aforementioned four primary oxides, they can be simply represented by the Bogue equations, where CaO, Al_2O_3, Fe_2O_3, and SiO_2 are denoted as C, A, F, and S, respectively (Thiery et al., 2018).In this notation, alite (tricalcium silicate) [$(CaO)_3 SiO_2$], belite (dicalcium silicate) [$(CaO)_2SiO_2$], celite (tricalcium aluminate) [$Ca_3Al_2O_6=3CaO\cdot Al_2O_3$], and brownmillerite (tetracalcium aluminoferrite) [$Ca_4Al_2Fe_2O_{10}=4CaO\cdot Al_2O_3\cdot Fe_2O_3$] are represented by C_3S, C_2S, C_3A, and C_3AF, respectively. When analyzing the elemental makeup of Ca, Al, Fe, and Si, which is typically done using X-ray fluorescence spectroscopy, we express them as a percentage of the corresponding oxides. For instance, Bogue calculations would yield C_3S=64.7%, C_2S=12.9%, C_3A=9.0%, and C_4AF=8.5%, respectively, if the experimentally measured clinker composition was CaO=65.6%, SiO_2=21.5%, Al_2O_3=5.2%, and Fe_2O_3=2.8% (Portland Cement Clinker, 2017). However, the chemical symbols for the components that make up cement are H, S, N, K, and CSH_2. These components are water (H_2O), sulphur trioxide (SO_3), sodium oxide (Na_2O), potassium oxide (K_2O), and gypsum ($CaSO_4\bullet 2H_2O$). Gypsum (calcium sulfate dihydrate) is denoted by the symbol CSH_2 since it is $CaO\bullet SO_3\bullet 2H_2O$. As such, the approximate composition of the cement clinker is different from the above values and is depicted in Table 2.1

Table 2.1: Approximate composition of the cement clinker

Compound	Formula	Notation	wt.%
Celite (tricalcium aluminate)	$Ca_3Al_2O_6$ [$3CaO \cdot Al_2O_3$]	C_3A	10
Brownmillerite (tetracalciumaluminoferrite)	$Ca_4Al_2Fe_2O_{10}$ [$4CaO \cdot Al_2O_3 \cdot Fe_2O_3$]	C_4AF	8
Belite (dicalcium silicate)	Ca_2SiO_4 [$2CaO \cdot SiO_2$]	C_2S	20
Alite (tricalcium silicate)	Ca_3SiO_5 [$3CaO \cdot SiO_2$]	C_3S	55
Sodium oxide	Na_2O	N	≤2
Potassium oxide	K_2O	K	
Gypsum (calcium sulfate dihydrate)	$CaSO_4 \cdot 2H_2O$ [$CaO \cdot SO_3 \cdot 2H_2O$]	CSH_2	5

Source: Powers and Brownyard (2009)

Cement comes in a variety of forms, including Portland cement, Siliceous and Calcareous Fly Ash (ASTM C618, 2017). The three main forms are fly ash, slag cement, and silica fume (Composition of Cement, 2017; Mindess and Young, 2008). They differ in terms of their chemical makeup; Table 2.1 lists the SiO_2, Al_2O_3, Fe_2O_3, CaO, MgO, and SO_3 contents of the cement clinker mentioned above. The remaining components may include additional substances like Na_2O and K_2O. Keep in mind that SO_3 stands for oxide of sulfur, and that gypsum ($CaSO_4 \bullet 2H_2O$) is the source of sulfur. Given in Table 2.2 are also composition of components by weight used to make different types of cement and properties such as specific surface area (SSA) obtained through Blaine analysis; Brunauer, Emmett and Teller (BET) and specific gravity (Gs) (Kosmatka and Panarese, 2008; Mamlouk and Zaniewski, 2009). General use of the Portland cement, Siliceous (ASTM C618, 2017) Fly Ash, Calcareous (ASTM C618, 2017) Fly Ash, slag

cement, and silica fume in Concrete is a primary binder, cement replacement, and property enhancer, respectively (Patentsgoogle.com, 2018).

Table 2.2: Composition of components as wt. % used to make different types of cement.

Component	Portland cement	Siliceous fly ash	Calcareous cement	Slag cement	Fume silica
SiO_2	21.9	52.0	35.0	35.0	85–97
Al_2O_3	6.9	23.0	18.0	12.0	0
Fe_2O_3	3.9	11.0	6.0	1.0	0
CaO	63.0	5.0	21.0	40.0	<1
MgO	2.5	0	0	0	0
SO_3	1.7	0	0	0	0
SSA (m^2g^{-1})	0.37 Blaine	0.42 Blaine	0.42 Blaine	0.42 Blaine	15–30 BET
SG	3.15	2.38	2.65	2.94	2.22

SSA=Specific surface area; SG=Specific gravity.

Source: Holland (2005); Kosmatka, Kerkhoff, Panerese (2002); Gamble (2016).

2.1.1 Portland cement

The type of cement that is used most frequently worldwide is Portland cement. Joseph Aspdin created it in England in the late 19th century from different varieties of hydraulic lime It is made by heating limestone ($CaCO_3$) with other materials such as clay to a temperature of about 1300-1500 °C in a kiln (Shetty, 2009). It releases carbon dioxide (CO_2) to form calcium oxide (CaO) that combines chemically with other materials to form calcium silicate ($CaSiO_3$) and other cementitious compounds. The 'clinker' which is the product is ground and little amount of gypsum is added which forms the ordinary Portland cement which turns out to be the most used

Portland cement in the construction industriesPortland cement can be either white or grey. However, due to his innovations in the 1840s, William Aspdin, Joseph Aspdin's son, came to be recognized as the creator of "modern" Portland cement (Courtland, 2011).

Calcareous, siliceous, argillaceous, and ferrifrous are some of the more than thirty (30) raw materials that are known to be utilized in the production of Portland cement. The various materials and oxides that are under these categories are in the cement mixture are;

i. Chalk ii. lime stone (Calcium carbonate) iii. Clay iv. Calcium oxide v. Silicon oxide

vi. Aluminum oxide vii. Iron (II) oxide

According to Kosmatka *et al.* (2002), Table 2.3 lists a few potential raw materials that could be utilized to create each of the major cement components.

Table 2.3: Raw ingredients used to provide each of the main cement elements

Calcium	**Silicon**	**Aluminium**	**Iron**
Limestone	Clay	Clay	Clay
Marl	Marl	Shale	Iron ore
Calcite	Sand	Fly ash	Mill scale
Aragonite	Shale	Aluminum	Shale
Shale	Fly ash		Blast furnace dust
Sea shells	Rice husk ash		
Cement kiln dust	Slag		

Source: Kosmatka *et. al.,* (2002)

The manufacturing processes of cement are**;**

i. Quarry

Cement facilities are typically placed close to the required market or to places with sufficient quantities of raw materials because of the ease of transportation and low cost of the fundamental elements of cement obtained from quarries. Drilling, blasting, excavation, as well as crushing, screening, and storage of raw materials, such as lime stone used in cement manufacture, are all part of this process. About 7% of the total CO_2 emitted during this process is caused by the operation of machinery (Mohammed, Collette, and Sean, 2013).

The first stage is to produce clinker from raw materials. Depending on the raw material's condition, this might be a dry, wet, semi-dry, or semi-wet process. Manufacturing cement from clinker is the second phase.

ii. Clinker production

Before entering a revolving kiln, bulk raw materials are transported, crushed, and homogenized. The kiln is a huge rotating pipe that can have a diameter of up to 6 meters and a length of 60 to 90 meters. This massive kiln is heated internally by a flame that burns at 2000°C. To facilitate the transportation of materials to the opposite end of the kiln, where they are rapidly cooled to 100–200°C, it is somewhat slanted (Hahn and Emory, 1994). Cement clinker is primarily composed of four oxides: silicon oxide (20%), calcium oxide (65%), alumina oxide (10%), and iron oxide (5%). These elements will mix uniformly (called a "slurry") at a temperature of approximately 1450°C to form new compounds, such as tricalcium silicate ($3CaO.SiO_2$), dicalcium silicate ($2CaO.SiO_2$), tricalcium aluminate ($3Ca.Al_2O_3$), and tetracalcium aluminoferrite ($4CaO.Al_2O_3.Fe_2O_3$). Cement solidifies as a result of these compounds hydrating. The final product generated at this step is referred to as "Clinker" and is stored in very huge silos.

iii. Cement production

This second stage, which is completed in the cement grinding mill, which is occasionally located distant from the clinker plant, involves adding gypsum (calcium sulphates) to the clinker together with other components like fly ash, blast furnace slag, and natural pozzolanas. Cement is created by processing the mixture into a fine, consistent powder. Subsequently, the cement is stored in silos until it is shipped in bulk or bags (Natesan, Steve, and Kenneth, 2003).

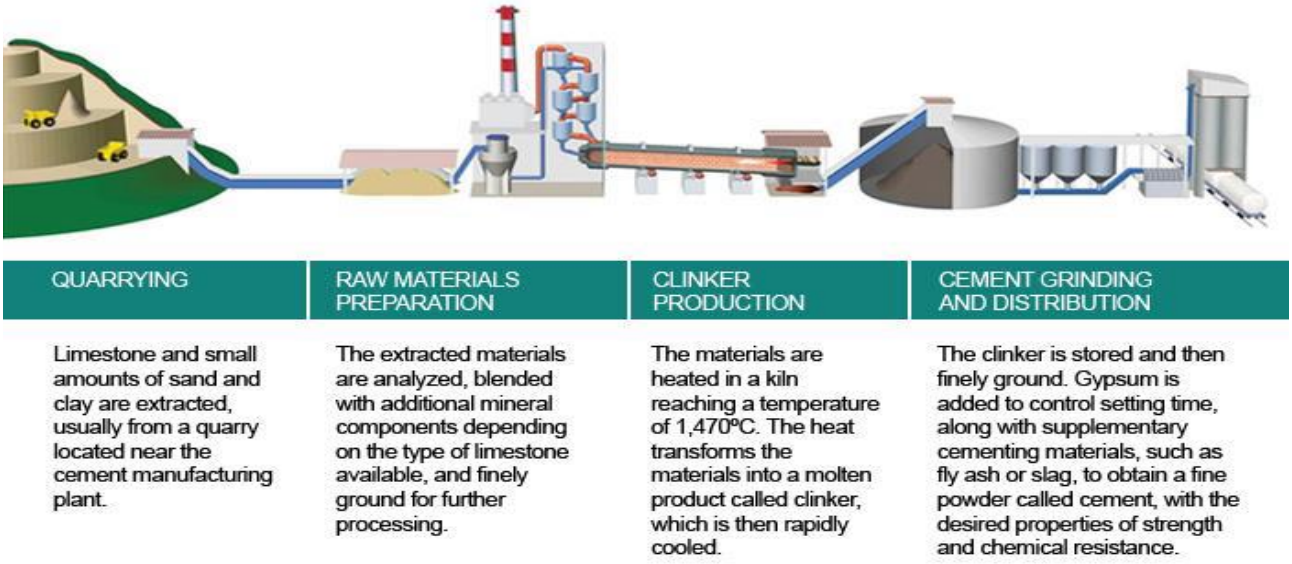

Figure 2.1 Cement raw materials processing (Hahn and Emory, 1997).

2.1.2 Chemical composition of Portland cement

In order to make cement, a mixture of calcareous and silicious material is burned at a high temperature along with lower amounts of alumina (Al_2O_3) and iron oxide (Fe_2O_3) (Potgieter, 2012). The different properties and characteristics of the Portland cement are greatly influenced by the proportions of these oxide compositions. The oxide composition limits present in ordinary Portland cement is presented in Table 2.4.

Table 2.4: Approximate Oxide Composition Limits of Ordinary Portland Cement

Oxide	Per cent content
$\mathbf{CaO}$	60–67
$\mathbf{SiO_2}$	17–25
$\mathbf{Al_2O_3}$	3.0–8.0
$\mathbf{Fe_2O_3}$	0.5–6.0
$\mathbf{MgO}$	0.1–4.0
Alkalies ($\mathbf{K_2O}$, $\mathbf{Na_2O}$)	0.4–1.3
$\mathbf{SO_2}$	1.3–3.0

Source: Shetty (2009)

These oxides which are present in the source materials combine with one another at high temperature to form complex compounds. The compounds which were identified by Bogue (1929) are called Bogue's compound as shown in Table 2.5.

Table 2.5: Major compounds of cement

Name of Compound	Formula	Formula Abbreviated
Tricalcium silicate	3 $CaO.SiO_2$	C_3S
Dicalcium silicate	2 $CaO.SiO_2$	C_2S
Tricalcium aluminate	3 $CaO.Al_2O_3$	C_3A
Tetracalciumaluminoferrite	4 $CaO.Al_2O_3.Fe_2O_3$	C_4AF

Source: Shetty (2009)

The oxide composition of a typical Portland cement, along with the corresponding calculated compound composition and minor oxides, is displayed in Table 2.6.

Table 2.6: The oxide content of ordinary Portland cement and the computed compound composition that follows

Oxide	Composition per cent	Using Bogue's equation to calculate the compound composition in percent

CaO	63	C_3S	54.1
SiO_2	20	C_2S	16.6
Al_2O_3	6.0	C_3A	10.8
Fe_2O_3	3.0	C_4AF	9.1
MgO	1.5	-	-
SO_2	2.0	-	-
K_2O,	1.0	-	-
Na_2O	1.0	-	-

Source: Shetty (2009).

2.1.4 Problems associated with Portland cement

At every step of the process, cement manufacture has an impact on the environment. These include the release of airborne pollutants such as dust, fumes, noise, and vibration from mechanical operation and quarry blasting. Portland cement's caustic nature leads to chemical burns. When exposed for an extended period of time, the powder's potentially harmful ingredients, such as crystalline silica and hexavalent chromium, might irritate the lung or even lead to lung cancer.

The major impacts of the cement production are;

i. CO_2 emissions during production: The biggest issue with the cement business is that it contributes significantly to global warming by emitting large amounts of CO_2. Nearly a ton of CO_2 is now released for every ton of cement produced. The direct process of heating calcium

carbonate, which yields lime and carbon dioxide, is what causes cement manufacture to release CO_2 into the environment. When its manufacturing results in the emission of CO_2, it is emitted indirectly through the consumption of energy (Matar and Elshurafa, 2017). Due to globalization, our cement industries contribute 10% of the world's man-made CO_2 emissions, 60% of which come from chemical processes and 40% from fuel burning. A 2018 Chatham House study indicated that the annual production of 4 billion tons of cement would result in 8% of global CO_2 emissions (Hendriks, Worell, de Jagar, Blok and Riemer, 2004). Improved efficiency is unlikely to change this, but substituting green cement (geopolymer cement) for some of the cement or replacing some of the cement with a supplementary cementing ingredient that does not emit CO_2 can greatly reduce these emissions.

ii. Energy used during production: The use of fossil fuels to run the kiln was shown to be responsible for around 40% of CO2 emissions, according to the World Business Council for Sustainable Development (WBCSD) (Mohammed *et al.,* 2013). One component of the overall energy usage at a cement plant is the electrical energy needed to power the plants. According to Table 2.7, a cement factory uses more than 50% of its electricity to power the raw meal components, the clinker's final grinding, and the gypsum in the finishing mill (Vazinram and Khodaparast, 2009). Although ball mills are still the most popular mills, a more recent generation of mills, including high grinding efficiency roller mills and HORO mills (pressure mills), is now readily available and has the potential to improve grinding efficiency while using less energy.

Table 2.7: Processes in a cement plant that use electricity.

Consumer	Energy Demand (kWh/t)	%
Extraction & Blending	5.5	5
Grinding of raw materials	26.4	24
Homogenization of raw meals	6.6	6
Production of Clinker	24.2	22
Grinding of cement	41.8	38
Conveying, packing, e.t.c	5.5	5
Total	110	100

Source: Stoiber, (2003).

Other minor impacts of cement productions are;

i. Nitrous oxide emissions

According to Silivia, Paolo, Ettore, and Mauro (2014), nitrous oxide (N_2O), the third-most significant greenhouse gas after carbon dioxide and methane, is responsible for around 6% of the greenhouse impact. The main pollutants released into the environment during cement manufacture are nitrogen oxides, with a contribution of NO of around 95% and N_2O of approximately 5%. According to Guseva, Potapova, Tichonova, and Shchelchkov (2002), there are three ways that nitrogen oxides can occur during the Portland cement clinker baking: heat nitrogen oxides (thermal NO_x), fast nitrogen oxides (fast NOx), and fuel nitrogen oxides (fuel NO_x). Due to the low denitrification efficiency of current denitrification methods, nitrogen oxide (NO_x) emissions from the cement industry have severely polluted the atmosphere (Cai, Wu, Ren, Lin, Zhou, and Lyu, 2020).

ii. Particulate air emissions

According to the majority of studies undertaken globally, cement manufacturing is the main source of particulate matter emissions, accounting for up to 40% of all industrial emissions and between 25% and 30% of all particulate matter emissions (Adeyanju and Okeke, 2019). Studies have also shown a possible link between prolonged exposure to fine particles and an increased risk of developing lung cancer, chronic bronchitis, and lung disease mortality (Ciobanu, Istrate, Tudor, and Voicu, 2021).

iii. Noise pollution

Due to noise pollution, cement industry workers are at risk of losing their hearing. Neurasthenia syndrome, which can cause high blood pressure, memory loss, and insomnia, is another side effect of prolonged exposure to these conditions (Ciobanu, Istrate, Tudor, and Voicu, 2021). Cement plants generate noise from a variety of sources. According to Thai, Kucera, and Bernatik (2021), the primary sources of noise are gas dynamic noise, which is produced by blowers, air compressors, and dust collectors; mechanical noise, which is produced by machines like mills and crushers; and electric-magnetic noise, which is produced by electric motors.

2.2 Supplementary cementitious materials (SCMs)

Materials that exhibit pozzolanic or hydraulic activity are supplementary cementitious materials. A hydraulic binder is a substance that, when exposed to water, can set and harden by producing cementitious products through a hydration process. According to Ruben, Gilles, and Jan (2012), iron blast furnace slags frequently exhibit "latent hydraulicity," meaning their hydraulic activity is lower than that of Portland cement and needs to be activated chemically or physically to start and speed up the hydration reaction. Chemical activation of blast furnace slags can be

accomplished by adding alkali-hydroxides, sulfates in the form of gypsum or anhydrite, or, more frequently, lime or materials that produce lime, such as Portland cement. It should be emphasized that materials with hydraulic properties can replace Portland cement to a far greater extent than those with pozzolanic properties.

As defined generally by ASTM C618 (2017), a pozzolan is a siliceous or siliceous and aluminous material that, by itself, has little to no cementitious value but that, at room temperature, chemically reacts with calcium hydroxide (lime) when finely divided and exposed to moisture. It should be noted that the definition of a pozzolan solely refers to the material's ability to react with lime and water; it has nothing to do with the material's origin. The term "pozzolanic activity" includes a measurement of this capacity (Felipe, Xiao and Kubicki, 2001).

2.2.1 Metakaolin (MK)

A siliceous substance known as metakaolin (MK) pozzolan is a siliceous material that, when finely separated from calcium hydroxide and in the presence of water, will chemically react to generate cementitious compounds. Additionally, using MK as a geopolymer or as a component of conventional cement lessens the cement industry's impact on the environment. MK and other cementitious materials are used to replace some cement in order to lessen the environmental impact of the cement industry (Alaa *et al.,* 2009) or as a source of new cementless products (Alaa, 2013). Kaolin or paper sludge following a proper thermal treatment are the main sources of MK. Kaolin as shown in Table 2.8, is made up of several compounds such as SiO_2, Al_2O_3, Fe_2O_3, TiO_2 etc. These compounds are responsible for the pozzolan activities of the kaolin. The colour of the kaolin differs based on the location it was obtained and it can be gotten from different communities in Nigeria.

Researchers continue to disagree on the ideal temperature for heating kaolin to produce MK with a high pozzolanic index. The precise length of the heating cycle is also still unknown. The ideal temperature range for heating kaolin to produce MK may be between 600^0C and 850^0C for times between 1hr and 12hr. These variations might be connected to the molecular make-up of MK (Alaa and Sayieda, 2011). However, most researchers preferred to use 700^0C for 12hr to obtain MK from kaolin (Alaa and Sayieda, 2011). The ideal temperature range for calcining sludge to produce MK is between 600^0C and 800^0C for 2 to 5 hours. According to the majority of researchers, calcination settings that were given a temperature of 700^0C for two hours were ideal (Alaa and Sayieda, 2011). Mention should be made of the fact that MK can also be produced by calcining locally-found lateritic soils (Ambroise, Murat, and Pera, 2009).

Chemical reaction between MK and hydrating cement results in a changed paste microstructure. MK enhances the mechanical characteristics and durability of concrete in addition to its beneficial effects. MK has been researched extensively as a pozzolan for concrete. Sabir et al. (2001) produced green cement for use in building using MK. The effects of MK on the characteristics of mortar and concrete were investigated by (Liew *et al.,* 2011). Siddique and Klaus (2009) looked at the ideal conditions for treating kaolin and paper sludge to create MK.

Table 2.8: Sources of kaolin in Nigeria and their chemical composition.

Deposit	Chemical composition (%)										
	SiO_2	Al_2O_3	Fe_2O_3	TiO_2	CaO	MgO	Na_2O	K_2O	SO_2	L.0.I	Colour
Ozubulu	60	26	5	5	Trace	Trace	Trace	Trace	-	-	White, light grey and dark brown
Nahuta	47	32	1.3	2.4	Trace	Trace	Trace	Trace	0.55	12.18	White, yellow, pink, grey and brown
Jagalwa River	50	30	1.4	2.4	Trace	Trace	Trace	Trace	-	-	-
Darazo	51.9	32.9	2.9	-	0.39	0.29	Trace	0.89	0.13	-	Orange, pink, brown and white grey
Kankara	43.3	36.7	0.21	Nil	Trace	1.49	Trace	0.7	-	11.10	Off-white with pink and patches
Onibode	43.1	36.1	3.1	1.9	Trace	Trace	Trace	Trace	-	12.65	-
Ifon	48	33.2	0.006	1.72	Trace	Trace	Trace	Trace	-	-	Pink
Okitipupa	50	29	-	-	-	-	-	-	-	10	-
Major Porter	45.6	35.2	2.7	-	Trace	Trace	Trace	Trace	-	-	-

Source: Alabi and Omojola (2013)

2.2.1.1 Properties of metakaolin

The physical and chemical properties of metakaolin according to Sanjay, Anil, and Subhash (2013) is as shown in Table 2.9 (a) and 2.9(b) respectively.

Table 2.9(a): Physical Properties of Kaolin.

Physical Properties	Description
Specific Gravity	2.4 to 2.6
Physical Form	Powder
Colour	Off White, Gray to Buff
Brightness	80 – 82 Hunter L
BET	15 m2/gram
Specific Surface	8 – 15 m2/g.

Source: Sanjay *et al*., (2013).

Table 2.9(b): Chemical Properties of Kaolin

Oxide	Composition
SiO_2	51-53%
Al_2O_3	42-44%
Fe_2O_3	<2.20%
TiO_2	<3.0%
CaO	<0.20%
MgO	<0.10%
Na_2O	<0.05%
K_2O	<0.04%
SO_4	<0.50%
P_2O_5	<0.2%
L.O.I	<0.50%

Source: Sanjay *et al*., (2013).

2.3 Supplementary Cementitious Materials (SCMs)

Additional cementitious materials (SCMs) include fly ash, silica fume, metakaolin, limestone flour, natural and synthetic pozzolans, and ground granulated blast furnace slag (GGBFS). When combined with the calcium hydroxide (CH) hydration product of portland cement, pozzolanic materials can become calcium silicate hydrate (CSH), which is not necessarily cementitious. The most reliable and enduring cement hydration product is CSH. Some substances are nonetheless regarded as SCMs even though they are not cementitious or pozzolanic. They act as catalysts for the synthesis of CSH, with limestone flour being one such substance. Because SCMs boost

concrete's durability and its benefits in terms of the economy and ecology, their usage in concrete mixtures has gained importance.

Binary blended Portland cement concrete mixtures have been using supplementary cementitious materials (SCMs) for nearly a century. They have, however, rarely been used in ternary combinations and are not thought to be common practice. The requirement for data and the difficulty of the materials have been the main causes of this lack of use. Technical, financial, and environmental advantages exist for ternary mixed cement. Because the second SCM can compensate for the first's flaws, ternary blends may be even more durable than binary blends. It should be observed, nevertheless, that the properties do not behave in a superpositional manner. The SCMs may interact, and ternary blends' attributes might be different from those of binary blends.

In an effort to prevent chloride ingress, Jones, Dhir, and Mgee (2007) investigated ternary mixed cement. To augment Portland cement systems, they added various mixtures of fly ash, silica fume, and ground granulated blast furnace slag (GGBFS). Their research showed that ternary blended cement often outperformed other binary and plain Portland cement concrete combinations in terms of chlorine resistance. After 30 days, certain ternary mixes revealed substantial chloride ingress, indicating the need for additional research on the best material combinations.

Shehata and Thomas (2011) evaluated the Alkali-Silica Reaction (ASR) resistance of binary and ternary mixed cement. According to their research, silica fume and Portland cement combined in binary form increased alkalinity after 28 days. However, the ternary mixtures of silica fume, fly

ash, and Portland cement used in their study were able to retain low alkalinity for up to 3 years while also limiting expansion to 0.04%.

Using GGBFS and silica fume, Thomas, Hopkins, and Perreault (2012) conducted a long-term investigation on the resilience of ternary mixed cement. Testing was done in a lab and at outdoor exposure sites for the study. In tough Canadian settings, slabs of various combinations were cast and exposed to heavy traffic and deicing salts. Two years were spent testing the slabs. The findings demonstrated that typical Portland cement slabs expand significantly as a result of ASR. None of the ternary mixes, however, demonstrated a sizable extension from ASR. With the exception of the slab containing up to 50% GGBFS, which scaled somewhat during the salt scaling tests, all slabs worked admirably. In the tests for quick chloride penetration, ternary blends fared noticeably better than all other mixes. The study found that ternary mixed cement concrete slabs outlasted all other regular and binary concrete slabs in terms of durability.

For the purpose of increasing strength, Menendez, Bonavetti, and Irassar (2002) investigated binary and ternary mixtures of Portland cement, GGBFS, and limestone. They came to the conclusion that Portland cement and GGBFS binary mixtures had lower early age strengths but higher later age strengths. Portland cement and limestone in binary mixtures exhibited strong early strengths but lower later age strengths. However, the early age and after-age strengths of ternary mixtures of Portland cement, limestone, and GGBFS were very high.

Similar strength gain tests were carried out by Khatib and Hibbert (2005) using metakaolin, GGBFS, and Portland cement. They also discovered that ternary mixtures of the materials preserved each binary combination's advantages while overcoming any drawbacks it had. Anwar studied the early age characteristics of blended cement concretes in 2006 utilizing fly ash and

silica fume. New properties (slump, air content, unit weight) and hardened properties (compressive strength, tensile strength, dynamic elastic modulus, and static young's modulus) were investigated on concrete specimens. The inclusion of fly ash increases the workability of the Concrete, and the results showed that the ternary mixes had desirable fresh qualities. The hardened properties revealed that fly ash tends to weaken materials at an early age, but that the addition of silica fume made up for this weakness.

Ternary mixes of Portland cement, limestone, and natural pozzolana were put to the test by Ghrici, Kenai, and Said-Mansour in 2007. Additionally evaluated were control combinations made of regular Portland cement, Portland cement and limestone, and Portland cement and raw pozzolana. The early age and long-term compressive and flexural strengths of the ternary blend were superior to those of the control mixtures, according to the results. The ternary blend also demonstrated improved chloride ion penetration and sulfate resistance. For usage in transportation constructions, Hale, Freyne, Bush, and Russell (2008) examined the characteristics of concrete mixtures incorporating GGBFS and fly ash. The purpose of the study was to find out whether ternary combinations of the materials outperformed binary combinations. In this study, three different kinds of cement were used. The key findings were that depending on the chemical makeup of the cement, the interaction between SCMs and cement varied substantially. Ordinary and binary blends often fared worse than ternary blends. Nevertheless, depending on the cement and SCM type employed, the ideal SCM replacement ranges differed substantially. Malhotra looked at the use of fly ash in concrete in 1999 as a means of lowering greenhouse gas emissions. A ton of CO_2 was thought to be released into the atmosphere for every ton of cement produced. The quantity of CO_2 that the cement industry emits into the atmosphere is reduced by lowering the amount of cement in concrete mixtures.

Mehta (1999) also investigated the advantages of utilizing more fly ash and GGBFS in concrete for the environment. He calculated that just 6% of the available fly ash was being used as a pozzolan in blended cement at the time, indicating that it is significantly underutilized. In the US, GGBFS is not as easily accessible. GGBFS is still available in a lot of places, though. Mehta came to the conclusion that the future of the concrete industry would be severely impacted by the use of fly ash and GGBFS as SCMs in concrete mixturesDamtoft, Lukasik, Herfort, Sorrentino, and Gartner published a report in 2008 detailing how the concrete sector contributed to the Climate Change Initiative. Hydraulic cement is the most extensively used building material, and it has a significant impact on sustainable development. A component of the study was devoted to SCM replacement in concrete in order to reduce CO2 emissions from the cement industry. They emphasized the need of reducing cement output by adopting binary, ternary, and quaternary blended cement. Marquez, Tikalsky, and Hanson (2009) investigated the reduction of CO2 emissions in cement plants that manufacture ternary blended cement. According to the findings, ternary mixed cements could lower CO2 emissions by up to 45%. CO2 emissions were reduced differently depending on the type of SCMs used in the concrete.

2.4 Aggregates

By lowering drying shrinkage, adding coarse particles throughout the concrete-making process enhances the properties of the hardened concrete. The aggregate's coefficient of thermal expansion significantly affects the concrete's overall strength. Conversely, excessive fine particles will make the concrete extremely flimsy.

Originally, aggregates were thought of as a straightforward filler for concrete, helping to minimize the quantity of cement required. Nonetheless, it is now understood that the kind of aggregate utilized in concrete can significantly affect the concrete's ability to be both flexible and

hardened. Since aggregates can account for up to 80% of the mixture in concrete, their characteristics are essential to the material's performance. Heavy-weight, normal-weight, light-weight, and ultra-lightweight aggregates are the four basic categories into which aggregates fall. However, the majority of concrete processes only use light- and normal-weight particles. For example, thermal insulation in light-weight concrete and nuclear radiation shielding in heavy-weight concrete are two specific uses for different aggregates.

Common forms of aggregates include manmade aggregates, shattered rocks, and natural sands and gravels. Typically, stream beds, dunes, alluvial deposits, and marine deposits contain natural sands and gravels. Compared to other aggregates, crushed rocks have the benefit of having their size customizable through the use of different size screens. Crushed aggregates are often made of igneous rocks like basalt, diorite, and granite; sedimentary rocks like limestone, though sandstone is also infrequently used; and metamorphic rocks, which are rarely employed because of their extremely varied mineral makeup.

The use of synthetic sands in concrete results in very poor workability. The uneven particle form of the produced sands causes this. The amount of water required for a certain level of workability (slump) is proportional to the amount of empty space in the aggregate. When the vacuum space is large, the amount of water required for a particular workability increases. In addition, unless additional cement is added, the strength of the concrete will be inadequate. In general, the void content of produced sand is higher than that of natural sand (Hudson, 2009).

The workability and strength of concrete are significantly impacted by the fines concentration of the generated sand. The larger surface area of the finer particles in aggregate combinations including too much or too fine sand might result in uneconomical concretes, according to the

Cement and Concrete Association of Australia's Guide to Concrete Construction. Hudson (2009) claims that compared to concrete manufactured with regular natural sand, concrete made with a high percentage of minus 75-micron material generates a more cohesive mix. Hudson went on to say that although artificial sand has better workability and compressive strength than natural sand, there is still a big drawback to using it in concrete: the way the finished product looks.

2.4.1 Chemical Composition of Aggregates

The chemical makeup or content of a concrete aggregate determines how the aggregates act in the concrete. Concrete's durability is heavily influenced by the type of aggregates used. Ferraris, David, and Clinton (2007) demonstrated that reactive aggregates expanded geometrically more than non-reactive aggregates in the same mix and condition of concrete. The results also demonstrated that reactive aggregate concrete gained more mass than non-reactive aggregate concrete. In the experiment, siliceous dolomite limestone was used as the reactive aggregate. According to them, the majority of concrete deterioration is caused by the Alkali Silica Reaction (A-S-R), a reaction between reactive silica and hydroxide ion (a byproduct of cement hydration) in the pore of concrete. The consequence is that if an aggregate is reactive to an alkaline media, particularly calcium hydroxide, the concrete created from it will be unstable. As a result, the aggregate may not be suitable for the production of Concrete. As a result, if the opposite is true, the aggregate will be acceptable for concrete manufacture.

2.4.2 Physical Properties of Aggregates

Aggregates are classed according to their shape. Some of the aggregates are rounded. Others have angular, extended, uneven, or other shapes. The size of the aggregate determines whether it is coarse or fine. According to BS 3797 (1964) and BS 877 (1967), aggregates 2mm and lower

are considered fine aggregates, whereas aggregates 3mm and above are called coarse aggregates. Some aggregates have a smooth texture, while others have a rough texture. The aggregates used in typical construction have relative densities ranging from 2.4 to 2.9 and weight densities ranging from 2400 to 2900 kg/m^3 (Mahajan, 2020). Aggregate specific gravity ranges from roughly 2.5 to 3.0, with an average value of about 2.68. The specific gravity of aggregates is used to determine their strength (IS 2386(Part 3):1963).

2.4.3 Classification of aggregates

The classifications of aggregates is done based on the various factors. They include:

a. Based on their geological origin

Aggregate based on their geological origin can be classified into natural and artificial aggregates

i. Natural aggregate

Neville and Brooks (2010) state that they are formed either by crushing a larger percentage of the parent rock or by weathering and abrasion. According to Shetty (2005), parent rocks include sedimentary rocks that were formed beneath the sea bed and hauled up, metamorphic rocks, and igneous rocks formed by the cooling of molten lava on the crust's surface (granite, basalt, and trap), deep within the crust (granite). Igneous or sedimentary rocks that have undergone extreme heat and pressure metamorphosis are the source of metamorphic rocks. The quality of both fresh and hardened concrete is affected by a variety of aggregate attributes that are influenced by the characteristics of their parent rocks, including chemical and mineral compositions, specific gravities, hardness, physical and chemical stability, and more (Neville and Brooks, 2010).

a. Artificial aggregate

Zongjin (2011), explains that these kinds of aggregates are manmade materials, resulting from products or by-products of industries. According to Faridah (2009), they produce light weight concrete of adequate strength and good heat insulation properties. Examples include blast furnace slag, expanded clay, etc., organic materials and by-products such as saw dust, wood chips, rice husk ask, palm kernel shells, periwinkle shells, etc.

b. Classification based on size

According to Shetty (2005), the following criteria influence the maximum size of aggregates that can be utilized in any given condition: section thickness, reinforcement spacing, clear cover to concrete element, mixing, handling, and putting processes. He also stated that the aggregates' maximum size should be as large as possible within the limit indicated, but should not be higher than one-fourth of the member's minimum thickness. Aggregates are divided as coarse and fine aggregates based on size.

i. Coarse aggregate

They are obtained through spontaneous disintegration or artificial crushing of rocks, according to Duggal (2008). Aggregates retained on a 4.75 mm sieve are considered coarse, with a maximum size of 80 mm.

ii. Fine aggregates

They are made from natural river sand, crushed stone sand made by breaking stones, and crushed gravel sand. They pass through a sieve with a diameter of 4.75 mm, and the smallest size of fine aggregates (sand) is 0.06 mm (Duggal, 2008).

c. Classification based on shape and texture

Shape is a crucial aspect of aggregate. According to Zongjin (2011), the difference in surface area generated by differing aggregate shapes impacts the workability of concrete. The characteristics of the source rock, as well as the type of crusher utilized, influence aggregate shape (Shetty, 2005). Shapes of aggregates include spherical, irregular or partially rounded, flaky, angular, elongated, and so on. The texture of aggregate refers to how polished or dull, smooth or rough the aggregate surfaces are. According to Shetty (2005), the factors determining aggregate surface texture depend on the hardness, grain size, pore structure of the rock, and the degree to which all the forces operating on the aggregates have smoothed or roughened the surface. Honeycombed, crystalline, rough, granular, and other characteristics are examples. The surface roughness of aggregate has a considerable impact on the fluidity of new concrete as well as the binding between aggregates and cement paste in hardened concrete (Zongjin, 2011).

2.4.4 Fine aggregate

Particles classified as fine aggregates are those that almost completely pass the 4.75 mm (No. 4) sieve, remain mostly on the 75 μm (No. 200) sieve, and pass the 9.5 mm (3/8 in.) filter. Because less cement is used, the fine aggregate should have a rounded form for improved workability and economy. The purpose of the fine aggregate is to function as a workability agent and to fill up any gaps in the coarse aggregate.

2.4.4.1 River sand

In the past, river sand was the most preferred choice for the fine aggregate component of concrete, but its overuse has raised environmental issues. Therefore, it's critical to identify inexpensive, environmentally friendly substitutes for river sand. The amount of sand used annually in the manufacturing of concrete alone is over 1000 million tons, making it uncommon

and restricted. The British standard BS 882: 1992 defines sand as aggregate that is able to pass through the BS410 test sieve's 5 mm size and does not contain more coarse aggregate than is permitted by this standard. This standard states that one type of sand created by crushing rocks for manufacturing purposes is crushed rock sand.The British standard limits the amount of tiny particles in crushed rock sand to 16% for ordinary use. However, BS standard 882 (1992) restricts the amount of material that can pass through a 150 micron sieve in the case of fine aggregate used in construction to 10%, 10%, and 15%, respectively. However, river sand is currently not accepted for use in construction under Iraqi standards. The use of nonconforming fine aggregate in concrete mixtures is nevertheless advised by ASTM Standard C33 (2003), provided that the final concrete satisfies all criteria.

2.4.4.2 Quarry dust

Quarry dust is a concentrated material used as fine aggregate that is produced as a byproduct of cutting and crushing stone. When a mountain is burst, the rock is crushed into little pieces known as quarry dust, which is produced during the process and ends up as waste and air pollution. On the other hand, by better utilizing natural resources, quarry dust can be employed in construction projects to lower construction costs. There is pressure on the majority of developing nations to switch out fine aggregate entirely or partially with an alternate material without sacrificing the quality of the concrete. Quarry dusts have been used in the construction industry for many different applications, such as fine aggregates, building materials, road construction materials, bricks, and tiles.

2.4.5 Coarse aggregate

Coarse-grained materials cannot be passed through a 4.75 mm hole sieve (No. 4). Particles that will pass through a 3-inch screen and are mostly retained on the 4.75 mm (No. 4) sieve are referred to as "coarse aggregate". The coarser the aggregate, the more economical the mix. Larger chunks provide less surface area of the particles than an equivalent amount of minuscule bits. The amount of cement and water required can be reduced by using coarse aggregate with the largest allowed maximum size.When aggregates are used in concrete forms, if the maximum size of coarse aggregates permitted is surpassed, the particles may interlock and form blocks or arches.This weakens the space below, making it a void or, at most, allowing only finer sand and cement particles to fill it. For coarse particles in concrete, the following characteristics are ideal:

i. Strength
ii. Hardness
iii. Toughness
iv. Hardness
v. Durability
vi. Shape of aggregates.

According to Table 2.10, the calculated F-ratio is 1.17 for the various quarry sites and 1.33 for the various aggregate sizes. According to Omopariola and Jimoh (2017), this suggests that there are no appreciable differences between the sample averages for the various aggregate sizes from the various quarry locations.

Table 2.10 Analysis of variance for Specific Gravity for the various sizes of aggregates and different Quarry Sites

Source of variation	**SS**	**Df**	**MS**	**F-**	**5%F-Limit**
Between different aggregate forms	0.023	(4-1) =3	$\frac{0.023}{3} = 0.008$	$\frac{0.008}{0.006} = 1.33$	F (3,9) =3.86
Between varieties of cements	0.002	(4-1) =3	$\frac{0.002}{3} = 0.007$	$\frac{0.007}{0.006} = 1.17$	F (3,9) =3.86
Residual factor/Error	0.053	9	$\frac{0.053}{9}$ $= 0.006$		
Total	0.078	15			

Source: Omopariola and Jimoh (2017)

For samples taken from every quarry site, the moisture content decreases as the size of the aggregates does. The moisture content readings for all of the coarse aggregate, however, are within the parameters set forth in earlier research. According to Omopariola and Jimoh (2017), extremely porous sandstone and expanded shale have moisture contents as high as 40%, while gravel has a moisture level of less than 1%. All aggregates obtained from different quarry sites have moisture contents that are lower than the acceptable value of 3% as stated in British Standard Institute's BS 882: (1992). Table 2.11 shows that the computed F-ratio is more than the table value of 3.86, with values of 5.75 for various aggregate sizes and 33.25 for various quarry

sites. This suggests that the sample means for both the varied aggregate sizes from the various quarry locations show substantial variances. 2017 (Omopariola and Jimoh).

Table 2.11 Analysis of variance for moisture content for the various sizes of aggregates and different Quarry Sites

Source of variation	**SS**	**Df**	**MS**	**F-**	**5%F-Limit**
Between different aggregate forms	0.007	(4-1) =3	$\frac{0.007}{3} = 0.023$	$\frac{0.023}{0.004} = 5.75$	F (3,9) =3.86
Between varieties of cements	0.4	(4-1) =3	$\frac{0.4}{3} = 0.133$	$\frac{0.133}{0.004} = 33.25$	F (3,9) =3.86
Residual factor/Error	0.04	9	$\frac{0.04}{9} = 0.004$		
Total	0.51	15			

Source: Omopariola and Jimoh (2017)

The water absorption of all aggregate sizes for all quarry sites is within the range of 1% to 3% specified in the literature and British Standards (2000). As a result, all of the tested aggregates had very low water absorption values and are hence ideal for use in concrete construction (Omopariola and Jimoh 2017). The computed F-ratio for the various aggregate sizes in Table 2.12 is 3.4, which is lower than the 3.86 number in the table. This suggests that there are no significant differences between the sample averages, leading to the conclusion that the differences in the water absorption values of various aggregate sizes are negligibleOn the other hand, the fact that the computed F-ratio for each quarry site is 36.4 and is higher than the table

value of 3.86 indicates that the sample averages are different, leading to the conclusion that the water absorption values at each quarry site vary.

Table 2.12 Analysis of variance for water absorption for the various sizes of aggregates and different Quarry Sites

Source of variation	SS	Df	MS	F-	5%F-Limit
Between different aggregate forms	0.05	(4-1) =3	$\frac{0.05}{3} = 0.17$	$\frac{0.17}{0.05} = 3.4$	F (3,9) =3.86
Between varieties of cements	5.45	(4-1) =3	$\frac{5.45}{3} = 1.82$	$\frac{1.82}{0.05} = 36.4$	F (3,9) =3.86
Residual factor/Error	0.47	9	$\frac{0.47}{9} = 0.05$		
Total	5.97	15			

Source: Omopariola and Jimoh (2017)

2.4.5.2 Crushed rocks

Crushed rock aggregates are used to create concrete, mortar, and asphalt by combining them with water and a binding agent like bitumen or cement. When making concrete or mortar, crushed rock aggregates such as sand, stone dust, gravel, crushed stone, crushed blast-furnace slag, and so forth are mixed with a binder like Portland cement. Aggregates can be produced artificially at quarries from broken rocks, or they can be naturally occurring in the form of sands and gravels.

The durability and strength of crushed rock aggregates have a role in their application in engineering building (Okeke, 2005). huge boulders (rip-rap), which are used as fill in huge construction projects, to finely powdered flour-sized particles, which are utilized in paint, glass, plastic, medicine, agricultural feed, soil conditioners, and many more industrial and domestic items, are all examples of aggregates.

Crushed rocks are made in quarries where the bedrock is first explosively blasted (shot) and then mechanically crushed into smaller pieces. All crushed stone fragments have angular shapes, and the crushing process produces all of the fragments' faces. Limestone, dolostone, sandstone, shale, and siltstone are the most prevalent forms of sedimentary rocks found in Indiana (Portland Cement Association, 2012).

2.5 Admixtures

Admixtures are materials that are added to the concrete mix to give it better qualities. Admixtures fall under a number of different categories. They include;

i. Air entraining Agents ii. Accelerating Agents iii. Retarders iv. Water Reducing or Plasticizers v. Superplasticisers vi. Bonding Admixtures vii. Water-Repelling Agents viii. Pigments ix. Porefillers x. Pozzolans

Different qualities of freshly-poured and hardened concrete are impacted by each of these different admixtures. A surface active agent, which is present in water-reducing plasticisers, has a characteristic akin to a detergent. These substances have an imbalanced electrical charge, and when placed in water, they float to the surface with the electrically charged end jutting out and the tail above the surface.

The Cement and Admixtures Association (2009) reported that two things would happen when a surface active agent is placed into a suspension of cement particles.

i. The cement particle's surface absorbs the surface active agent's "tail," which has a negative charge sticking out into the water. As a result, the cement particles do not aggregate, leaving more surface area open for the water's reaction. The discharge of water from a cement particle floc occurs simultaneously. The combined effects make the cement mix easier to deal with.

ii. Since the direction of the surface active agents prevents the air bubble from adhering to cement particles, entrapped air is also more easily released.

2.6 Concrete

Concrete is a composite material made up of coarse granules (the aggregate) mixed with a matrix of materials (the cement paste), which fills in the spaces between the aggregate particles and holds them together. The qualities of fresh concrete, such as workability, are important because they can influence the equipment used to handle and consolidate concrete as well as the properties of the hardened concrete. Concrete is made by combining fine particles, coarse aggregates, cement, and water. According to Oyenuga (1999), concrete is a composite inert substance comprised of a binder course (cement) and a mineral filler (body), or aggregates and water. It is possible to predict the properties of concrete, a structural and building material, by carefully organizing and controlling its component parts. The cement is hydrated with water to form a bond between the components. On the other hand, an excessive amount of water could weaken the final concrete.

The maximum size of aggregates, surface texture, shape, strength, and stiffness of aggregate particles are some of the factors that determine how much strength can be developed by a

workable, properly placed mixture of cement, aggregates, and water (Shetty, 2000). According to Jackson (2011), the primary ingredients of concrete, a composite material, are natural aggregates like sand and gravel (river stone). Additional artificial aggregates include slags from blast furnaces, expanded clay, and broken bricks. Concrete is divided into many categories based on its components and application method. Concrete can be divided into two categories: heavy-weight concrete and light-weight concrete, depending on its constituent parts (Abuguo, 2004). For this investigation, heavy-weight concrete will be taken into account. Practically every civil engineering project uses concrete. It is utilized in constructions for everything from the foundation to the roof. Conversely, tension is not where concrete excels. As a result, while designing with reinforced concrete, it is presumed that the concrete in the member's tension zone has failed (BS 8110, part 3, 1985).

2.6.1 Types of concrete

The various types of concrete used for construction purposes are listed below:

i. **Normal Strength Concrete**

   Cement, water, and aggregate are the basic components that we need to mix to create concrete with typical strength. The strengths of these concrete varieties range from 10 MPa to 40 MPa. Depending on the properties of the cement and the climate where it is placed, normal strength concrete might take anywhere from 30 to 90 minutes to set initially.

ii. Plain Concrete

The plain concrete will not have any reinforcement. The main ingredients of the combination are cement, aggregates, and water. The most commonly used mix design is the usual 1:2:4. The density of plain concrete will be between

2200 and 2500 kg/m^3. The range of the compressive strength is 200–500 kg/cm^2. Buildings and pavements are the main uses for these types of concrete in areas where there is less need for high tensile strength. These types of concrete offer excellent levels of durability pleasure.

iii. Reinforced Concrete

The concrete that has reinforcement added to it to support the tensile strength is referred to as reinforced cement concrete. Plain concrete is strong in compression but weak in tension. Therefore, sustaining the tensile stresses will be the responsibility of the reinforcing location. R.C.C. operates through the joint action of reinforcing and plain concrete. Rods, bars, or meshes are all possible forms of steel reinforcement used in concrete. As reinforcement, fibers are now being created as well.

iv. Precast Concrete

Different structural parts can be produced and cast in the factory in compliance with the requirements, then delivered to the assembly location. These concrete units are referred to as precast concrete. Precast concrete pieces include things like concrete lintels, stair rails, precast walls and poles, and many more parts. The advantage of these units is that they may be assembled quickly because only assembly is needed. Because everything is made on-site, quality is assured. Ensuring their passage is the only safety precaution.

v. Lightweight Concrete

Concrete that is classified as lightweight will have a density of less than 1920 kg/m3. We will have lightweight aggregates thanks to the usage of lightweight aggregates in concrete design. The crucial component that affects the density of the concrete is the aggregate. Pumice, perlites, and scoria are examples of lightweight aggregates.

vi. High-Density Concrete

Heavyweight concrete can be defined as concrete with a density of between 3000 and 4000 kg/m^3. Heavy weight aggregates are utilized here. The coarse aggregates are made of crushed rocks. Barytes is the most often used heavy weight aggregate. The most typical applications for these aggregates include the construction of nuclear power plants and related projects. The construction will be better able to withstand any form of radiation thanks to the large weight aggregate.

vii. Air Entrained Concrete

These concrete kinds contain 3 to 6% of the concrete that is purposefully entrained with air. Foams or gas-foaming agents are added to the concrete to create air entrainment. Resins, alcohols, and fatty acids are only a few instances of air entraining substances.

2.6.2 Properties of Fresh Concrete

Plastic or recent concrete may be molded into any shape because it is a newly mixed substance. The fresh and hardened states are affected by the proportions of cement, aggregates, and water in the mixture (Shetty, 2004).

2.6.2.1 Workability

A concrete mix's workability, according to Jackson and Dhir (2006), is how easily it can be moved from the mixer to its ultimate compacted shape. Consistency, mobility, and compatibility are the three key traits. Wetness or fluidity are measured in terms of consistency. Mobility refers to how easily a mixture may flow into and fill a mold or form. A mixture's compatibility is determined by how easily it can be fully compressed to release all trapped air. Workability is often assessed using the slump, compacting factor, vibe consist meter, and flow tests.

i. **Slump**

This test primarily evaluates the plastic concrete's consistency. A slump increases as a result of a rise in water content or a decrease in the percentage of fine aggregate. True slump, shear slump, and collapse Slump are the three forms of slump that are typically observed (Neville, 2009). Mixtures that are coherent and rich show a true slump. A collapsing slump is frequently the result of segregation of the constituent materials and is typically linked with extremely wet mixtures and poor-quality concrete. Shear droop, which is more frequently found in leaner mixtures, is an indication of a loss of cohesiveness and is typically connected to severe mixtures.

i. Compacting Factor Test

This test provides a direct and reasonably reliable evaluation of the workability of Concrete by measuring the level of compaction imparted to Concrete for a specified amount of work.

ii. Vebe consistometer Test

Despite being widely acknowledged as a test that primarily assesses workability, it is not frequently employed. The time it takes to vibrate a conventional concrete cone into a flat, compressed cylinder is measured in seconds in this test (BS 1881: part 04).

Workable concrete is defined as having very little internal friction between particles or being able to overcome the frictional resistance provided by the reinforcements or framework surface within the concrete with minimal compactive effort.

Workability is influenced by a number of variables, including water content, mix proportion, aggregate size, aggregate grading, and surface roughness.

i. Water Content

Shetty (2004) noted that the amount of water in a given volume of concrete will have a big impact on how easily it can be worked. One of the key parameters impacting workability is fluidity, which increases with increased water content per cubic meter of concrete.

ii. Mix Proportions

Workability is significantly impacted by the cement to aggregate ratio. As the ratio of cement to aggregate increases, the concrete gets thinner. Aggregate mobility is limited in lean concrete because there is less paste available for lubricating per unit surface area of aggregate. The mix is more cohesive and easier to work with when the aggregate to cement ratio is lower, on the other hand.

iii. Size of Aggregate

Larger particles have less surface area, thus more paste is needed to lubricate the surface and reduce internal friction, and more water is required to wet the surface. Using aggregates with larger particle sizes for a given amount of paste and water will produce improved workability. Concrete's workability is influenced by the shape of the particles, claims Shetty (2012).

iv. Grading of Aggregate

One of the elements affecting workability is this. The least amount of voids are present in a given volume of a well-graded aggregate. A better lubricating effect can be achieved when there are fewer total voids since other parameters remain constant. Excess paste makes the mixture cohesive and prevents particle segregation. The less vacant material there is and the higher the workability, the better the grading.

v. Surface Texture

Aggregates with a rough surface have a larger surface area than aggregates with a smooth surface but the same volume, surface roughness has an impact on workability. According to the preceding discussions, aggregates with a rough texture will have low workability whereas those with a smooth or glassy texture will have higher workability.

2.6.3 Properties of Hardened Concrete

Hardened concrete offers several beneficial characteristics. Among the main characteristics of hardened concrete are strength, deformation under load, durability, permeability, strength, and shrinkage. According to Jackson and Dhir (2006), strength is Concrete's most important quality.

However, shrinkage and permeability ought to be important considerations in water-holding structures.

2.6.3.1 Strength

The greatest load (stress) that concrete can support is referred to as its strength. The water to cement ratio typically has an impact on concrete's strength. According to Walker and Bloem (2009), it has been demonstrated that the following elements can affect the strength that a workable concrete may generate for a given concrete and suitable aggregate.

i The ratio of cement to aggregate ii. Grading, surface texture, shape, strength, and stiffness of the aggregate particle iii. Maximum size of aggregate iv. Strength of the mortar v. The bond between the mortar and the coarse aggregate vi. The coarse aggregate, i.e., its strength, is its ability to resist stresses applied.

The various tests carried out to determine the strength of the hardened concrete are;

i. Compressive Strength

The concrete's compressive strength is influenced by its unit weight. According to Ding and Zongjin (2004), the aggregate/binder ratio and type have an effect on the compressive strength of concrete. As aggregates, they used sintered alumina, dead burnt magnesia, and river sand. Their results show that when the aggregate/binder ratio rises, compressive strength falls. Furthermore, at the same aggregate/binder ratio, the mix made with magnesium sand or aluminum sand was found to have a higher compressive strength than the mix made with river sand. It was also shown in the same investigation that the compressive strength decreased as the ratio of cement to water increased. Their experimental results showed that, for all aggregate to cement ratios,

compressive strength decreases as the water to cement ratio increases and vice versa. Compressive strength of a concrete cube can be obtained from Equation (2.1)

$$Fc = \frac{P}{A} \quad (2.1)$$

Where;

Fc = compressive strength

P = crushing load

A = cross-section area of concrete cube

ii. **Tensile Strength**

When designing concrete runways and roadways, the tensile strength of concrete is crucial. Jackson and Dhir (2006) assert that concrete members must also be able to bear tensile pressures brought on by any restriction on contraction caused by drying or temperature changes. Typically, it is assumed that concrete's tensile strength is equivalent to about one-tenth of its compressive strength. However, this may differ based on the technique employed to gauge tensile strength and the type of concrete.

iii. Flexural strength

This is one of Concrete's mechanical characteristics. Typically, concrete is not made to withstand direct flexure. However, it can be used to predict the load at which cracking will appear (Neville, 2013). Unreinforced concrete constructions like motorways and airport runways are also of importance. Procedures for flexural tests are laid out in BS 1881, part 118 of the code of practice.

Flexural strength of a concrete can be obtained using Equation (2.2)

$$FS = \frac{failure\ load}{loaded\ area\ of\ beam} \quad (2.2)$$

It has been demonstrated that the lateral tensile strain in a cylinder under uniaxial compression and the beam in flexure are of comparable magnitudes at the site of beginning cracking (Berugo, 2010). The splitting tensile strength at a specific age and the modulus of rupture also have a linear connection (Melis, 2015).

iv. Young modulus

The ratio of normal stress to corresponding strain for tensile or compressive stresses below the material's proportional limit is known as the concrete's modulus of elasticity. The first component of the stress-strain curve of concrete under compression is linear when the loading is of low intensity and brief duration, supporting the usage of the modulus of elasticity. However, with a continuous load, inelastic creep causes the stress-strain curve to diverge, even at very moderate values. Additionally, creep and shrinkage effects will cause concrete to behave non-linearly. As a result, according to Neville and Brooks (2010), the initial tangent modulus is a measurement of the dynamic modulus of elasticity.

For a linear elastic analysis, one should use the static modulus of elasticity. Several definitions of modulus of elasticity are available, as indicated in Figure 2.2. These include initial tangent modulus, tangent modulus (at a defined stress level), and secant modulus (at a specified stress level). According to Neville and Brooks (2010), the average value of Ei under service load conditions is believed to be the secant modulus, which is the slope of a line drawn from the

origin to the stress-strain curve point that corresponds to 40% of the failure stress.

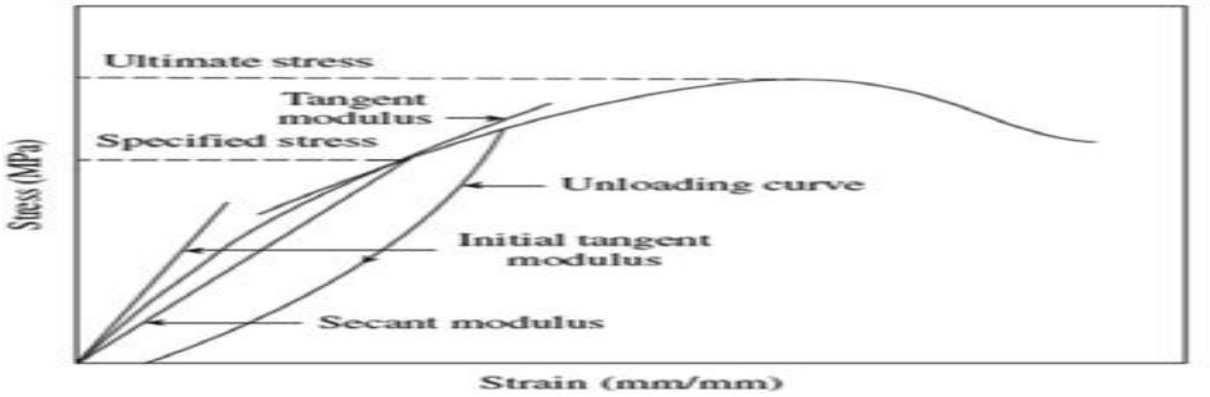

Figure 2.2:Various definitions of modulus of elasticity of concrete

Source: Neville and Brooks (2010).

The strength of concrete can be affected by some factors, namely;

i. Water/Cement Ratio

The strength of the cement paste is a major factor in cement strength (Shetty, 2012). Shetty (2012) claims that the results of the experiment show that the paste's strength determines how strong cement paste is. In other words, the strength of the paste is inversely proportional to the amount of cement and air or water present. The strength of Concrete is only affected by the water/cement ratio, so long as the mixture is workable, according to Abram's water/cement ratio equation (Ferraris *et al.*, 2007).

ii. Aggregate

The aggregate, the matrix, the contact between the two, or any combination of these may fail in concrete under stress. "Aggregates are typically stronger than the concrete itself, and in such cases, the aggregate strength has little effect on the strength of concrete," according to (Arthur and Peter, 2011). Concrete cannot be strong without the aggregate matrix contact, also known as the bond. Aggregate shape, surface roughness, and cleanliness all impact bond strength.

Aggregates with a high surface roughness or angular or irregular shapes will create a stronger bond between the aggregate and the matrix than smooth, rounded aggregates. Nevertheless, the reduced water-to-cement ratio needed for the same workability may make up for the corresponding loss in strength. According to Jackson and Dhir (2006), "aggregate shape and surface texture affect the tensile strength more than the compressive strength." A thin layer of contaminants, like silt and clay, on the aggregate surface hinders the formation of a strong bond.

iii. Influence of Curing

The hydration of the cement component requires curing concrete, according to Jackson and Dhir (2006). Temperature affects both the quantity and pace of hydration for a specific concrete as well as the physical characteristics of the hydration products. In general, the longer concrete is submerged in water, the stronger it becomes. Most people agree that the first 28 days are when concrete created with regular Portland cement and kept in typical conditions develops roughly 75% of its strength.

iv. Deformation

Concrete can withstand deformation up to a specified applied load in its hardened state. It sags when it is laden. With an increase in load, the deformation grows. Elastic deformation is the distortion brought on by an increase in load.

2.6.3.2 Durability

Rugged weather conditions and the chemical environment are the main issues with concrete's durability. Concrete with air inclusions appears to be more durable than other types. Compared to concrete without air entrainment, they are more freeze-thaw resistant. The cement mortar's entrained air can withstand the hydraulic pressure brought on by the water leaving the

aggregates, protecting the concrete from harm. It is encouraging that concrete can now withstand chemical attacks.

The effects of water absorption, stress relaxation, and self-desiccation on the alkali silica reaction in mortar with a low water/cement ratio were examined by (Ferraris *et al.*, 2007). The aggregates utilized in the studies were silica dolomitic limestone and non-reactive limestone (with 0.01% expansion at 14 days ASTM C1260). The results showed that the mixture containing silica dolomitic limestone developed to a maximum of 0.43% at 30 days, whereas the later mix grew to a maximum of 0.02% at the same time. Mass increased greater in the former mixture than in the latter.

Laukaitis, Zurauskas, and Keriene (2003) investigated how polystyrene granules affected the cement composites' thermal properties. According to their findings, the coarse granule composites with matching mass values of 108 kg/m^3, 220 kg/m^3, and 260 kg/m^3 had respective thermal conductivity coefficients of 0.0754 W/mK, 0.0868 W/mK, and 0.0981 W/mK. For fine granules of the density, the coefficients are 0.0723 W/mk, 0.0803 W/mK, and 0.0883 W/mK, in that order. The findings of their study indicated that heat conductivity increased with composite density and decreased with density.

In a study to test the bond strength of concrete made with various aggregates, Yassar (2006) showed that normal-weight aggregate concrete had a lower bond strength than light-weight aggregate concrete. Three different kinds of concrete were examined. They were foamed concrete, light-weight aggregate concrete, and normal-weight aggregate concrete. The results indicated that the concrete using normal-weight particles had the highest compressive strength. The properties to study under durability of concrete are;

i. Water absorption capacity

Concrete has the ability to absorb liquids, such as water or aqueous solutions, by capillary action. Absorptivity (sometimes called sorptivity) is the rate at which this happens, and it is determined by the moisture gradient that is already present at the surface as well as the size and connectedness of the concrete's capillary pores (Neil and Dhir, 2006). Concrete's pore structure can be effectively represented by measuring the rate of absorptionConcrete absorbs water through capillary action, and this process is known as capillary water absorption. The phenomenon occurs because of the fineness of the concrete's capillary pores. According to Khatib and Clay (2003), capillary action is a better water penetration test to gauge the quality of concrete for above-ground projects like buildings.

ii. Shrinkage

The hardened concrete may contract. Concrete shrinks as a result of three different processes: plastic shrinkage, autogenous shrinkage, and drying shrinkage. Plastic shrinkage is the settlement of solids and the loss of free water from plastic concrete. As the concrete dries and hardens, shrinkage is another name for the volume contraction that occurs. Asuquo (2007) asserts that shrinkage is brought on by the capillary tension of the water that is still present in the concrete. In contrast, dry concrete expands when submerged in water, restoring a large portion of the volume lost during shrinkage. Ordinary concrete experiences final shrinkage in the range of 0.0001 % to 0.0007 % depending on the original water content, environmental temperature, humidity, and aggregate type.

iii. Sulphate attack

One of the issues with concrete's durability is sulphate attack. Sulphate attack is frequently explained in terms of the interaction between the solid cement hydration products and the ions of

sulfuric acid in solution. Soil, groundwater, rivers, saltwater, cooling towers, industrial waste, and cations such sodium, potassium, magnesium, and calcium ions are the sources of sulfate ions (Lee, Moo, and Swamy, 2005). Because of its complex behavior and various overlapping reactions, it has been challenging to pinpoint the specific nature of the processes of sulphate assault (Lee *et al.*, 2005).

The main issue with material evaluation is the varied attack form in sulfate settings (Chabrelie, Muler, and Skrivener, 2011). The permeability of concrete, water/cement ratio, cement type (i.e., cement composition), exposure conditions, cation type in Sulphate salts, Sulphate ions concentration, environment, and exposure length are some of the variables that determine how much Sulphate affects concrete. Under this attack, the concrete's microstructure is altered. Although the severity of these changes can vary, they frequently involve physical attack brought on by salt accumulation in pores and chemical Sulphate attack (Manu, Menashi, and Jan, 2002; Skalny, Marchand, and Odler, 2003). Common damages include cracking, expansion, and a loss of bond between the cement paste and aggregate. Although there is some debate over the precise mechanisms causing the expansion (Manu *et al.*, 2002; Tian and Cohen, 2000; Karakurt *et al.*, 2011), the expansion brought on by Sulphate assault is typically linked to the creation of gypsum and ettringite.

2.6.3.3 Some Other Properties of Concrete

Concrete qualities can generally be divided into;

i. **Optical:** This attribute of Concrete gauges how it reacts to light.

ii. **Physical:** This characteristic establishes how Concrete appears to the eye. The property has a significant impact on the finished concrete work's looks. Concrete's physical characteristics depend on the design and workmanship.

iii. **Thermal:** This is the concrete's capacity to withstand a certain amount of heat for a certain amount of time. It depends on the Concrete's composition of materials and design. Concrete design codes outline various fire resistances for concrete.

2.7 Reviews on past works done Metakaolin/Quarry dust Concrete

The compressive strength of various concrete mixtures modified with calcined kaolin was investigated by Huat (2006). Kaolin was calcined at various temperatures ranging from 600^0C, 650^0C, 700^0C, 750^0C, and 800^0C for three hours. Calcined kaolin was used in place of cement at weight ratios of 0%, 5%, 10%, 15%, 20%, and 30%. The fixed w/b ratio was 0.56. The findings showed that 8% calcined kaolin treated at 750^0C had the highest 28-day compressive strength, followed by 8% calcined kaolin treated at 800^0C. The improvements in the 28-day compressive strength were 9.71% and 5.1%, respectively, after kaolin's calcination at 750 and 8000C. Thermal activation of kaolin was carried out by Cara, Gianfranco, Luigi, Paola, Ulrico, and Massimo (2006), at 530^0C, 630^0C, and 800^0C for 100 min. According to their findings, thermal activation at 6300C seems to be a good balance between economics and activation. At lengthy curing durations, the reactivity at 630 and 800^0C produced values that were similar.

As seen from the literature review in this section, the optimum MK level in the mixture was affected by the chemical make-up of the MK source as well as the temperature and length of the calcination process for the kaolin. When converting source kaolin to MK, it is preferable to use 850^0C for 3 hours in order to get the best 28-day compressive strength if the source kaolin contains a high alumite content (about 22%). On the other hand, 650^0C for 3 hours is sufficient

to transform source kaolin into reactive MK if the alumite content is less than 7%. In keeping with this, the calcination temperature and time of the kaolin are significant factors that determine the ideal MK replacement level. According to several publications, the optimal conditions for producing high reactive MK are kaoline calcinations at 850^0C for three hours. However, Rashad (2013) fully addresses this matter.

For a design mix of M20 grade concrete, Venkatarama (2004) investigated the effects of a 0%, 20%, 30%, 40%, and 50% partial replacement of sand with quarry dust. Quarry dust was found to be quite helpful in ensuring excellent concrete cohesion due to its high fines content. Quarry dust's thorough pozzolanic reaction with the concrete admixture enhanced micro aggregate filling, concrete durability, and pozzolanic reaction. Higher surface area aggregates needed more water in the mixture to sufficiently wet the particle surfaces and retain a certain workability. It goes without saying that adding more water to the mixture will reduce the concrete's quality. It was shown that the percentage of sand replaced by quarry dust grows as the slump value does.

The compressive and flexural strengths of foam concrete with quarry dust were about 40% higher than the control foam concrete, according to Kamarulzaman's (2008) study on the subject. Sand replacement by quarry dust up to 30% was found to increase the properties of foam concrete.

According to Viswanadha, Rama, and Sindhu (2014), they looked at the impact of metakaolin replacements of 0%, 10%, 15%, and 20% on the compressive strength of concrete cubes. 91 days of curing and 28 days of testing were used to determine the compressive strength for M50 grade. The results are summarized in Table 2.13 and the graph is displayed in Figure 2.3.

Table 2.13: Compressive Strength of M50 Grade Concrete

S/No	% metakaolin	Compressive strength (N/mm^2)	
		28 days	**90 days**
1	0	59	61.34
2	10	60.20	62.12
3	15	61.86	63
4	20	57.1	58.3

Source: Viswanadha *et al.*, (2014)

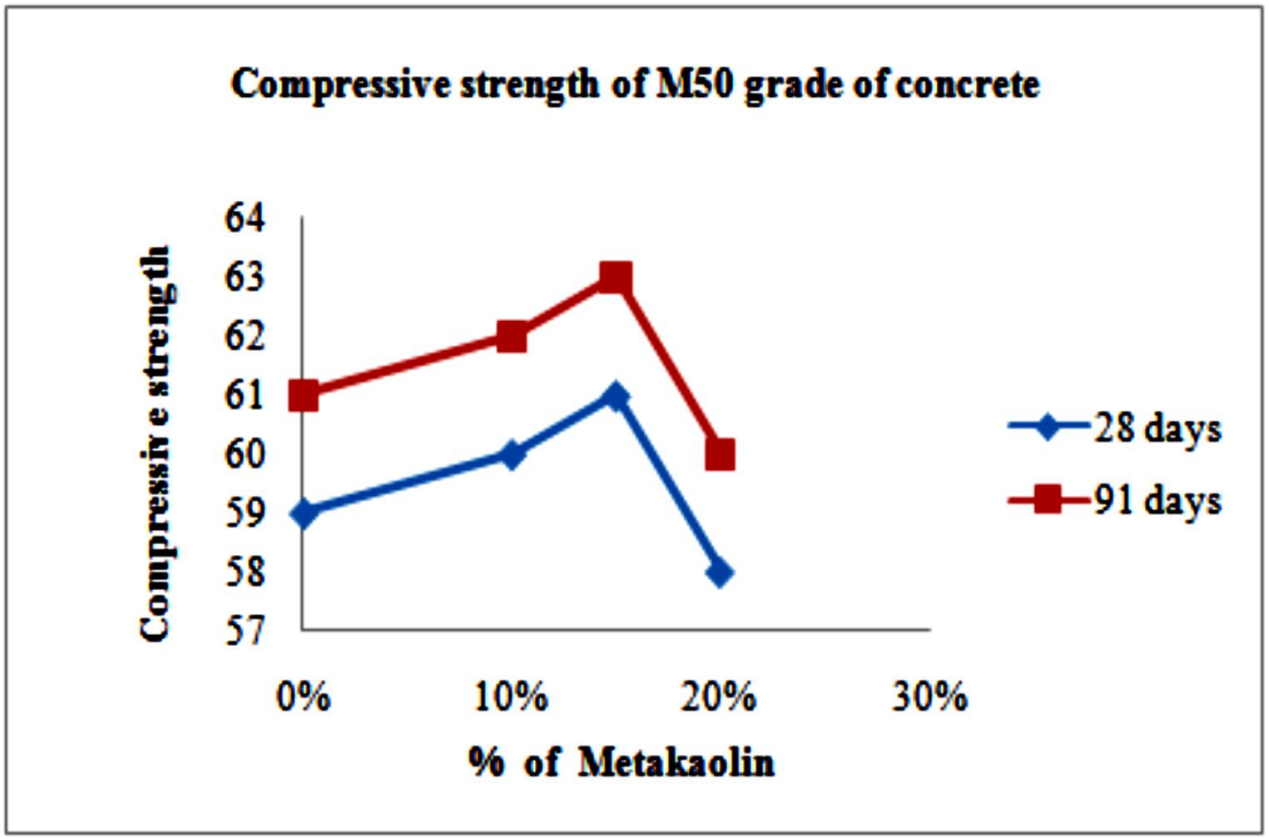

Figure 2.3. Compressive Strength of M50 Grade of Concrete

Source: Viswanadha *et al.*, (2014)

Table 2.13 displays the compressive strength of M50 grade concrete with 15% cement replacement by Metakaolin and no cement replacement at all. After 28 days, the strength rises from 0% metakaolin to 15% metakaolin. The strength decreases as the percentage of metakaolin replacement in cement increases, and the maximum compressive strength is reached at 15% cement replacement by metakaolin. The strength obtained after 91 days of curing is higher than the strength obtained after 28 days of curing, as Table 2.13 and Figure 2.3 demonstrate.

According to Khater (2014), Figure 2.4 displays the results of compressive strength as a function of metakaolin concentration and curing time up to 90 days at w/b ratios of 0.60 and 0.30, respectively. The results show an increase in compressive strength at any metakaolin addition with curing time due to binder buildup and formation in the open pores caused by cement hydration as well as the pozzolanic interaction of metakaolin with CH. The pozzolanic activity of metakaolin and PC hydration work together in PC-MK systems, but the rate of clinker hydration in PC determines how quickly strength develops.

The literature indicates that the main factors influencing the contribution of metakaolin to strength are the filler effect, the dilution effect (physical effect), and the pozzolanic reaction of metakaolin with CH (chemical effect), which results in the formation of additional CSH and CSAH phases (Wild, Khatib, and Jones 1996). wherein in addition to the pozzolanic reaction, the pozzolanic effect is dependent upon the filling or physical effects of the smaller particles in the mixture. The main reasons for the increase in relative strength are the filler effect, which accelerates PC hydration initially, and the rise in C-S-H binder phases brought on by the reaction between CH released from cement hydration and the SiO2 component of metakaolin, as later

shown by XRD, when PC is substituted with up to 25% of Mk. The relative strength decline beyond 25% in the case of w/b = 0.60 and 20% Mk in the case of w/b = 0.30 may be caused by the cessation of the pozzolanic reaction as well as the overcoming of the filler effect by dilution effect, which results in a decrease in the relative strength, or the overcoming of the filling effect over the pozzolanic one as the source of liberated lime (PC) decreases. It is observed that strength decreases due to the dilution effect of metakaolin as well as very fine pore structure and narrow particle size distribution, which need much water content to contribute to the reaction. At lower water content, the increase of Mk beyond 20% needs more water and therefore decreases structure compaction that is accompanied by decreases in cement content (the source of CH required for pozzolanic reaction), where the cement used liberates 24-25% calcium hydroxide, this ratio would favor the creation of C_2ASH_8 if fully hydrated, according to the competitive hydration reaction theory put forward by Murat (1983). The water demand is nevertheless sufficient for mortar durability even at increased water contents, which in turn led to an increase

in Mk of up to 25% and a maximum strength augmentation.

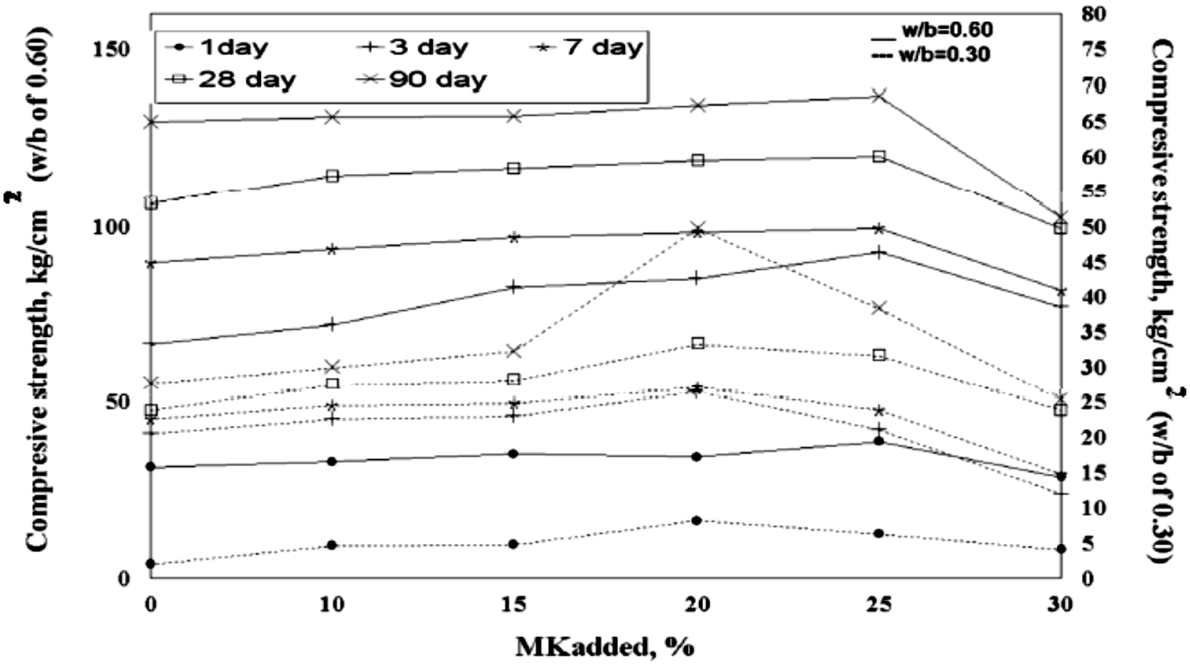

Figure 2.4: Compressive strength at different hydration ages of the different blended cement (OPC-MK) mortar pastes with water/binder ratios of 0.60 and 0.30
Source: Khater (2014).

According to Jadhao and Shelorkar (2013), they investigated the impact of Metakaolin replacement percentage on High Grade (HGC) water permeability. The variation in water penetration depth in HGC with 4%, 6%, and 8% of Metakaolin (Metacem85) content. In contrast to the increase in Metakaolin (Metacem-85) content, the depth of penetration decreases by 11.33mm, 14.33mm, and 16.33mm, respectively. The filling effect of the Metakaolin (Metacem-85) causes a decrease in penetration depth with an increase in its content. Comparing concrete specimens with 4%, 6%, and 8% Metakaolin (Metacem-85) content to control concrete specimens, the percentage reduction in water penetration depth is 49.26%, 62.30%, and 71.00%, respectively.

2.8 Multiple Regression Analysis

The first time cross-validation techniques were used, multiple regression analysis was the setting. Multiple regression analysis is used to predict a dependent or criterion variable using two or more independent or predictor variables. Examine Equation (2.3), which is an example of a regression model for n observations and p independent variables.

$$\mathbf{Y = XB + e,} \tag{2.3}$$

Where Y is an *n* x 1 column vector containing data on the dependent variable (criterion);

X is an *n* x (*p* + 1) matrix containing data on the predictor (independent) variables;

B is a (*p* + 1) x 1 column vector containing estimated regression coefficients, and

e is an ***n*** x 1 column vector containing error terms (residuals).

One of the primary objectives of multiple regression analysis is to establish a regression equation that can be used in additional samples to predict an unknown criterion variable using known data on the predictor variables. When performing multiple regression analysis, the Ordinary Least Squares (OLS) method is usually used to calculate regression coefficients (B). Equation (2.4) can be used to find values of the regression coefficients that minimize prediction error (residuals) and provide the best fit of the data to the model.

$$\mathbf{e = Y - XB = Y - \hat{Y},} \tag{2.4}$$

Where $\hat{Y}$ is an *n* x 1 column vector containing predicted Y values for the sample.

When the following conditions are satisfied, OLS yields the best, unbiased regression coefficients: (1) no measurement error; (2) zero mean for the residuals; (3) constant variance for

the residuals; (4) no inter-correlation for the residuals; and (5) normal distribution for the residuals (Hamilton, 2012).

The sample squared multiple correlations can be used to estimate the population squared multiple correlation (ρ^2) and determine the percentage of the criterion variable's variance that is explained by the predictor variables after the regression equation has been established and predicted Y values ($\hat{Y}$) have been obtained in a sample for which data on both the predictor and criterion variables are available. The squared multiple correlations are equivalent to the squared zero-order correlation between the sample's predicted Y values ($\hat{Y}$) and the observed criterion variables (Y) (Pedhazur, 1982). Higher values of the squared multiple correlations were previously used to indicate higher predictive accuracy, or how well the sample equation would function in additional representative samples from the population. As an additional indicator of predictive accuracy, the sample mean square error of prediction (MSEP) was employed. This is the mean squared difference between the sample's predicted Y values ($\hat{Y}$) and the criterion variables (Y), as shown in Equation (2.5):

$$\mathbf{MSEP} = \sum\left(Y - \hat{Y}\right)^2/(\boldsymbol{n} - \boldsymbol{p} - \mathbf{1}) \qquad (2.5)$$

Where n is the number of observations, *p* is the number of independent variables.

Lower values of the MSEP indicate a less predictive error and, consequently, better predictive accuracy of the regression model. The MSEP is an estimate of the population MSEP ($2e^{\sigma}$). Unfortunately, researchers would usually find that the squared multiple correlations were smaller than those found in the original sample and that the MSEP was underestimated in the original sample when they applied regression equations with the fixed regression coefficients established in one sample to other data (Mosteller and Tukey, 1977). Shrinkage, which can be quantified as

the difference between multiple squared correlations obtained from samples other than the original one from which the regression equation was developed, is the finding of smaller squared multiple correlations in samples other than the one from which the regression equation was developed (Pedhazur, 1982). Shrinkage happens as a result of the model being built within a sample being dependent upon its unique characteristics. As a result, rather than necessarily reflecting the characteristics of the population or samples from the population, the regression model will represent the features of that particular sampleAs a result, the regression model created for a sample will always overestimate the model's fit and fit that sample more closely than other samples. Fit overestimation is caused by OLS regression estimation, which yields optimal regression coefficients for the best possible model-to-data fit. As such, it "capitalizes on chance" events that happen in that specific set of data (Mosteller and Tukey, 1977 Two metrics of predictive validity, represented as w^2 and d^2, respectively, were suggested by Browne (1975) for the population sample equation. These measures are comparable to the squared multiple correlation and the MSEP. The sample MSEP and sample squared multiple correlation are hopeful indicators of the population validity of the sample regression model.

2.8.1 Response surface modeling

A collection of statistical and mathematical techniques known as response surface modeling (RSM) can be applied to develop, improve, and optimize processes (Myers and Montgomery, 2002; Akinoso, Aboaba, and Olajide, 2011). RSM is most commonly employed when multiple input variables may have an impact on a single process quality attribute or performance metric. As a result, the response might be regarded as a performance indication or quality attribute. The scientist or engineer is in charge of the input variables, also referred to as independent variables.Response surface methodology includes empirical statistical modeling to establish a

suitable approximating relationship between the yield and the process variables, optimization techniques to identify the values of the process variables that yield desirable response values, and experimental techniques to explore the space of the process or independent variables. In practice, RSM application is required to create an approximate model of the real response surface. A physical mechanism that is unknown to us usually drives the genuine response surface underneath. The approximation model is an empirical model that is based on observed data from the process or system. A group of statistical methods known as multiple regression can be used to create the many kinds of empirical models needed in RSM. Equation (2.6) provides the first-order multiple linear regression model with two independent variables.

$$Y=\beta_0 + \beta_1 x_1 + \beta_2 x_2 + \varepsilon \qquad (2.6)$$

The independent variables are often called predictor variables or regressors. The term "linear" is used because Equation (2.6) is a linear function of the unknown parameters β_0, β_1,β_2,.

In general, the response variable *y* may be related to *k* regressor variables. The model

$$Y=\beta_0 + \beta_1 x_1 + \beta_2 x_2 + \ldots.. + \beta_k x_k + \varepsilon \qquad (2.7)$$

is called a multiple linear regression model with *k* regressor variables.

The parameters β_j, $j=0,1,\ldots k,$ are called the regression coefficients. Models that are more complex in appearance than Equation (2.7) may often still be analyzed by multiple linear regression techniques. When an interaction term is added to the first-order model in two variables, the equation is presented in Equation (2.8);

$$Y=\beta_0 + \beta_1 x_1 + \beta_2 x_2 + \beta_{12} x_1 x_2 + \varepsilon \qquad (2.8)$$

The second-order response surface model in two variables is is presented in Equation (2.9);

$$Y=\beta_0 + \beta_1 x_1 + \beta_2 x_2 + \beta_{11} x_1^2 + \beta_{22} x_2^2 + \beta_{12} x_1 x_2 + \varepsilon \qquad (2.9)$$

In general, any regression model that is linear in the parameters (the β-values) is a linear regression model, regardless of the shape of the response surface that it generates (Kathleen, Natalia and Jeff, 2004).

Figure 2.5 depicts the optimization outcomes in Minitab 17 using the response surface method, according to Annisa, Hariyadi, and Jauhar (2019). The proportions for each independent variable that yield the best response variable are displayed in the graph's results. Amounting to 121.53 gr, the variable Silica Fume is at a level of 0.0510. The sand variable is at level 0.0493, which is 1409.86gr, and the cement variable is at level 0.2888, or 514.65 gr. The optimization's results demonstrate the ideal composition that a mortar can achieve when silica fume is added in amounts up to 23.6%.

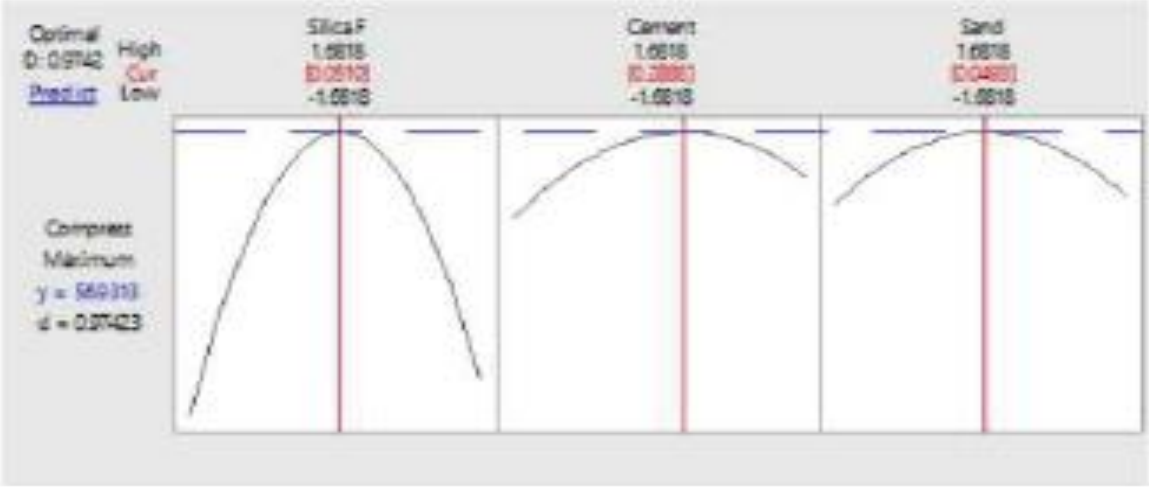

Figure 2.5: Optimum plots for the proportions of each independent variable
Source: Annisa *et al*. (2019)

This response surface optimization method's output is afterwards retested to determine the quality confirmation design generated. Based on the optimization results, this confirmation design was created with three samples of different material composition. This confirmation

design, which involved examining the mortar's physical and mechanical characteristics, was also used to evaluate the mortar's absorption and pH levels.

The results of evaluating the mortar combination with 23.6% silica fume obtained from the optimal plot were compared with mortar without silica fume content, according to Annisa *et al.* (2019). The compressive strength of mortar without additional silica fume components is 25.6 MPa. The confirmatory mortar optimization results' compressive strength value improved to 55.8 MPa. The amount is depicted in Figure 2.6.

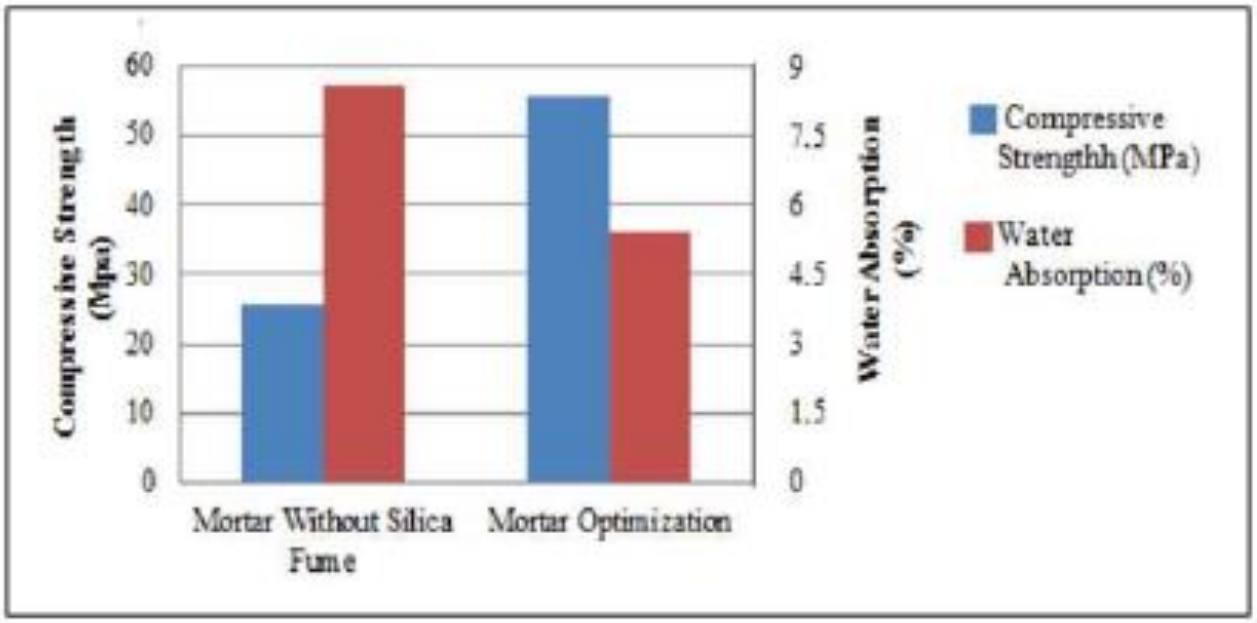

Figure 2.6: Comparison of mortar testing result
Source: Annisa *et al.* (2019).

According to Annisa *et al.* (2019), the 56-day-old specimen is submerged in water for 24 hours to perform the water absorption test on mortar. After the surface is dry and there are no more water drips, the weight of the mortar is calculated. The evaluated item is then placed in an oven set at 1100 degrees for 24 hours before being weighed once more. Figure 2.7 contrasts a mortar without silica fume with one that has been improved by including 23.6% silica fume. Mortar developed using response surface technologies can absorb water up to 5.43% less efficiently than

silica mixes with an absorptive capacity of 8.84%. Table 2.14 displays the outcomes of a 56-day mortar optimization.

Table 2.14: Results of absorption test on mortar

S/N	Silica Fume (gr)	Cement (gr)	Sand (gr)	SSD (gr)	SD (gr)	WA (%)	Average WA (%)
1	0	600	1400	306.53	279.34	8.87	
2	0	600	1400	311.75	283.99	8.905	8.848
3	0	600	1400	294.24	268.44	8.768	
4	121.53	514.66	1409.86	299.7	285.89	4.608	
5	121.53	514.66	1409.86	297.56	281.23	5.488	5.438
6	121.53	514.66	1409.86	293.75	275.48	6.22	

SSD: Saturated Surface Dry SD: Surface Dry WA: Water Absorption
Source: Annisa *et al.* (2019).

Ayobami, Bamidele, Joseph, Tolulope, and Samuel (2019) shown that adding metakaolin to concrete improves strength up to 10% replacement. The compressive strength began to decrease as more was added. The highest strength was found with 10% metakaolin addition across all ages. However, the strength was remained higher than the control at 15% and 20% (Figure 2.10). However, at percentages more than 20%, there was a loss in compressive strength when compared to 0% metakaolin. The projected R-Squared of 0.766 agrees reasonably with the "Adjusted R Squared" of 0.809 in Table 2.15 "Adeq. Precision" measures the signal-to-noise ratio. A ratio greater than 4 is preferred. The model ratio of 15.712 suggests that the signal is adequate. This model can be used to forecast the effect of metakaolin, cement, and age on metakaolin concrete compressive strength.

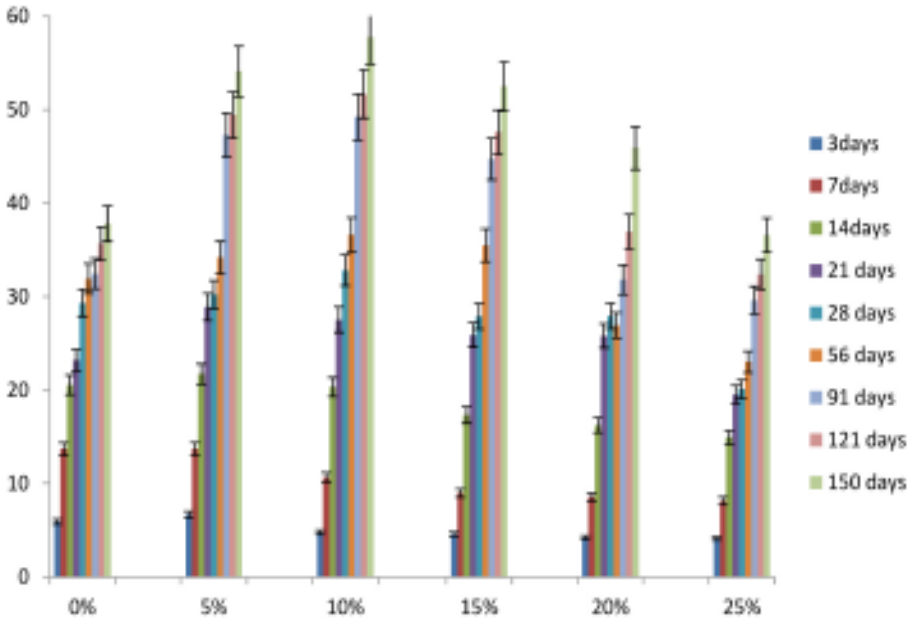

Figure 2.7: Compressive Strength of dehydroxylated kaolinitic clay versus age
Source: Ayobami *et al.*, (2019).

Table 2.15: ANOVA for response surface (quadratic model)

Source	**Sum of Squares**	**Df**		**F value**	**Prob> F**	
Model	2074.283	9	230.4759	26.00548	<0.0001	Significant
A	623.8372	1	623.8372	70.38995	<0.0001	
B	0.449426	1	0.449426	0.05071	0.8229	
C	0.750283	1	0.750283	0.084657	0.7724	
A^2	472.1313	1	472.1313	53.27239	<0.0001	
B^2	0.008533	1	0.008533	0.000963	0.9754	
C^2	0.006395	1	0.006395	0.000722	0.9787	
AB	38.7879	1	38.7879	4.376588	0.0422	
AC	46.28101	1	46.28101	5.222064	0.0272	
BC	0.000165	1	0.000165	0.0000186	0.9966	
Residual	389.9539	44	8.862589			
Cor Total	2464.237	53				

Source: Ayobami *et al.*, (2019).

The model equation in terms of actual factor is given in Equation (2.5) as follows;

$$\text{Compressive Strength} = -184.70 + 1.60\,A - 0.14\,B + 813.61\,C - 1.61\,A^2 + 1.77\,B^2 - 768.30\,C^2 + 4.08\,A{\cdot}B - 3.19\,A{\cdot}C - 0.35\,B{\cdot}C \quad (2.5)$$

Where: A – age of concrete,

B – metakaolin,

C – cement.

As shown in Equation (2.5), the addition of cement and metakaolin had a good influence on the strength qualities of the created self-compacting concrete. The normal plot of residuals on the experimental run fits the predicted values well. Figure 2.8 indicates that there were no outliers in the experimental runs. Figure 2.8 also depicts the model's predictability plot to account for future events. The predicted data points clustered around the actual data points, indicating less over-fitting, and yielded a predicted R-squared value of 0.767.

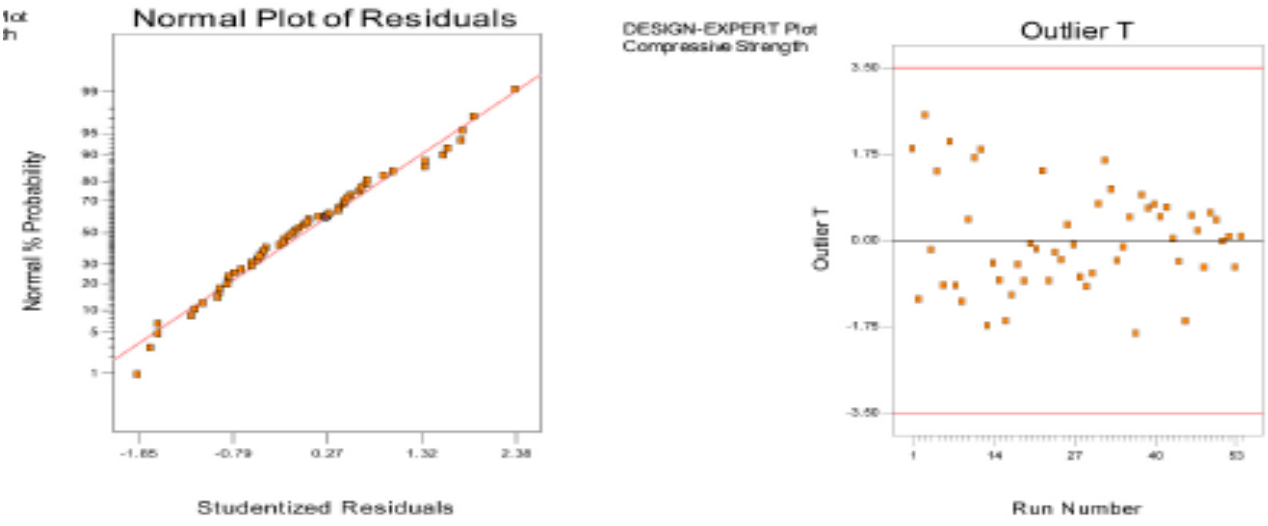

Figure 2.8: Diagnostic plots of residuals and outlier against experimental runs

Source: Ayobami *et al.*, (2019).

2.9 Related review works done on Metakaolin

Bucher, Diederich, Escadeillas, and Cyr (2017), found that the presence of metakaolin can result in adequate fly ash and slag concrete strength when comparing the service life of metakaolin-based concrete exposed to carbonation with blended cement containing fly ash, blast furnace slag, and limestone filler, cement, and concrete.

Mohammed and Gomathi (2017) researched the strength qualities of concrete using metakaolin (Mk), and discovered that 10% Mk is the best dosage that may be used in conjunction with a superplasticizer. They also discovered that the best proportion of Mk is 10% for split tensile strength, flexural strength, and modulus of elasticity. The addition of Mk to concrete reduced workability, which had to be compensated for by the inclusion of superplasticizers.

In Nigeria, Ibrahim, Okoli, and Dahiru (2016) compared the characteristics of regular portland cement (OPC) concrete with binary concrete including Mk produced from Kankara kaolin. They discovered that binary concrete containing Mk had a 25.8% lower workability than OPC. They discovered that adding Mk to binary concrete resulted in faster early age strength development than ordinary OPC concrete and increased compressive and tensile strength.

In order to determine whether Nigerian kaolin clay could be used as concrete material, Baba and Usman (2011) studied the thermal treatment of Kankara kaolin clay to produce metakaolin as a partial replacement of cement in the production of concrete and the parameters for converting Kankara kaolin clay to Mk. It was discovered that Kankara kaolin can partially substitute cement and that the ideal thermal condition for calcining it was 6500C for 90 minutes. They also came to the conclusion that 10% is the ideal replacement rate for cement when using Kankara metakaolin.

The advantages of metakaolin in high performance concrete (HPC) were examined by Kurtins (2011). He claims that because of its large surface area and reactivity, metakaolin boosts the compressive strength, impermeability, and durability of concrete.

According to Rafat and Juvas (2008), the extra cementing ingredient has become a crucial component of concrete mix designs for high strength and high performance. Water penetration into concrete by capillary action is reduced when cement is partially replaced with metakaolin. The mechanical and long-term strength qualities of cement paste, mortar, and concrete are improved with metakaolin. The plastic density of the mixtures was reduced by partially replacing the cement.

Rafat and Juvas (2008) claim that metakaolin has a filler effect that enhances the pozzolanic reaction and speeds up cement hydration. In this investigation, heated metakaolin that has been mixed with concrete is exposed. The strength of these specimens at 100^0C increases as they are heated to higher temperatures like 100^0C, 200^0C and 300^0C.

According to Abdul Razak (2005), adding 5%, 10%, or 15% of metakaolin to cement has a positive impact on the mechanical qualities of the material.

Khatib and Hibbert (2005) studied the effects of substituting slag and metakaolin for cement on the characteristics of concrete. Twelve mixes were looked at, four of which contained 0% Mk and slag contents ranging from 0% to 80% of the total cementitious materials (CM), four of which contained 10% Mk and slag contents ranging from 0% to 70% of the CM, and the last four of which contained 20% Mk and slag contents ranging from 0% to 60% of the CM. Comparing mixtures with 30% and 50% slag to mixes without Mk, the concrete strength increased at 10% Mk, especially at 7 and 14 daysThe pace of strength gain slows down after 28 days. Strength

trends at 20% Mk are comparable to those at 10%. Additionally, the strength values obtained at 10%Mk are not appreciably higher, indicating that Mk replacement above 20% may not be required. For all mixes with and without slag, it was discovered that the flexural strength increased in the presence of Mk, and the trend in the flexural strength after 90 days is comparable to that of compressive strength.

Due to the strong pozzolain activity of MK, Frias, Sanchez de Rojas, and Cabrera (2000) found that MK mortars provide a modest heating rise when compared to a mortar made entirely of Portland cement. When it came to hydration heat, MK-blended mortar had behaviors that were more similar to those of silica fume than fly ash at different percentages.

According to Fries (2000), replacing 15% of the cement with more Metakaolin boosts the strength of concrete. Following then, concrete's tensile and compressive strengths will decline.

Abdul Razak (2005) employed metakaolin and silica fumes at 5%, 10%, and 15% by mass as substitutes for cement in his investigation. The investigation came to the conclusion that 97% of regarded strengths are within 5% of real value at ages 28 days and more.

CHAPTER THREE

MATERIALS AND METHODS

3.1 Materials

The materials utilized for producing concrete used for the experimental study areas follows; Portland cement, kaolin, river sand, quarry dust, 20mm granite chippings, superplasticizer and water.

3.1.1 Kaolin

The kaolin samples were sourced in a natural state from Umuariaga–Umudike in Ikwuano Local Government Area of Abia State, Nigeria, as shown in Figure 3.1. The soft and greyish lump samples were sun dried for 3 days and broken down into smaller particles by using an electric grinding machine, then sieved using a 150μmm sieve in the laboratory before the calcination. The quartering method was used to place 5kg of the grounded samples in a Muffle furnace in batches due the furnace size. The samples were treated at temperatures of 650^0C, 750^0C and 850^0C for 90mins to produce the metakaolin which is a pozzolanic material that was used for making concrete. After the heating, the samples were cooled to room temperature at ambient conditions to avoid crystallization of amorphous metakaolin. Plate 3.1 shows the extraction of the kaolin from the natural ground, Plate 3.2 presents the calcination process of the kaolin, while Plate 3.3 displays the sample of metakaolin produced.

3.1.2 Portland cement

The cement used for this research was the BUA (CEM II A-L 42.5N) ordinary portland cement that conforms to BS EN 197-1 (2011) and was obtained in 50 kg bags from a retailer's shop

located at Timber market, Naze, Owerri, Imo state. Plate 3.4 depicts a sample of the Portland cement.

3.1.3 River sand

The river sand was obtained from Otammiri at Nekede, Owerri West in Imo state. The moisture content, particle size distribution, specific gravity and bulk density tests were carried out. The sample was kept in saturated surface dry (SSD) condition according to BS 812:109 (1990) before used in the concrete production.

3.1.4 Quarry dust

The quarry dust was obtained from a quarry site at Ishiagu, Ivo Local Government Area in Ebonyi state. It was kept in a saturated surface dry (SSD) condition according to BS 812:109 (1990) for the concrete production. The particle size distribution was determined to ensure the elimination of unwanted size of the materials. Similarly, the moisture content, specific gravity and bulk density were carried out so as to determine the soundness of the material. Plate 3.5 presents a sample of the quarry dust adopted in making the concrete.

3.1.5 Granite chippings

The coarse aggregate in the form of granite chippings was obtained from a quarry site at Ishiagu, Ivo Local Government Area, Ebonyi state. The moisture content test was carried out and it was kept in a saturated surface dry (SSD) condition in agreement with BS 812:109 (1990). The particle size distribution, specific gravity and bulk density tests were also conducted. The nominal size of the granite chippings used was 20mm. Plate 3.6 shows sample of the chipping.

3.1.6 Superplasticizer

A high performance water reducing and retarding superplasticizer COSTARMIX 200R which is of Type D and G in consonance with ASTM-C494/C494-81 (2017), was purchased from Lagos state. It is a polymer based high ranged water reducing admixture designed to produce high slump concrete with increase in workability, durability and low permeability of the metakaolin blended concrete.

3.1.7 Water

The water used to activate the hydration of the binder was one fit for drinking. It was used according to the water/binder ratio of 0.4 to produce the concrete specimens.

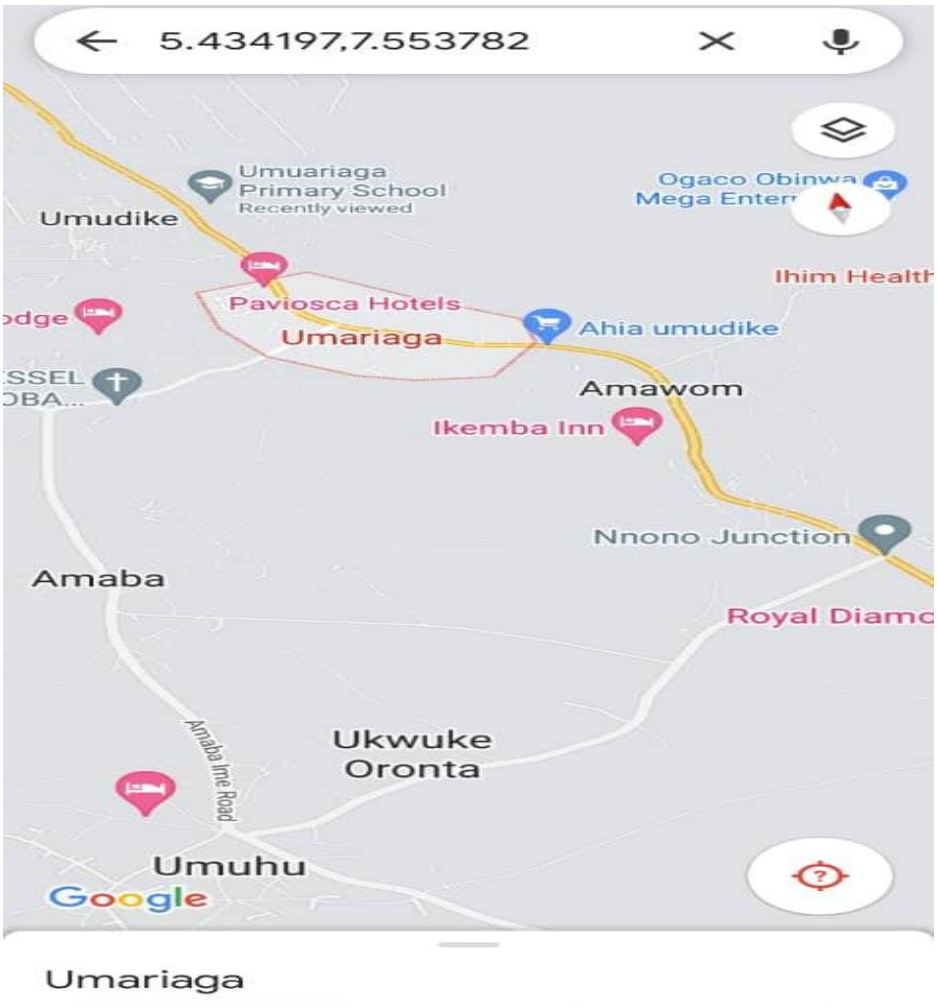

Figure 3.1: Google map showing the Umuariga-Umudike community in Abia State, Nigeria.

Plate 3.1: Kaolin Extraction

Plate 3.2: Calcinations of kaolin

Plate 3.4: Ordinary Portland cement

Plate 3.3: Sample of Metakaolin

Plate 3.5: Sample of quarry dust

Plate 3.6: Sample of granite chipping

3.2 Methods

The various tests to determine the properties of the constituents of the concrete, fresh and hardened concrete, and on the experimentally generated results are all are discussed in this section.

3.2.1 Characterization of the materials used in the research

The chemical property of the metakaolin at different temperature and the various properties of the fine and coarse aggregates used in the study were determined as follows:

3.2.1.1 Determination of the chemical properties of metakaolin

Samples of metakaolin obtained by calcining kaolin at various temperature of 650^0C, 750^0C and 850^0C using an electric muffle furnace, were subjected to the X-Ray Fluorescence (XRF) test corresponding to the ASTM C 618-94 (1994). This test was done in order to determine the oxides compositions of the metakaolin. X-rays produced by an X-ray tube of the XRF spectrometer were used to irradiate the metakaolin samples, resulting to the elements present in the samples emitting fluorescent X-rays with different energies. A component of the spectrometer called energy-dispersive (EDXRF) instrument was used to measure these energies, consequently identifying and quantifying the elements present in the metakaolin samples (Biljana Alexandra and Ljiljana 2010).

3.2.1.2 Determination of the specific gravity of the metakaolin

The specific gravity (G_S) of the metakaolin was determined by using the pycnometer method in accordance with BS 1377-2 (1990). The main apparatus used were the density bottle, stopper,

funnel, spatula and weighing balance. After the procedure was carried out, the specific gravity of the metakaolin was determined by applying Equation (3.1).

$$\text{Specific Gravity } (G_S) = \frac{W_2 - W_1}{(W_4 - W_1)(W_3 - W_1)} \quad (3.1)$$

Where: W_1 = Weight of density bottle

W_2= Weight of density bottle + Sample

W_3 = Weight of density bottle + Water (full) + Sample

W_4= Weight of density bottle + Water (full)

3.2.1.3 Moisture content of the aggregates

The moisture content test was carried out on the river sand, quarry dust and granite chipping according to the BS 812-109 (1990) and ASTM D2016-74 (1987). A clean container was weighed to the nearest 0.1g as m_1 . The mass of the coarse and fine aggregates used were 1000g and 0.5g respectively and recorded as m_2.They were placed with the container in an oven at a temperature of 105 ± 5^0C for 24hrs. The mass of the oven dry samples were weighed and recorded as m_3. The Equation 3.2 was then applied in determing the moisture content of the various aggregates.

$$MC = \frac{m_2 - m_3}{m_3 - m_1} \times 100\% \quad (3.2)$$

Where: MC = Moisture content expressed as a percentage.

m_1 = mass of container (g)

m_2 = mass of container and wet sample (g)

m_3 = mass of container and dry sample (g).

3.2.1.4 Water absorption of the aggregates

Using the pycnometer method according to BS 812:2 (1995), 1kg of the samples were used for the test accordingly. The samples were thoroughly washed, in the 75μm and 5mm sieve for the fine and coarse aggregates respectively, to remove finer particles. The aggregates were spread out and exposed to sunlight until all visible films of water were removed. They were independently weighed and the weight obtained was recorded as 'A'. The aggregates were placed on a tray and put into an oven at 105 ± 5^{0C} for 24hrs. The sample was cooled in an airtight container before being weighed. The weight obtained was recorded as 'D'. The water absorption for the three aggregates were then calculated using the Equation (3.3).

$$\text{Water absorption}(\%) = \frac{100(A-D)}{D} \quad (3.3)$$

Where A= mass of the saturated surface dry aggregates in air (g)

D= mass of the oven dry aggregates in air (g)

3.2.1.5 Determination of the specific gravity of the aggregates

The specific gravity (G_S) of the aggregates were aslo determined by using the pycnometer method in accordance with BS 1377:2 (1990). The apparatus and procedures followed are similar to those discussed in section 3.2.1.2. Equation (3.1) was also used to determine the specific gravity of the river sand, quarry dust and granite chippings respectively.

3.2.1.6 Particle size distribution test on the aggregates

The quantification of the percentage of each particle size that pass through sieves with square openings of varying standard apertures (or diameters) results in the particle size distribution of aggregates. A 2000g sample of aggregate is subjected to a sieve analysis to establish the grade. Several standard sieves are nested or piled on top of one another, with the aperture size rising from bottom to top. The sieves are typically shaken or vibrated to help a sample of aggregate move from the top to the bottom. Procedures for the test are given in accordance to BS 812-103 (1990). Highlights of this procedure are shown in Plates 3.7

The coefficient of uniformity (C_U) and coefficient of curvature (C_C) were calculated using the Equation (3.4) and Equation (3.5) respectively.

$$C_U = \frac{D_{60}}{D_{10}} \tag{3.4}$$

$$C_C = \frac{D_{30}^2}{D_{60} \times D_{10}} \tag{3.5}$$

Where D_{10} = The size at which 10% of the particles are finer.

D_{30}= The size at which 30% of the particles are finer.

D_{60}= The size at which 60% of the particles are finer.

3.2.1.7 Bulk density test on aggregates

This was determined in accordance with BS 812: Part 2 (1995) for coarse and fine aggregates used for this research. The relationship given in Equation (3.6) was used to determine the bulk density of the samples:

$$\text{Bulk Density } (\rho) = \frac{W_1 - W}{V} \quad (3.6)$$

Where W_1 = Weight of container + sample

W = Weight of empty container

V = Volume of container.

3.2.1.8 Specific gravity of superplasticizer

Similar to the metakaolin and aggregates, specific gravity test was conducted on the COSTARMIX 200R superlasticizer used in making the concrete. Specifications agreeing with the BS 1377-2 (1990) was followed. Equation (3.1) was adapted in determining the specific gravity of the superlasticizer.

3.2.2 Cement-metakaolin blended concrete

The concrete samples used for this study were prepared based on the properties of the various materials as well as the mix proportions. The properties and characteristics of the concrete are functions of the constituent materials' properties as well as the various mix proportions.

3.2.2.1 Mix design of the cement-metakaolin blended concrete

The concrete mix design was prepared to achieve a compressive strength of 30 MPa based on the properties and proportion of the mix components as shown in appendix A. The mix was prepared with a water/binder ratio of 0.4 according to Building Research Establishment Manual (1997), for both the river sand and quarry dust concrete. To improve the workability of the mix, superplasticizer with a dosage 1.3% of the binder was used. The design gave a mix proportion of

1: 1.68: 2.32 for river sand and 1: 1.42: 2.04 for quarry dust concrete. The steps carried out for the mix design for the river sand and quarry dust are presented in appendices A1 and A2 respectively. The proportions of the components for the various replacement levels are presented in Table 3.1.

Table 3.1: Mix proportioning of the cement-metakaolin blended concrete

River sand Concrete								Quarry dust concrete						
S/N	**Mix ID**	**OPC (kg/m^3)**	**MK (kg/m^3)**	**FA (kg/m^3)**	**CA (kg/m^3)**	**Water (kg/m^3)**	**SP (% binder)**	**MIX ID**	**OPC (kg/m^3)**	**MK (kg/m^3)**	**FA (kg/m^3)**	**CA (kg/m^3)**	**Waetr (kg/m^3)**	**SP (% binder)**
1	$0\%MK_{RS}$	475	0	798	1102	190	1.3	$0\%MK_{QD}$	525	0	744.15	1070.85	210	1.3
2	$5\%MK_{RS}$	451.25	23.75	798	1102	190	1.3	$5\%MK_{QD}$	498.75	26.25	744.15	1070.85	210	1.3
3	$10\%MK_{RS}$	427.5	47.5	798	1102	190	1.3	$10\%MK_{QD}$	472.5	52.5	744.15	1070.85	210	1.3
4	$15\%MK_{RS}$	403.75	71.25	798	1102	190	1.3	$15\%MK_{QD}$	446.25	78.75	744.15	1070.85	210	1.3
5	$20\%MK_{RS}$	380	95	798	1102	190	1.3	$20\%MK_{QD}$	420	105	744.15	1070.85	210	1.3
6	$25\%MK_{RS}$	356.25	118.75	798	1102	190	1.3	$25\%MK_{QD}$	393.75	131.25	744.15	1070.85	210	1.3
7	$30\%MK_{RS}$	332.5	142.5	798	1102	190	1.3	$30\%MK_{QD}$	367.5	157.5	744.15	1070.85	210	1.3
8	$35\%MK_{RS}$	308.75	166.25	798	1102	190	1.3	$35\%MK_{QD}$	341.25	183.75	744.15	1070.85	210	1.3
9	$40\%MK_{RS}$	285	190	798	1102	190	1.3	$40\%MK_{QD}$	315	210	744.15	1070.85	210	1.3
10	$45\%MK_{RS}$	261.25	213.75	798	1102	190	1.3	$45\%MK_{QD}$	288.75	236.25	744.15	1070.85	210	1.3
11	$50\%MK_{RS}$	37.5	237.5	798	1102	190	1.3	$50\%MK_{QD}$	262.5	262.5	744.15	1070.85	210	1.3

3.2.2.2 Production of the cement-metakaolin blended concrete cube specimen

The procedures adopted for production of the blended concrete was done according to BS 1881-125 (1986) and BS 1881-108 (1983), and the steps are listed below:

i. The production of the grade C30 concrete was done using 150×150×150mm size of concrete cube mould, with cement partially replaced with metakaolin for both the river sand and quarry dust concrete respectively., in accordance to

ii. A total of ten (10) different percentage replacements of portland cement with metakaolin were investigated. These replacement values ranged from 5% to 50% at interval of 5%. A control point of 0% replacement was adopted.

iii. Using Table 3.1, the proportions of the river sand, cement and the metakaolin were weighed and thoroughly hand-mixed together before the addition of the granite chippings. Then, the water and superplasticizer were added in their appropriate quantities. The blended concrete was poured in three layers and tamped with 35 strokes in three different cube moulds for each percentage of replacement, this was done for the 650^0C, 750^0C and 850^0C metakaolin samples. The same process was repeated for the blended concrete with quarry dust as fine aggregate. Plate 3.9 shows the mixing of the constituents of the blended concrete.

iv. The workability of the freshly mixed concrete was checked by carrying out the slump test as depicted in Plate 3.10.

v. The blended concrete was de-moulded after 24hours and cured in a water tank under room temperature for 7 and 28 days as shown in Plate 3.11 and Plate 3.12.

vi. The number of samples produced for compressive strength, young modulus and water absorption are presented in Table 3.2.

Table 3.2 Summary of the number of cubes produced

Tests	**Specimen types**	**Temperature**		
		650°C	**750**°C	**850**°C
Compressive strength	Cubes	132	132	132
Young Modulus	Cubes	-	-	-
Absorption capacity	Cubes	66	66	66
Sub total		198	198	198
Total		**594**		

3.2.2.3 Slump test on the fresh cement-metakaolin blended concrete

The slump test was carried out according to BS 1881,102 (1983) by filling a specified mould of height 300mm having diameter at the top and base as 100mm and 200mm respectively, with freshly mixed blended concrete and measuring the slump after the removal of the mould. The mould is firmly held on a sampling tray and then filled with fresh concrete in three layers with approximately one–third of the height of the mould. Each layer is tamped with 25 strokes uniformly distributed using a 16mm diameter and 600mm tamping rod. The mould is carefully removed vertically after it is fully filled with the fresh concrete. A measuring rule is used to ascertain the difference between the height of the mould and the highest point of the sample to the nearest 5mm after the mould has been removed. Values obtained are illustrated in Table 4.10a and Table 4.10b. Plates 3.10 clearly describes the process.

3.2.2.4 Bulk density test on the hardened cement-metakaolin blended concrete

After 28 days curing, one set (3 cube) of concrete specimen were taken out from storage for density test in accordance to clause 6.2.3 in BS 1881-114: 1983. These specimens were prepared in SSD (Saturated Surface Dry) condition by removing water from the surfaces. Then SSD mass

of samples in air (m) was measured and the volume of the samples were calculated from their dimension in m^3. The density of concrete was calculated using Equation (3.7):

$$\rho = \frac{m}{v} \tag{3.7}$$

Where ρ = density of the hardened concrete

m = mass of the saturated sample in air (kg)

v = volume of the samples (m^3) (calculated from their cross-sectional dimension and height).

3.2.2.5 Compressive strength test on the hardened cement-metakaolin blended concrete

A total of 132 cubes of the concrete were produced from cement blended with metakaolin calcinated at 650^0C, 750^0C and 850^0C respectively. These consist of three replicates for each percentage of replacement for the river sand and quarry dust blended concrete. The concretes were cured in a curing tank containing distilled water at room temperature for 7 and 28 days respectively. After curing, the samples were surfaced wiped before carefully placing them in the testing machine as shown in Plate 3.13. The compressive strength were obtained in accordance with BS 1881-116 (1983) and the values calculated from Equation (3.8):

$$F_{cu} = \frac{crushing\ load(N)}{surface\ area(A\ mm^2)} \tag{3.8}$$

Where F_{cu} = Compressive strength of the hardened concrete.

The percentage of compressive development from 1day to 7days and from 7days to 28days for all the samples produced were determined using Equation (3.9) and Equation (3.10) respectively.

$$\%\ of\ compressive\ strength\ development\ (1day - 7days) = \frac{F_{cu(7days)}}{F_{cu}(C30)} \times 100 \qquad (3.9)$$

where; F_{cu} (7days) = Compressive strength of the concrete at 7days

F_{cu}(C30)= Compressive strength of concrete grade 30 (30MPa)

$$\%\ of\ compressive\ strength\ development(7days - 28days) = \frac{F_{cu(28days)} - F_{cu(7days)}}{F_{cu(7days)}} \times 100$$

(3.10)

where; F_{cu}(7days) = Compressive strength of the concrete at 7days

F_{cu}(28days)= Compressive strength of concrete at 28days

3.2.2.6 Determination of young modulus of elasticity

The young modulus of elasticity (Ec) was obtained from the compressive strength results according to ACI building code 318 with a concrete unit weight between 1500 kg/m^3 and 2500 kg/m^3 . The relationship is given in Equation (3.11) as shown:

$$E_c = \gamma_c^{1.5}\ 0.043 F_c^{1/2} \qquad (3.11)$$

E_c = young modulus of elasticity (MPa)

γ_c = unit weight of concrete (kg/m^3)

F_{cu} = 28 days compressive strength

3.2.2.7 Water absorption test on hardened cement-metakaolin blended concrete

The water absorption capacity of the hardened concrete was determined according to BS 812-2(1975).Three samples were placed in an oven for 72hours at 105 ± 5^{0C} .The samples were removed after drying and weighed and the weights were recorded as w_d. The samples are then immersed in a water tank and removed after 1hour. Samples were surface dried using a cloth before being weighed again. This new weight was recorded as w_w. The water absorption of the samples were then calculated using Equation (3.12):

$$\text{Water absorption} = \frac{Ww-WD}{WD} \times 100\% \quad (3.12)$$

where;

W_W = wet cubes,

W_D = dried cubes

Plate 3.14 shows some of the test procedures.

3.2.3 Development of the Multivariate Regression models using Response surface methodology

The response surface method (RSM) is seen as a powerful approach for resolving complex problems through the development of statistical interaction between factors (independent variables) and responses (dependent variables). The process of developing predictive models through RSM is initiated with the collection of the experimental data and the responses using the historical design (HD) and performing experimental programs. The independent variables used were Mass of cement (X_1), and mass of metakaolin (X_2) with compressive strength, young modulus and water absorption capacity as dependent variables. The maximum and minimum limits for the independent variables were stipulated for both the river sand concrete and quarry

dust concrete as shown in Table 3.3. The eleven (11) experimental runs were incorporated into the design and analyzed to obtain the multivariate regression models for the dependent variables used in the study. The flow chart depicting the process for the multivariate regression analysis using response surface methodology is presented in Figure 3.2.

Table 3.3. Historical Design experimental range

		River sand Concrete		Quarry dust concrete	
Variable	Unit	Minimum value (-1)	Maximum value (+1)	Minimum value (-1)	Maximum value (+1)
Cement	Kg	0.97	1.95	1.08	2.15
Metakaolin	Kg	0	0.97	0	1.08

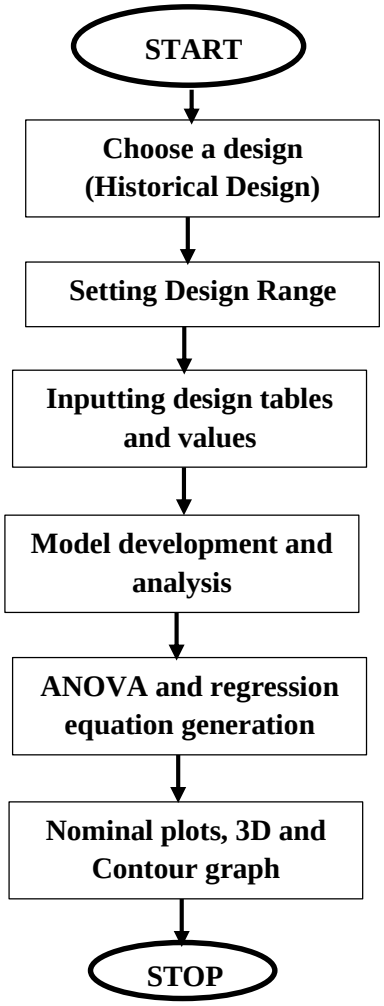

Figure 3.2: Flow chart for the multivariate regression model design using RSM

3.2.4 Model prediction and comparison with experiment results.

The models for the dependent variables were developed from the regression analysis of the dependent variables using the response surface methodology. A second order polynomial equation shown in Equation (3.13) was used to determine the relationships that exist between dependent and independent variables.

$$Y = \beta_0 + \sum_{i=1}^{k} \beta_i x_i + \sum_{i=1}^{k-1} \sum_{j=2}^{k} \beta_{ij} x_i x_j + \sum_{i=2}^{k} \beta_{ii} x_i^2 \qquad (3.13)$$

Where the predicted response (Compressive strength, Young modulus and Water absorption) is represented by Y. The x_i and x_j are independent parameters affecting the dependent responses, while β_0, β_i, β_{ii}, and β_{ij} are the regression coefficients for intercept, linear, quadratic, and interaction terms, respectively; and k is the number of parameters. The experimental values were compared with the predicted values obtained in order to evaluate the accuracy of the model.

3.2.5 Check for adequacy of model predictions using ANOVA

To examine the effects of independent parameters and their mutual interaction, the regression coefficients were used to generate 3-D surface plot from the fitted two factor interaction (2FI) equations. Moreover, the results of the analysis of variance (ANOVA) were developed through the RSM models which was analyzed statistically for future use. For a model to be acceptable, a relative change of less than 0.2 between the adjusted R^2 and predicted R^2, a value of adequate precision greater than four (>4), with a low standard deviation of each response must be obtained (Zahid, Shafiq and Jalal 2018).The Prob > F which should be less than 0.05 is a strong indicator

of a statistically significant model with a 95% confidence level (Subasi, Sahin and Kaymaz, 2016). Moreover, the adequacy of the models were examined to obtained results which was compared with the predicted.

Plate 3.8: Bulk density test

Plate 3.7: Sieve analysis test

Plate 3.9: Mixing of binary concrete

Plate 3.10: Workability Test (Slump test)

Plate 3.11: Moulding and de-moulding of cement-metakaolin blended concrete cubes

Plate 3.12: Curing of cement-metakaolin blended concrete cubes

Plate 3.13: Compressive strength testing of cube samples

Plate 3.14: Cement-metakaolin blended concrete cubes for water absorption test

CHAPTER FOUR

RESULTS AND DISCUSSIONS

4.1 Results

The results presented in this chapter are obtained from the tests carried out on the materials used and concrete samples. They are presented and discussed in this chapter.

4.1.1 Chemical Properties results of metakaolin

The X-ray fluorescence (XRF) test results for the metakaolin treated at 650^0C, 750^0C and 850^0C are presented in Table 4.1. Table 4.2 compares the percentage of the major oxides present in the metakaolin and their requirements according to ASTM C-618:1994.

Table 4.1: Chemical composition of metakaolin produced at different temperatures

Oxides	**Percentage composition (%)**		
	650^0C	750^0C	850^0C
Aluminium oxide (Al_2O_3)	34.54	34.86	35.51
Silicon oxide (SiO_2)	56.50	58.62	55.94
Iron trioxide (Fe_2O_3)	2.82	2.95	2.61
Titanium oxide (TiO_2)	1.34	1.37	1.24
Vanadium oxide (V_2O_5)	0.03	0.03	0.03
Manganese oxide (MnO)	0.03	0.03	0.03
Potassium oxide (K_2O)	0.66	0.65	0.62
Phosphorus Pentoxide(P_2O_5)	0.13	0.14	0.16
Germanium oxide(Ga_2O_3)	0.01	0.01	0.01
Chromium(III)Oxide(Cr_2O_3)	0.02	0.02	0.02

Sulfur Trioxide(SO_3)	0.07	0.07	0.13
Zinc Oxide(ZnO)	0.05	0.06	0.10
Magnesium Oxide(MgO)	1.40	1.83	1.45
Niobium Pentoxide(Nb_2O_5)	0.02	0.02	0.03
Arsenic trioxide(As_2O_3)	0.0020	0.0015	0.0017
Lead(II)Oxide(PbO)	0.02	0.02	0.02
Zirconium dioxide (ZrO_2)	0.11	0.11	0.12
LOI	1.90	1.50	1.10

Table 4.2: Comparism of the major oxides of metakaolin with ASTM C-618 requirement

Metakaolin	T= (SiO_2) + (Al_2O_3) + (Fe_2O_3) (%)	ASTMC-618 **(Class N)** 'T' requirement (%)	(SO_3) content (%)	**ASTM C-618 (Class N) %** SO_3 **requirement**	Moisture Content (MC) **(ClassN)** (%)	**ASTM C-618 %** MC **(ClassN) requirement**
650^0C	93.9	70 (Minimum)	0.07	4.0 (maximum)	Nil	3.0 (maximum)
750^0C	96.4		0.07		Nil	
850^0C	94.1		0.13		Nil	

4.1.2 Specific gravity results of the metakaolin

The test results obtained from Equation (3.1) for the specific gravity of the metakaolin treated with different temperatures are depicted in Table 4.3.

Table 4.3: Summary of results of specific gravity of metakaolin

Temperatures	**Specific gravity (G_S)**
650^0C	2.62
750^0C	2.74
850^0C	2.66

4.1.3 Moisture content results of the aggregates

Table 4.4 presents the test results for the moisture content of the granite chippings river sand and the quarry dust, used as coarse and fine aggregates obtained from Equation (3.2).

Table 4.4: Summary of moisture content results of aggregates

S/No	**Type of aggregate**	**Moisture content (MC) %**			
		MC1	**MC2**	**MC3**	**AV MC (%)**
1	Granite chippings	1.7316	1.4903	2.2113	1.8111
2	River sand	1.5015	2.0905	1.9436	1.9436
3	Quarry dust	2.6400	2.4410	2.5500	2.5437

4.1.4 Water absorption results of the aggregates

Table 4.5 shows the values for water absorption capacity calculated from Equation (3.3) for the various aggregates used for this study.

Table 4.5: Summary of water absorption results of aggregates

S/No	**Type of aggregate**	**Water absorption (WA) %**			
		WA1	**WA2**	**WA3**	**AV WA (%)**
1	Granite chippings	0.3152	0.4703	0.2313	0.3390
2	River sand	0.1015	0.2121	0.1622	0.1586
3	Quarry dust	0.2400	0.2410	0.2130	0.2313

4.1.5 Specific gravity results of the aggregates

The results obtained from Equation (3.1) for the specific gravities of the granite chippings, river sand and quarry dust are presented in Table 4.6.

Table 4.6: Summary of the specific gravity of the aggregates

Temperatures	**Specific gravity (G_s)**
Granite chippings	2.95
River sand	2.75
Quarry dust	2.79

4.1.6 Particle size distribution test results on the aggregates

The sieve analysis results for the particle size distribution carried on the river sand,quarry dust and granite chippings are shown in Table 4.7a , Table 4.7b and Table 4.7c respectively. The grain distribution curves are presented in Figure 4.1a and Figure 4.1b. Equation (3.4) and Equation (3.5) were used to obtain the coefficient of uniformity (C_u) and coefficient of curvature (C_c) respectively.

Table 4.7a: Results of the sieve analysis of river sand

LABORATRY	**CIVIL LAB**	**TEST 1:1**	**CLIENT**
Test date:	**10-Nov-2021**	**River sand**	**Ibe and Co.**
Specification	BS 1377:PART 2:1990		

Pan mass ($g^{m)}$	100		
Initial dry sample mass + ($g^{m)}$	2100	Fine %	0.98
Initial dry sample mass ($g^{m)}$	2000	Acceptance Criteria (Fine)	4(Max.)
Used dry sample mass + ($g^{m)}$	2100	Finess Modulus	3.4
Washed dry sample mass ($g^{m)}$	2000	Acceptance Criteria (FM)	2 - 4
		C_u	15.56

				C_c			2.93	
Sieve Sizes	**Mass of Sieve (g)**	**Mass of Sieve + Sample Retained (g)**	**Mass of Sample Retained (g)**	**Mass of Sample Passing (g)**	**% Retained**	**Cumulative % Retained**	**% Passing**	**BS 882:1973 (Zone 1)**
4.75mm	444.0	444.0	0	200g	0	0	100	90-100
2.36mm	428.8	938.3	509.5	1490.5	25.48	25.48	74.53	60-95
1.18mm	362.2	1038.6	676.4	814.1	33.82	59.3	40.71	30-70
600µm	336.1	660.4	324.3	489.8	16.22	75.52	24.49	15-34
300µm	321.8	606.9	285.1	204.7	14.26	89.78	10.24	5-20
150µm	281.7	414.6	132.9	71.8	6.65	96.43	3.59	0-10
75µm	263.6	315.8	52.2	19.6	2.61	99.04	0.98	-
Pan	243.7	263.3	19.6	0	0.98	100	0	-
TOTAL			2000					

Table 4.7b: Results of the sieve analysis of quarry dust

LABORATRY	**CIVIL LAB MOUAU**	**TEST 1:1**	**CLIENT**
Test date:	**17-NOV-2021**	**Quarry dust**	Ibe and Co
Specification	BS 1377:PART 2:1990		

Pan mass	(g^m)	100		
Initial dry sample mass +	(g^m)	2100	Fine %	5.62
Initial dry sample mass	(g^m)	2000	Acceptance Criteria (Fine) %	16 (Max)
Used dry sample mass +	(g^m)	2100	Fineness Modulus	3.14
Washed dry sample mass	(g^m)	2000	Acceptance Criteria (FM)	2-4
			C_u	12.31
			C_c	2.25

Sieve size (mm)	**Mass of sieve size (g)**	**Mass of sieve + sample retained (g)**	**Mass of sample retained**	**Mass of sample passing (g)**	**percentage retained**	**Cumulative percentage retained**	**(%) passing**	**BS 882:1973 Zone1**
4.75	444.0	444.0	0	2000	0	0	100	90-100
2.36	428.8	909.14	480.34	1519.66	24.02	24.02	75.98	60-95
1.18	362.2	871.38	509.18	1010.48	25.46	49.48	50.52	30-70
600µm	336.1	735.58	399.48	611	19.97	69.45	30.55	15-34
300µm	321.8	585.38	263.58	347.42	13.18	82.63	17.37	5-20
150 µm	281.7	402.14	120.44	226.98	6.02	88.65	11.35	0-10
75µm	263.6	378.14	114.54	112.44	5.73	94.38	5.62	-
PAN	243.7	356.14	112.44	0	5.62	100	0	-
			2000					

Table 4.7c: Results of the sieve analysis on granite chippings

LABORATRY	**CIVIL LAB**	**TEST 1:1**	**CLIENT**
Test date:	**10-Nov-2021**	**Granite**	**Ibe and Co.**

Specification	BS 1377:PART 2:1990		
Pan mass (g^m)	100		
Initial dry sample mass + (g^m)	2100	Fine %	-
Initial dry sample mass (g^m)	2000	Acceptance Criteria (Fine)	-
Used dry sample mass + (g^m)	2100	Finess Modulus	5.67
Washed dry sample mass (g^m)	2000	Acceptance Criteria (FM)	5.5-8.0
		C_u	2.11
		C_c	1.1

Sieve size (mm)	**Mass of sieve size (g)**	**Mass of sieve + sample retained (g)**	**Mass of sample retained (g)**	**Mass of sample passing (g)**	**percentage retained**	**Cumulative percentage retained**	**(%) Passing**
28.00	543.9	543.9	0	2000	0	0	100
19.05	477.3	982.9	505.6	1494.4	25.28	25.28	74.72
13.20	489.3	1320.8	831.5	662.9	41.575	66.86	33.15
11.20	655.6	942.9	287.3	375.6	14.365	81.22	18.78
9.50	448.1	717.6	269.5	106.1	13.475	94.695	5.31
6.70	481.3	573.3	92	14.1	4.6	99.295	0.71
4.76	444.0	448.7	4.7	9.4	0.235	99.53	0.47
PAN	243.7	253.1	9.4	0	0.47	100	0
			2000				

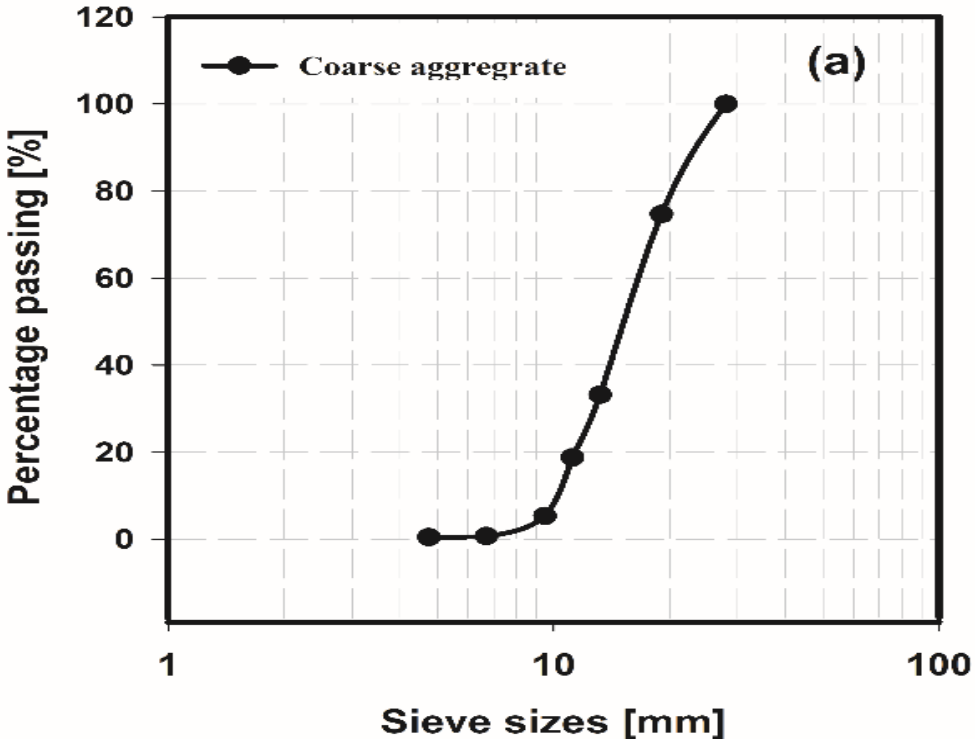

Figures 4.2a: Particle size distribution for coarse aggregates

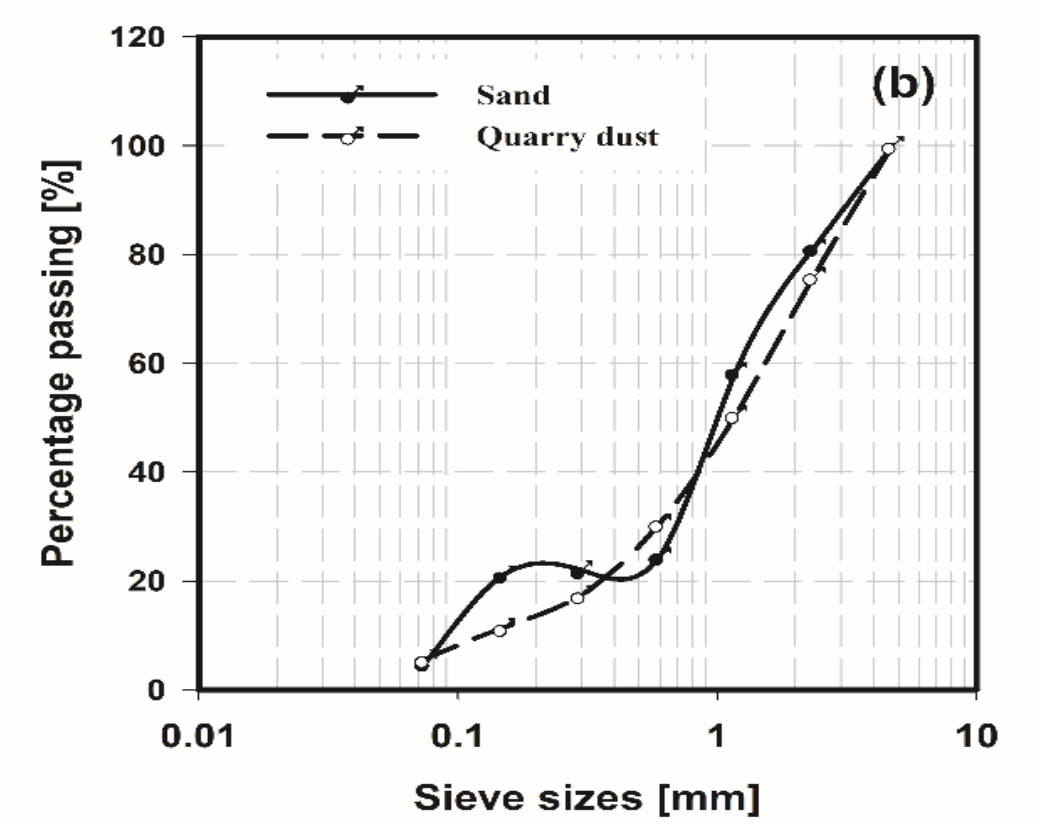

Figures 4.1b: Particle size distribution for fine aggregates

4.1.7 Bulk density test results on aggregates

Table 4.8 presents the results of the bulk densities of the granite chippings, river sand and quarry dust obtained from Equation (3.6).

Table 4.8: Summary of the bulk density results on aggregates

S/No	Type of aggregate	Bulk density (ρ) (kg/m^3)	
		Compacted	Un-compacted
1	Granite chippings	1310	1192
2	River sand	1411	1248
3	Quarry dust	1695	1491

4.1.8 Specific gravity result of the superplasticizer

The specific gravity result for the superplasticizer calculated using Equation (3.1) is shown in Table 4.9.

Table 4.9: Specific gravity of the superlasticizer

Superplasticizer	**Specific gravity (G_S)**
COSTARMIX 200R	1.2

4.1.9 Slump test result on the fresh cement-metakaolin blended concrete

The slump test results for the workability of the fresh cement-metakaolin blended concrete for both river sand and quarry dust are presented in Table 4.10a and Table 4.10b respectively.

Table 4.10a: Slump values of fresh concrete produced with river sand as fine aggregate

Specimen (Percentage replacement of cement with MK)	**Slump values 650^0C (mm)**	**Slump values 750^0C (mm)**	**Slump values 850^0C (mm)**
0%MK_{RS}	112	112	112
5%MK_{RS}	111	110	110
10%MK_{RS}	108	110	109
15%MK_{RS}	105	108	107
20%MK_{RS}	98	103	101
25%MK_{RS}	94	101	96
30%MK_{RS}	80	89	85
35%MK_{RS}	64	72	68
40%MK_{RS}	32	45	40
45%MK_{RS}	26	37	30
50%MK_{RS}	21	24	21

Table 4.10b: Slump values of fresh concrete produced with quarry dust as fine aggregate

Specimen (Percentage replacement of cement with MK)	**Slump values 650^0C (mm)**	**Slump values 750^0C (mm)**	**Slump values 850^0C (mm)**
0%MK_{QD}	98	98	98
5%MK_{QD}	92	96	94
10%MK_{QD}	91	95	94
15%MK_{QD}	88	93	90
20%MK_{QD}	85	91	88
25%MK_{QD}	78	87	83

30%MK_{QD}	63	74	69
35%MK_{QD}	56	67	62
40%MK_{QD}	40	48	47
45%MK_{QD}	29	36	32
50%MK_{QD}	18	24	21

4.1.10 Bulk density test results on the hardened cement-metakaolin blended concrete

The bulk density results on the hardened cement-metakaolin blended concrete was obtained using Equation (3.7) and presented in Table 4.11.

Table 4.11: Bulk density results of the cement-metakaolin blended concrete made from different fine aggregate.

		Bulk density (kg/m^3)						
S/NO	**Mix ID**	**River sand concrete**			**Mix ID**	**Quarry dust Concrete**		
		28days				**28days**		
		650^{0}C	750^{0}C	850^{0}C		650^{0}C	]750^{0}C	850^{0}C
1	0%MK_{RS}	2521.48	2521.48	2521.48	0%MK_{QD}	2518.5	2518.5	2518.5
2	5%MK_{RS}	2518.52	2518.52	2515.56	5%MK_{QD}	2500.74	2521.48	2503.70
3	10%MK_{RS}	2503.70	2515.56	2509.63	10%MK_{QD}	2480	2509.63	2494.81
4	15%MK_{RS}	2500.74	2509.63	2497.78	15%MK_{QD}	2491.85	2503.70	2483.93
5	20%MK_{RS}	2497.78	2500.74	2494.81	20%MK_{QD}	2482.96	2500.74	2485.93
6	25%MK_{RS}	2474.07	2488.89	2485.93	25%MK_{QD}	2453.33	2456.29	2450.37
7	30%MK_{RS}	2468.15	2474.07	2471.1	30%MK_{QD}	2414.81	2408.9	2426.67
8	35%MK_{RS}	2450.37	2456.29	2453.33	35%MK_{QD}	2405.93	2417.8	2411.86
9	40%MK_{RS}	2426.67	2444.4	2441.48	40%MK_{QD}	2373.33	2408.9	2376.29
10	45%MK_{RS}	2405.93	2426.67	2411.85	45%MK_{QD}	2293.33	2420.7	2358.52
11	50%MK_{RS}	2385.19	2405.93	2391.1	50%MK_{QD}	2266.67	2444.4	2331.85

4.1.11 Compressive strength test on the hardened cement-metakaolin blended concrete

The compressive strength test results on the hardened cement-metakaolin blended concrete made with both river sand and quarry dust was obtained using Equation (3.8) and presented in Table

4.12a with graphical representations illustrated in Figure 4.2a, Figure 4.2b, Figure 4.2c and Figure 4.2d. Table 4.12b and Table 4.12d presents the percentage of strength development from day 1 day to 7 days and from 7 days to 28 days for concrete using river sand, while Table 4.12c and Table 4.12e shows same for quarry dust. The percentage of compressive development from 1 day to 7 days and from 7 days to 28 days for all the samples produced were determined using Equation (3.9) and Equation (3.10) respectively.

Table 4.12a: Compressive strength result for the cement-metakaolin blended concrete

		Compressive strength (N/mm^2)												
S/	**Mix ID**	**River sand concrete**						**Mix ID**	**Quarry dust Concrete**					
No		**7days**			**28days**				**7days**			**28days**		
		650^{0}C	750^{0}C	850^{0}C	650^{0}C	750^{0}C	850^{0}C		650^{0}C	750^{0}C	850^{0}C	650^{0}C	750^{0}C	850^{0}C
1	0%MK_{RS}	19.63	19.63	19.63	32.17	32.17	32.17	0%MK_{QD}	19.42	19.42	19.42	31.16	31.16	31.16
2	5%MK_{RS}	21.75	22.30	21.89	33.10	35.58	34.08	5%MK_{QD}	21.28	21.60	21.34	32.66	33.95	33.08
3	10%MK_{RS}	22.47	24.02	22.80	35.32	37.83	37.02	10%MK_{QD}	22.39	23.67	22.62	34.51	35.33	34.97
4	15%MK_{RS}	27.21	27.56	27.37	38.92	40.08	39.79	15%MK_{QD}	26.68	27.33	26.76	36.14	37.19	36.30
5	20%MK_{RS}	27.29	27.91	27.72	37.97	42.05	40.98	20%MK_{QD}	26.93	27.83	27.04	36.48	38.02	36.30
6	25%MK_{RS}	24.74	26.71	25.68	28.86	30.05	29.94	25%MK_{QD}	22.59	26.61	22.70	28.76	28.94	28.83
7	30%MK_{RS}	19.56	23.88	20.66	25.74	27.74	27.55	30%MK_{QD}	19.24	22.80	19.53	26.45	27.81	27.06
8	35%MK_{RS}	16.83	19.12	17.76	21.28	24.97	24.69	35%MK_{QD}	15.60	18.31	16.12	18.18	24.05	19.35
9	40%MK_{RS}	11.70	16.59	16.03	14.24	18.30	18.15	40%MK_{QD}	10.65	15.15	14.67	12.37	17.55	15.64
10	45%MK_{RS}	8.22	10.42	9.29	11.54	15.31	15.28	45%MK_{QD}	8.01	9.66	9.03	9.19	12.43	10.87
11	50%MK_{RS}	6.78	8.10	6.91	8.42	13.02	12.55	50%MK_{QD}	6.02	7.53	6.75	6.77	8.13	7.64

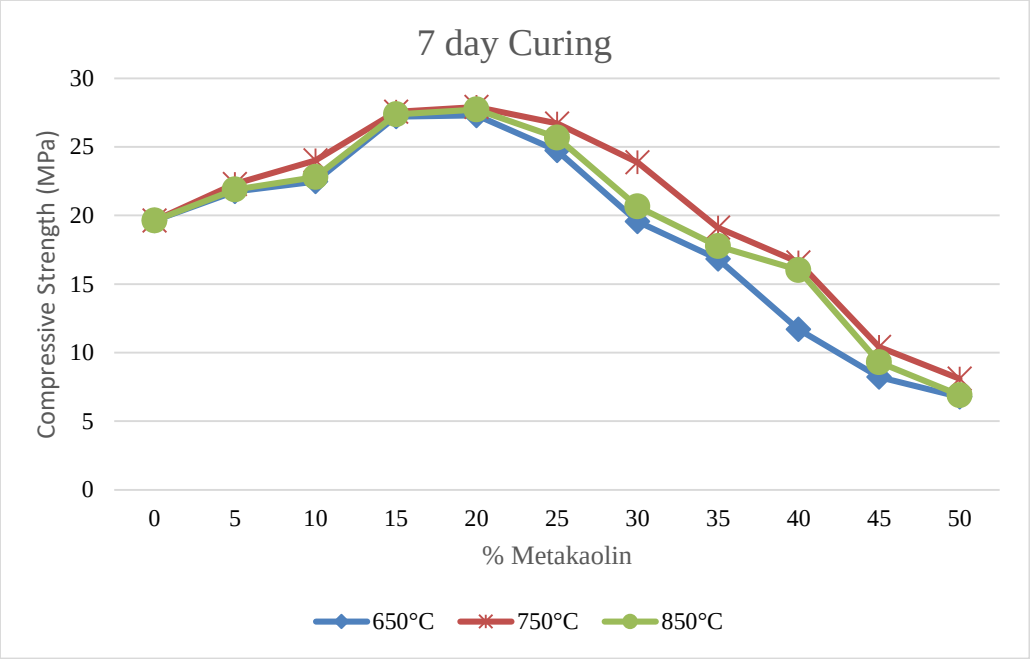

Figure 4.2a: Compressive strength of the concrete against the percentage of replacement of cement with metakaolin using river sand as fine aggregate

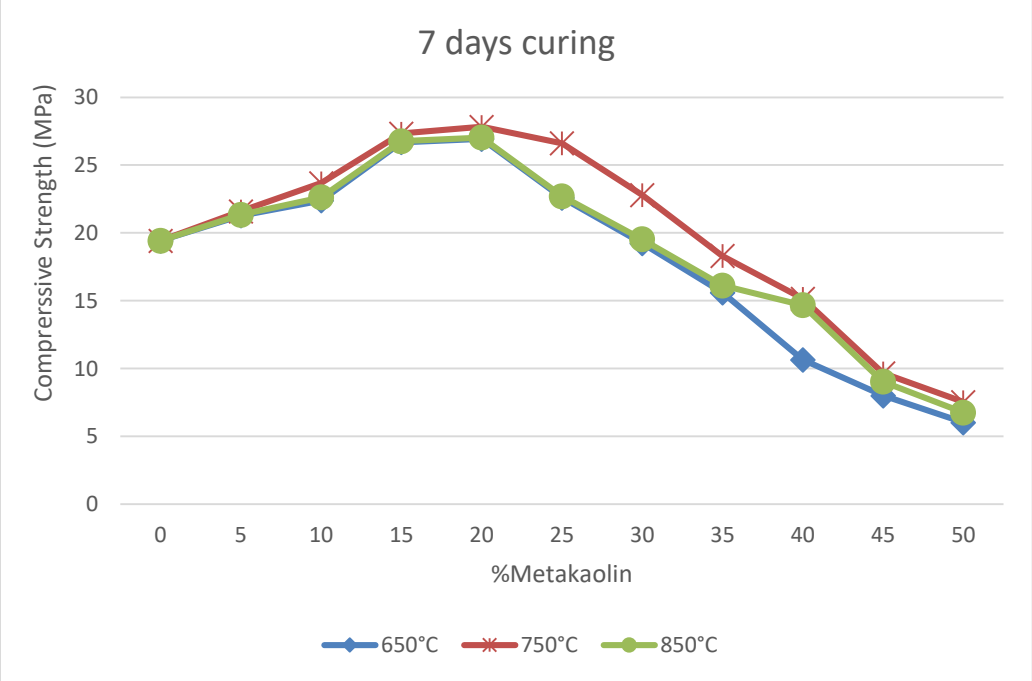

Figure 4.2b: Compressive strength of the concrete against the percentage of replacement of cement with metakaolin using quarry dust as fine aggregate.

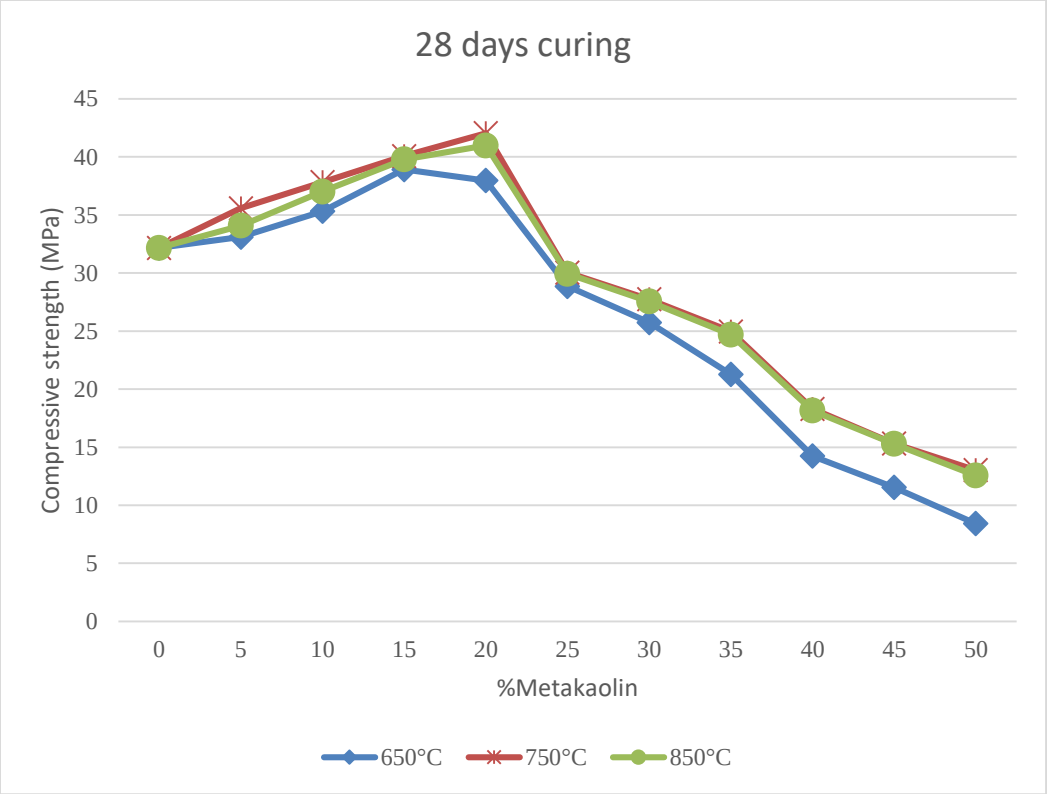

Figure 4.2c: Compressive strength of the concrete against the percentage of replacement of cement with metakaolin using river sand as fine aggregate

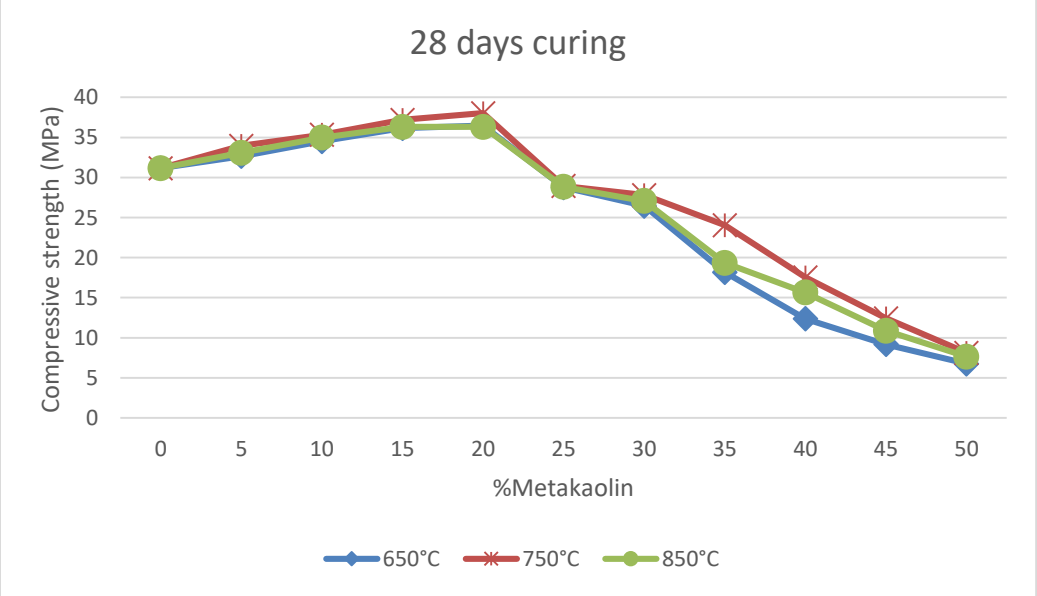

Figure 4.2d: Graphical representation of the compressive strength of the concrete against the percentage of replacement of cement with metakaolin using quarry dust as fine aggregate.

Table 4.12b: Percentage strength development of the cement-metakaolin blended concrete from 1 day to 7 days (River Sand)

Specimen	650^0C (%)	750^0C (%)	850^0C (%)
$0\%MK_{RS}$	65.43	65.43	65.43
$5\%MK_{RS}$	72.50	74.33	72.95
$10\%MK_{RS}$	74.89	80.05	75.99
$15\%MK_{RS}$	90.70	91.88	91.22
$20\%MK_{RS}$	90.98	93.03	92.40
$25\%MK_{RS}$	82.45	89.02	85.60
$30\%MK_{RS}$	65.20	79.60	68.87
$35\%MK_{RS}$	56.10	63.74	59.20
$40\%MK_{RS}$	39.01	55.30	53.44
$45\%MK_{RS}$	27.40	34.72	30.96
$50\%MK_{RS}$	22.60	27.00	23.02

Table 4.12c: Percentage strength development of the cement-metakaolin blended concrete from 1 day to 7 days (Quarry dust)

Specimen	650^0C (%)	750^0C (%)	850^0C (%)
$0\%MK_{QD}$	64.72	64.72	64.72
$5\%MK_{QD}$	70.92	72.01	71.13
$10\%MK_{QD}$	74.63	78.90	75.41
$15\%MK_{QD}$	88.93	91.10	89.21
$20\%MK_{QD}$	89.78	92.78	90.13
$25\%MK_{QD}$	75.31	88.70	75.67
$30\%MK_{QD}$	64.12	76.01	65.10
$35\%MK_{QD}$	52.01	61.02	53.72
$40\%MK_{QD}$	35.52	50.49	48.89
$45\%MK_{QD}$	26.70	32.20	30.01
$50\%MK_{QD}$	20.05	25.10	22.51

Table 4.12d: Percentage strength development of the cement-metakaolin blended concrete from 7 days to 28 days (River Sand)

Specimen	650^0C (%)	750^0C (%)	850^0C (%)
$0\%MK_{RS}$	63.88	63.88	63.88
$5\%MK_{RS}$	52.18	59.55	55.69
$10\%MK_{RS}$	57.19	57.49	62.37
$15\%MK_{RS}$	43.04	46.23	45.38
$20\%MK_{RS}$	39.14	50.77	47.84
$25\%MK_{RS}$	16.65	12.50	16.59
$30\%MK_{RS}$	31.60	16.16	33.35
$35\%MK_{RS}$	26.44	30.60	39.02
$40\%MK_{RS}$	21.71	10.31	13.23

45%MK_{RS}	40.39	46.93	64.48
50%MK_{RS}	24.19	60.74	81.62

Table 4.12e: Percentage strength development of the cement-metakaolin blended concrete from 7 days to 28 days (Quarry dust)

Specimen	**650^{0}C (%)**	**750^{0}C (%)**	**850^{0}C (%)**
0%MK_{QD}	60.45	60.45	60.45
5%MK_{QD}	53.48	57.18	55.01
10%MK_{QD}	54.13	49.26	54.60
15%MK_{QD}	35.46	36.08	35.65
20%MK_{QD}	35.46	36.62	38.72
25%MK_{QD}	27.31	8.76	27.00
30%MK_{QD}	37.47	21.97	38.56
35%MK_{QD}	16.22	31.35	20.74
40%MK_{QD}	16.04	15.84	6.61
45%MK_{QD}	14.73	28.67	20.74
50%MK_{QD}	12.46	7.97	4.30

4.1.12 Young modulus of elasticity results on the cement-metakaolin blended concrete

The young modulus of elasticity results obtained from Equation (3.11) on the cement-metakaolin blended concrete for both river sand and quarry dust are shown in Table 4.13. Figure 4.3a and Figure 4.3b presents the graphical representation of the results for concrete using river sand and quarry dust respectively.

Table 4.13: Young modulus of elasticity of the cement-metakaolin blended concrete

Young Modulus of elasticity (GPa)								
S/NO	**Mix ID**	**River sand concrete**			**Mix ID**	**Quarry dust Concrete**		
		28days				**28days**		
		650^{0}C	750^{0}C	850^{0}C		650^{0}C	750^{0}C	850^{0}C
1	0%MK_{RS}	30.88	30.88	30.88	0%MK_{QD}	30.34	30.34	30.34
2	5%MK_{RS}	31.27	32.42	31.67	5%MK_{QD}	30.73	31.72	30.98
3	10%MK_{RS}	32.01	33.25	32.89	10%MK_{QD}	31.19	32.13	31.69
4	15%MK_{RS}	33.55	34.32	33.86	15%MK_{QD}	32.15	32.85	32.07
5	20%MK_{RS}	33.08	34.88	34.30	20%MK_{QD}	32.45	33.16	32.64
6	25%MK_{RS}	28.43	29.27	29.16	25%MK_{QD}	28.02	28.16	28.01
7	30%MK_{RS}	26.75	27.87	27.72	30%MK_{QD}	26.24	26.81	26.74
8	35%MK_{RS}	24.06	26.16	25.96	35%MK_{QD}	21.61	25.07	22.40
9	40%MK_{RS}	19.39	22.23	28.09	40%MK_{QD}	17.49	21.29	19.69
10	45%MK_{RS}	18.04	20.11	19.91	45%MK_{QD}	14.32	18.06	16.24

11	50%MK_{RS}	14.53	18.31	17.81	50%MK_{QD}	12.07	14.82	12.85

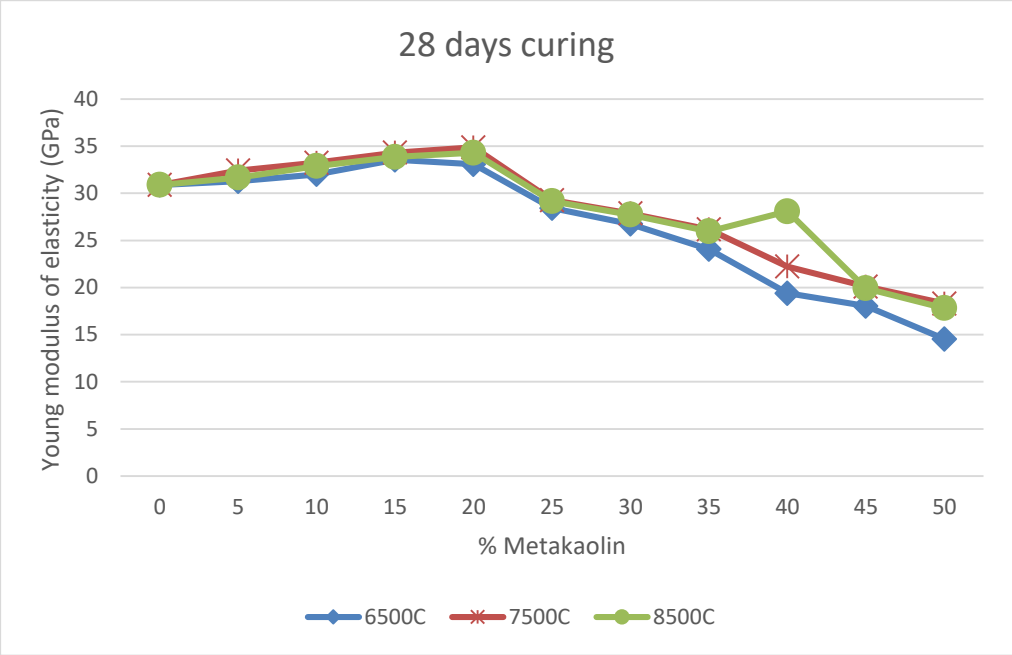

Figure 4.3a: Young modulus of elasticity of the concrete against the percentage of replacement of cement with metakaolin using river sand as fine aggregate

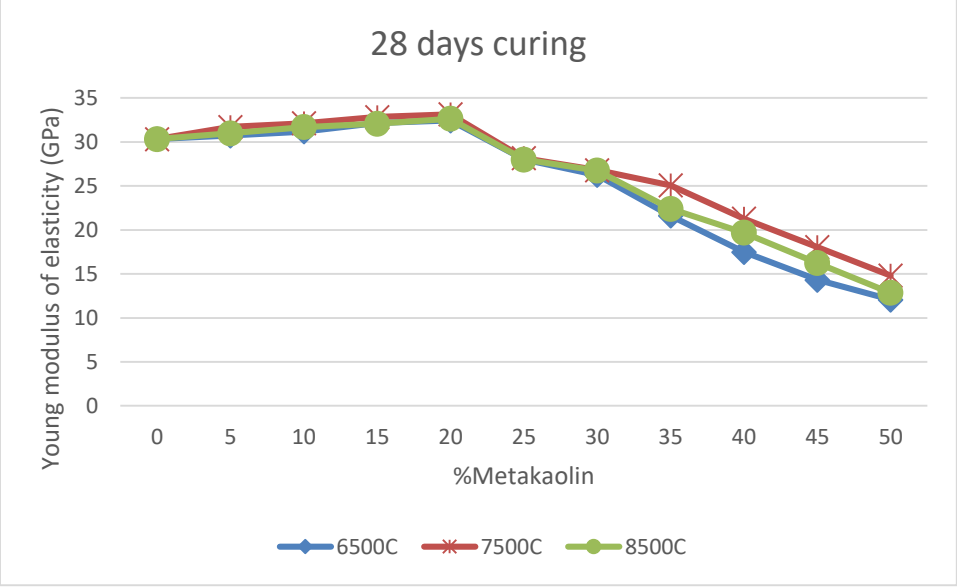

Figure 4.3b: Young modulus of elasticity of the concrete against the percentage of replacement of cement with metakaolin using quarry dust as fine aggregate

4.1.13 Water absorption test results on hardened cement-metakaolin blended concrete

Table 4.14 shows the results for the water absorption on the hardened concrete obtained from Equation 3.12. Figure 4.4a and Figure 4.4b demonstrate the results graphically for river sand and quarry dust concrete respectively.

Table 4.14: Water absorption of the cement-metakaolin blended concrete

Water Absorption (%)								
S/No.	**Mix ID**	**River sand concrete**			**Mix ID**	**Quarry dust Concrete**		
		28days				**28days**		
		650^0C	750^0C	850^0C		650^0C	750^0C	850^0C
1	$0\%MK_{RS}$	1.70	1.70	1.70	$0\%MK_{QD}$	2.16	2.16	2.16
2	$5\%MK_{RS}$	1.58	1.45	1.57	$5\%MK_{QD}$	1.68	1.44	1.56
3	$10\%MK_{RS}$	1.46	1.33	1.46	$10\%MK_{QD}$	1.57	1.33	1.46
4	$15\%MK_{RS}$	1.34	1.22	1.33	$15\%MK_{QD}$	1.46	1.21	1.33
5	$20\%MK_{RS}$	1.22	1.10	1.22	$20\%MK_{QD}$	1.46	1.33	1.45
6	$25\%MK_{RS}$	1.60	1.47	1.47	$25\%MK_{QD}$	2.72	1.59	1.71
7	$30\%MK_{RS}$	1.98	1.73	1.86	$30\%MK_{QD}$	2.63	1.84	1.85
8	$35\%MK_{RS}$	2.25	2.12	2.25	$35\%MK_{QD}$	3.05	2.20	2.63
9	$40\%MK_{RS}$	2.77	2.90	2.64	$40\%MK_{QD}$	3.22	3.02	2.81
10	$45\%MK_{RS}$	2.91	3.19	3.31	$45\%MK_{QD}$	4.84	3.73	4.08
11	$50\%MK_{RS}$	3.57	3.34	3.46	$50\%MK_{QD}$	5.58	4.59	5.50

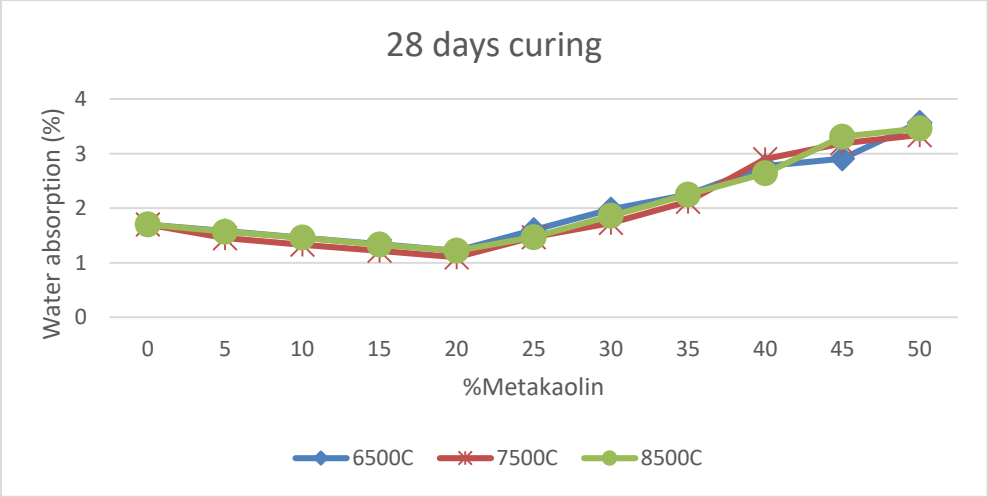

Figure 4.4a: Water absorption of the concrete against the percentage of replacement of cement with metakaolin using river sand as fine aggregate

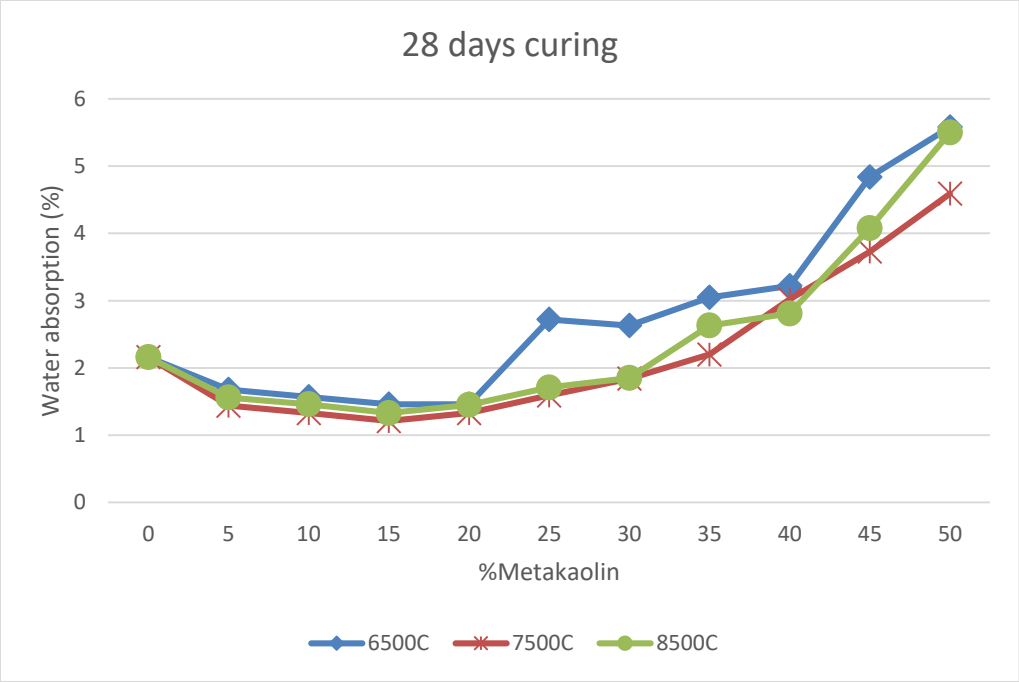

Figure 4.4b: Water absorption of the concrete against the percentage of replacement of cement with metakaolin using quarry dust as fine aggregate

4.1.14 Multiple regression analysis for the cement-metakaolin blended concrete

The multiple regression analysis of the experimental result for the best cement-metakaolin blended concrete based on the compressive strength, young modulus of elasticity and water absorption was obtained at 750ºC for both the river sand and quarry dust. The experimental result of the blends at 750ºC were statistically analyzed with the Historical Design (HD) in Response Surface Methodology (RSM) in Design Expert Software version 13.0. The regression equations and analysis of variance (ANOVA) of the compressive strength, young modulus and water absorption were evaluated and the results presented in this section.

4.1.14.1 Regression model for the compressive strength of cement-metakaolin blended concrete at 750ºC metakaolin production temperature

The statistical analysis for the compressive strength of the cement-metakaolin concrete blend for both river sand and quarry dust at 750ºC was done using the independent and response values shown in Table 4.15. The multiple regression analysis of the experimental data gave a two factor interaction (2FI) equation that is, Equation (4.1) and Equation (4.2) for river sand and quarry dust concrete respectively. The 2FI models developed depict the interaction between the compressive strength and the actual values of the independent variables (that is, mass of cement and metakaolin). The equations in terms of actual factors can be used to make predictions about the responses for given levels of each factor.

Table 4.15: Design data for compressive strength of the cement-metakaolin blended concrete using river sand and quarry dust at 750ºC metakaolin production temperature.

	River sand concrete			Quarry dust concrete		
Run	Factor 1 A:Cement kg	Factor2 B:Metakaolin kg	Response1 Comp.Strength MPa	Factor 1 A:Cement kg	Factor2 B:Metakaolin kg	Response1 Comp.Strength MPa
1	1.95	0	32.17	2.15	0	31.16
2	1.85	0.1	35.58	2.05	0.11	33.95
3	1.75	0.2	37.83	1.94	0.22	35.33
4	1.64	0.29	40.3	1.83	0.32	37.19
5	1.56	0.39	42.08	1.72	0.43	38.02
6	1.46	0.49	30.05	1.61	0.54	28.94
7	1.37	0.58	27.74	1.51	0.65	27.81
8	1.27	0.68	24.97	1.4	0.75	24.05
9	1.17	0.78	18.3	1.29	0.86	17.55
10	1.07	0.88	15.31	1.18	0.97	12.43
11	0.97	0.97	13.02	1.08	1.08	8.13

The procedures used to generate Equation (4.1) for the compressive strength of cement-metakaolin blended concrete produced using river sand for metakaolin at 750ºC is illustrated in Figure 3.2.

$$Compressive\ Strength = +574.89798 - 277.38749(CEM) - 351.45619(MK) + 48.92976(CEM)(MK) \quad (4.1)$$

Where; CEM = Cement content (kg)

MK = Metakaolin content (kg)

Similarly, procedures used to generate Equation (4.2) for the compressive strength of cement-metakaolin blended concrete produced using quarry dust for metakaolin at 750ºC is illustrated in Figure 3.2.

$$Compressive\ Strength = -33.07048 + 30.35123(CEM) - 41.68140(MK) + 44.15918(CEM)(MK) \quad (4.2)$$

Where; CEM = Cement content (kg)

MK = Metakaolin content (kg)

4.1.14.2 Regression model for the young modulus of elasticity of the cement-metakaolin blended concrete at 750ºC metakaolin production temperature

The statistical analysis for the young modulus of the cement-metakaolin concrete blend for both river sand and quarry dust at 750ºC was done using the independent and response values shown in Table 4.16. The multiple regression analysis of the experimental data gave a two factor interaction (2FI) equation that is, Equation (4.3) and Equation (4.4) for river sand and quarry dust concrete respectively. The 2FI models developed depict the interaction between the young modulus and the actual values of the independent variables (that is, mass of cement and metakaolin). The equations in terms of actual factors can be used to make predictions about the responses for given levels of each factor.

Table 4.16: Design data for young modulus of elasticity of the cement-metakaolin blended concrete using river sand and quarry dust at 750ºC metakaolin production temperature.

	River sand concrete			**Quarry dust concrete**		
Run	Factor 1 A:Cement (kg)	Factor2 B:Metakaolin (kg)	Response1 Young modulus (GPa)	Factor 1 A:Cement (kg)	Factor2 B:Metakaolin (kg)	Response1 Young modulus (GPa)
1	1.95	0	30.88	2.15	0	30.34
2	1.85	0.1	32.42	2.05	0.11	31.72
3	1.75	0.2	33.25	1.94	0.22	32.13
4	1.64	0.29	34.32	1.83	0.32	32.85
5	1.56	0.39	34.88	1.72	0.43	33.16
6	1.46	0.49	29.27	1.61	0.54	28.16
7	1.37	0.58	27.87	1.51	0.65	26.81
8	1.27	0.68	26.16	1.4	0.75	25.07
9	1.17	0.78	22.23	1.29	0.86	21.29
10	1.07	0.88	20.11	1.18	0.97	18.06
11	0.97	0.97	18.31	1.08	1.08	14.82

The steps used to generate Equation (4.3) for the young modulus of elasticity of cement-metakaolin blended concrete produced using river sand for metakaolin at 750ºC is illustrated in Figure 3.2.

$$Young\ Modulus = +270.50474 - 122.51212(CEM) - 165.21082(MK) + 27.58260(CEM)(MK) \quad (4.3)$$

Where; CEM = Cement content (kg)

MK = Metakaolin content (kg)

Similarly, procedures used to generate Equation (4.4) for the young modulus of elasticity of cement-metakaolin blended concrete produced using quarry dust for metakaolin at 750ºC is illustrated in Figure 3.2.

$$Young\ Modulus = +55.09240 - 11.20912(CEM) - 53.52617(MK) + 24.68764(CEM)(MK) \quad (4.4)$$

Where; CEM = Cement content (kg)

MK = Metakaolin content (kg)

4.1.14.3 Regression model for the water absorption of cement-metakaolin blended concrete at 750ºC metakaolin production temperature

The statistical analysis for the water absorption of the cement-metakaolin concrete blend for both river sand and quarry dust at 750ºC was done using the independent and response values shown in Table 4.17. The multiple regression analysis of the experimental data gave a two factor interaction (2FI) equation that is, Equation (4.5) and Equation (4.6) for river sand and quarry dust concrete respectively. The 2FI models developed depict the interaction between the water absorption and the actual values of the independent variables (that is, mass of cement and metakaolin). The equations in terms of actual factors can be used to make predictions about the responses for given levels of each factor.

Table 4.17: Design data for water absorption of the cement-metakaolin blended concrete using river sand and quarry dust at 750ºC metakaolin production temperature.

	River sand concrete			**Quarry dust concrete**		
Run	Factor 1 A:Cement (kg)	Factor2 B:Metakaolin (kg)	Response1 Water absorption (%)	Factor 1 A:Cement (kg)	Factor2 B:Metakaolin (kg)	Response1 Water absorption (%)
1	1.95	0	1.7	2.15	0	2.16
2	1.85	0.1	1.45	2.05	0.11	1.44
3	1.75	0.2	1.33	1.94	0.22	1.33
4	1.64	0.29	1.22	1.83	0.32	1.21
5	1.56	0.39	1.1	1.72	0.43	1.33
6	1.46	0.49	1.47	1.61	0.54	1.59
7	1.37	0.58	1.73	1.51	0.65	1.84
8	1.27	0.68	2.13	1.4	0.75	2.23
9	1.17	0.78	2.9	1.29	0.86	3.02
10	1.07	0.88	3.19	1.18	0.97	3.73
11	0.97	0.97	3.34	1.08	1.08	4.59

The procedures used to generate Equation (4.5) for the water absorption of cement-metakaolin blended concrete produced using river sand for metakaolin at 750ºC is illustrated in Figure 3.2.

$$Water\ Absorption = -21.65367 + 11.95313(CEM) + 18.70849(MK) - 4.78724\ (CEM)(MK) \quad (4.5)$$

Where; CEM = Cement content (kg)

MK = Metakaolin content (kg)

Similarly, procedures used to generate Equation (4.6) for the water absorption of cement-metakaolin blended concrete produced using quarry dust for metakaolin at 750ºC is illustrated in Figure 3.2.

$$Water\ Absorption = +18.60661 - 7.69463(CEM) + 1.65257(MK) - 6.42813(CEM)(MK) \quad (4.6)$$

Where; CEM = Cement content (kg)

MK = Metakaolin content (kg)

4.1.15 Model prediction and comparison with the experimental results.

The models obtained were used to predict the compressive strength, young modulus and water absorption of the cement-metakaolin blended concrete. Values obtained were compared to those generated experimentally, while the effects of independent parameters and their

mutual interactions with the aid of the regression coefficients were used to generate the contour plot and 3-D surface plot from the fitted two factor interaction (2FI) equations. The results are presented in this section.

4.1.15.1 Comparison between the experimental and model predicted compressive strength results for the cement-metakaolin blended concrete.

The compressive strength generated experimentally and the model predicted results for cement-metakaolin blended concrete using river sand and quarry dust are shown in Table 4.18 and Table 4.19 respectively.

Table 4.18: Statistical report on the compressive strength of cement-metakaolin blended concrete using river sand at 750ºC metakaolin production temperature.

Run order	Actual value	Predicted value	Residual
1	32.17	33.99	-1.82
2	35.58	35.64	-0.0575
3	37.83	36.3	1.53
4	40.3	41.33	-1.03
5	42.08	34.87	7.21
6	30.05	32.7	-2.65
7	27.74	29.91	-2.17
8	24.97	25.88	-0.9114
9	18.3	20.87	-2.57
10	15.31	14.88	0.4258
11	13.02	10.96	2.06

Table 4.19**:** Statistical report on the compressive strength of cement-metakaolin blended concrete using quarry dust at 750ºC metakaolin production temperature.

Run order	Actual value	Predicted value	Residual
1	31.16	32.18	-1.02
2	33.95	34.52	-0.5725
3	35.33	35.49	-0.1581
4	37.19	34.99	2.2
5	38.02	33.87	4.15
6	28.94	31.68	-2.74
7	27.81	29.01	-1.2

8	24.05	24.53	-0.4773
9	17.55	19.23	-1.68
10	12.43	12.86	-0.4276
11	8.13	6.2	1.93

Figure 4.5a and Figure 4.5b illustrate the relationship between actual and predicted compressive strength values for cement-metakaolin concrete using river sand and quarry dust respectively, while Figure 4.6a and Figure 4.6b presents the normal probability of residuals

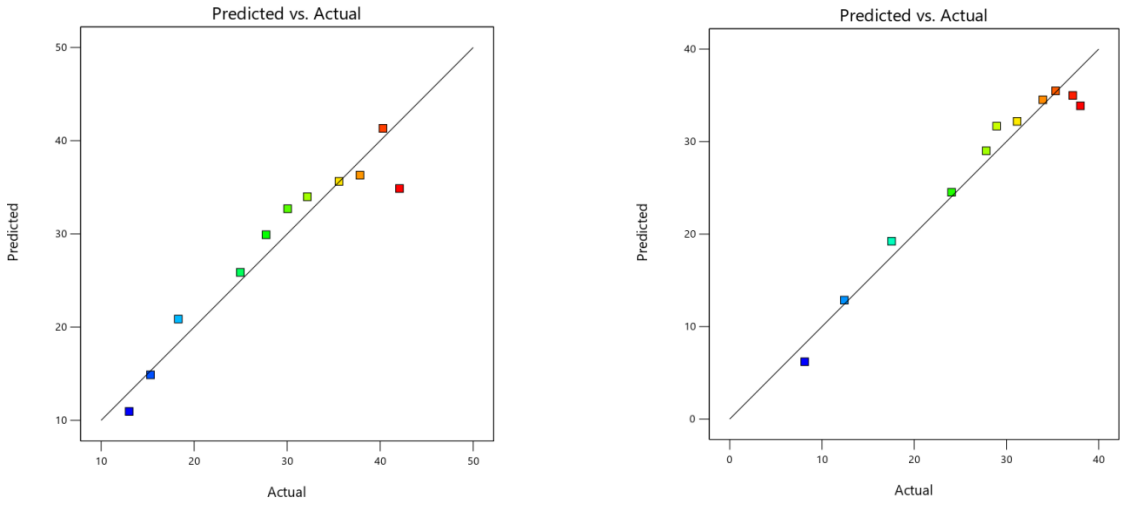

(a) (b)

Figure 4.5: Correlation between Predicted and experimental compressive strength of the cement-metakaolin blended concrete using river sand and quarry dust at 750ºC metakaolin production temperature.

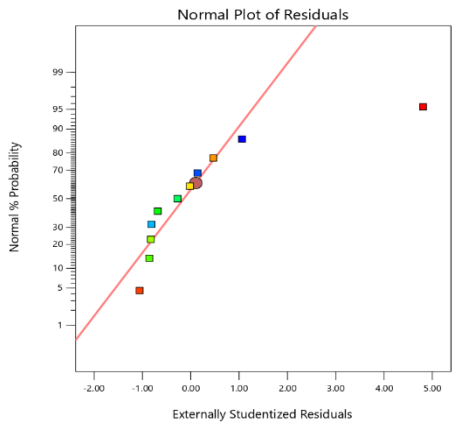

(a)

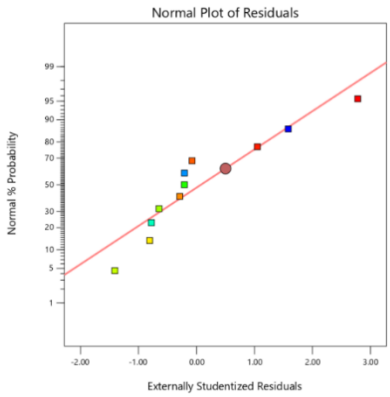

(b)

Figure 4.6: Diagnostic plots of residual against experimental runs for the compressive strength of the cement-metakaolin blended concrete using river sand and quarry dust at 750ºC metakaolin production temperature.

Figure 4.7a and Figure 4.7b show the contour plots for cement-metakaolin concrete using river sand and quarry dust respectively, while Figure 4.8a and Figure 4.8b presents and 3D plots respectively.

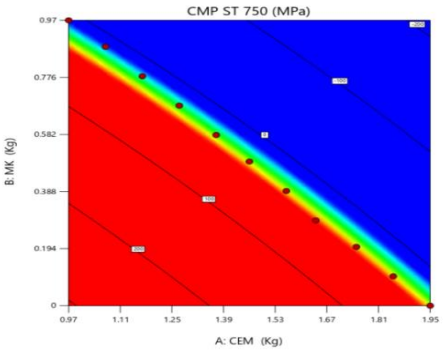

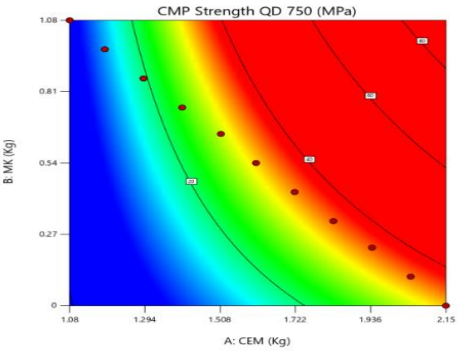

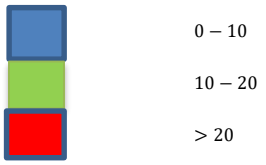

Compressive strength (Mpa)

(a)

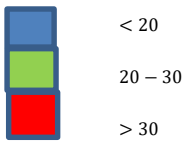

Compressive strength (Mpa)

(b)

Figure 4.7: Contour plots for the compressive strength of the cement-metakaolin blended concrete using river sand and quarry dust at 750ºC metakaolin production temperature.

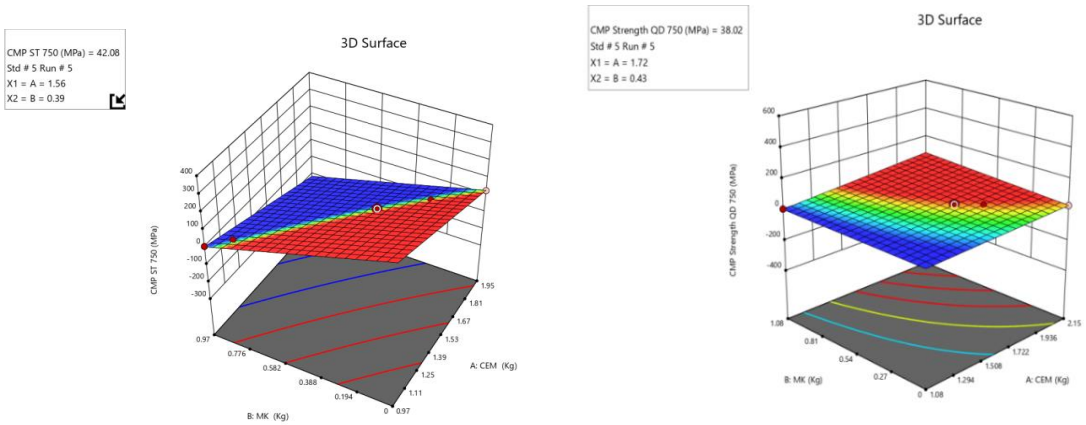

(a) (b)

Figure 4.8: 3D plots for the compressive strength of the cement-metakaolin blended concrete using river sand and quarry dust at 750ºC metakaolin production temperature.

4.1.15.2 Comparison between the experimental and model predicted young modulus of elasticity results for the cement-metakaolin blended concrete.

The young modulus of elasticity obtained experimentally and the model predicted results for cement-metakaolin blended concrete using river sand and quarry dust are shown in Table 4.20 and Table 4.21 respectively.

Table 4.20: Statistical report on the young modulus of elasticity of cement-metakaolin blended concrete using river sand at 750ºC metakaolin production temperature.

Run order	Actual value	Predicted value	Residual
1	30.88	31.61	-0.7261
2	32.42	32.44	-0.0190
3	33.25	32.72	0.5297
4	34.32	34.79	-0.4720
5	34.88	31.73	3.15
6	29.27	30.42	-1.15
7	27.87	28.76	-0.8880
8	26.16	26.39	-0.2313
9	22.23	23.47	-1.24
10	20.11	20.00	0.1070
11	18.31	17.37	0.9440

Table 4.21: Statistical report on the young modulus of elasticity of cement-metakaolin blended concrete using quarry dust at 750ºC metakaolin production temperature.

Run order	Actual value	Predicted value	Residual
1	30.34	30.99	-0.6528
2	31.72	31.79	-0.0729
3	32.13	32.11	0.0224
4	32.85	31.91	0.9416
5	33.16	31.06	2.1
6	28.16	29.61	-1.45
7	26.81	27.61	-0.7955
8	25.07	25.18	-0.107
9	21.29	21.99	-0.6986
1	30.34	30.99	-0.6528
2	31.72	31.79	-0.0729

Figure 4.9a and Figure 4.9b illustrate the relationship between actual and predicted young modulus of elasticity values for cement-metakaolin concrete using river sand and quarry dust respectively, while Figure 4.10a and Figure 4.10b presents the normal probability of residuals

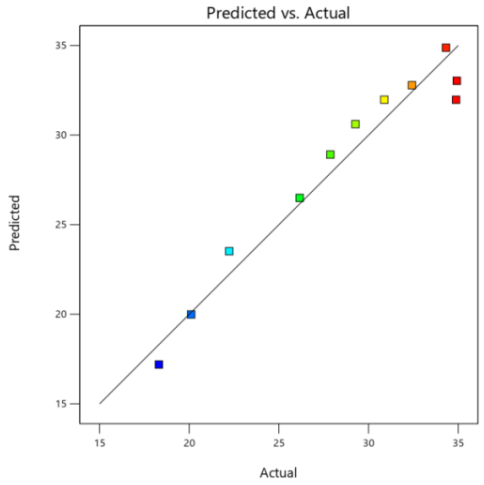

(a)

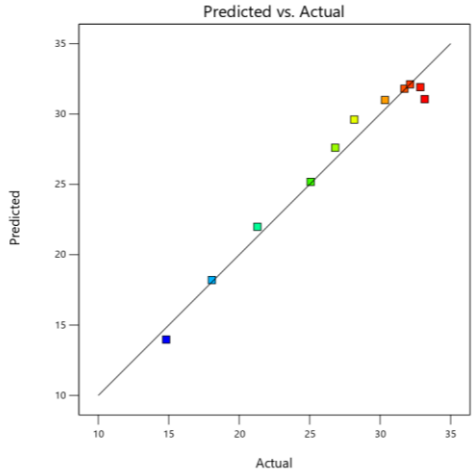

(b)

Figure 4.9: Correlation between Predicted and experimental young modulus of elasticity of the cement-metakaolin blended concrete using river sand and quarry dust at 750ºC metakaolin production temperature.

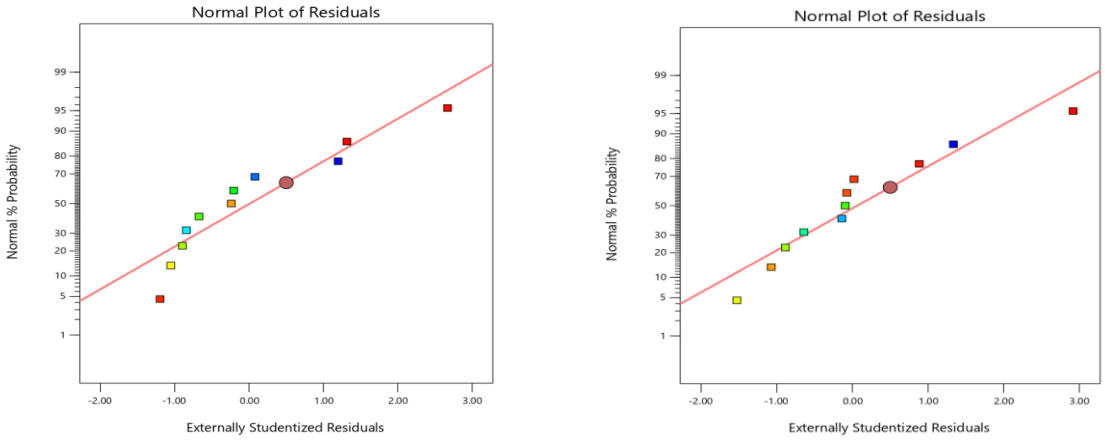

(a) (b)

Figure 4.10: : Diagnostic plots of residual against experimental runs for the young modulus of elasticity of the cement-metakaolin blended concrete using river sand and quarry dust at 750ºC metakaolin production temperature

Figure 4.11a and Figure 4.11b show the contour plots for cement-metakaolin concrete using river sand and quarry dust respectively, while Figure 4.12a and Figure 4.12b presents and 3D plots respectively.

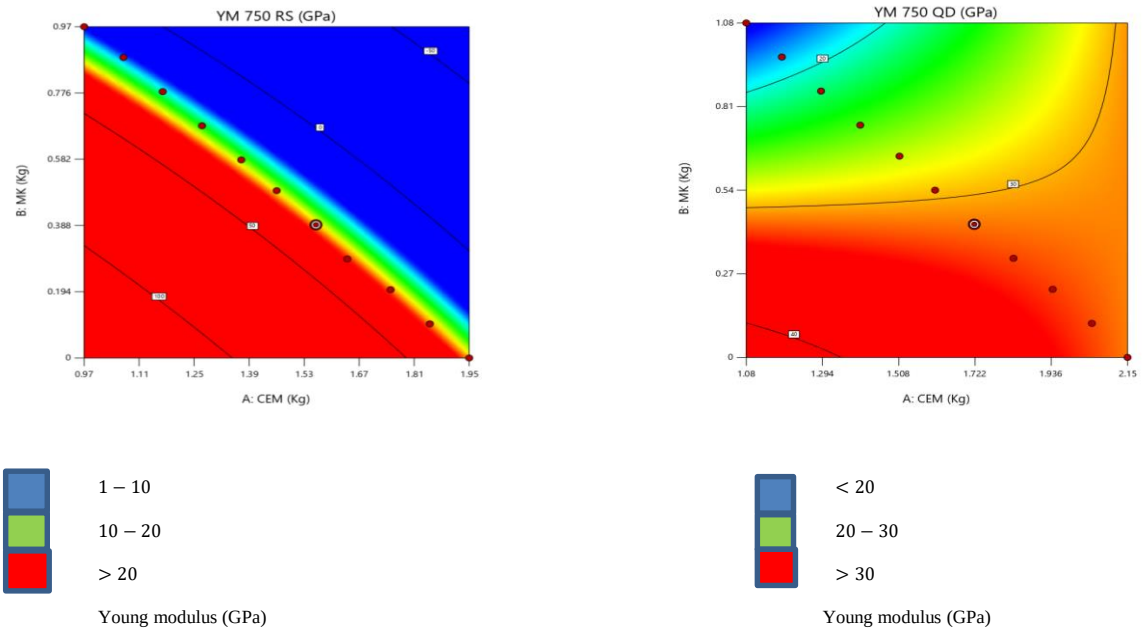

(a) (b)

Figure 4.11: Contour plots for the young modulus of elasticity of the cement-metakaolin blended concrete using river sand and quarry dust at 750ºC metakaolin production temperature.

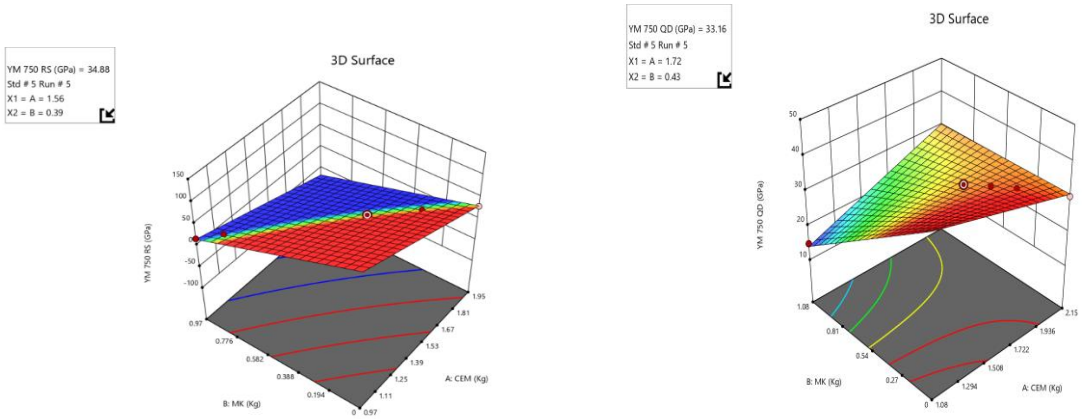

(a) (b)

Figure 4.12: 3D plots for the young modulus of elasticity of the cement-metakaolin blended concrete using river sand and quarry dust at 750ºC metakaolin production temperature.

4.1.15.3 Comparison between the experimental and model predicted water absorption results for the cement-metakaolin blended concrete.

The water absorption generated experimentally and the model predicted results for cement-metakaolin blended concrete using river sand and quarry dust are shown in Table 4.22 and Table 4.23 respectively.

Table 4.22: Statistical report on the water absorption of cement-metakaolin blended concrete using river sand at 750ºC metakaolin production temperature.

Run order	Actual value	Predicted value	Residual
1	1.7	1.65	0.0451
2	1.45	1.44	0.0052
3	1.33	1.33	-0.0005
4	1.22	1.1	0.1219
5	1.1	1.38	-0.277

6	1.47	1.54	-0.0703
7	1.73	1.77	-0.0391
8	2.13	2.11	0.0157
9	2.9	2.56	0.3447
10	3.19	3.09	0.098
11	3.34	3.58	-0.2438

Table 4.23: Statistical report on the water absorption of cement-metakaolin blended concrete using quarry dust at 750ºC metakaolin production temperature.

Run order	Actual value	Predicted value	Residual
1	2.16	2.06	0.0968
2	1.44	1.56	-0.1249
3	1.33	1.3	0.0309
4	1.21	1.29	-0.0799
5	1.33	1.33	0.0018
6	1.59	1.52	0.068
7	1.84	1.75	0.0873
8	2.23	2.32	-0.094
9	3.02	2.97	0.0496
10	3.73	3.77	-0.0423
11	4.59	4.58	0.0066

Figure 4.13a and Figure 4.13b illustrate the relationship between actual and predicted young modulus of elasticity values for cement-metakaolin concrete using river sand and quarry dust respectively, while Figure 4.14a and Figure 4.14b presents the normal probability of residuals

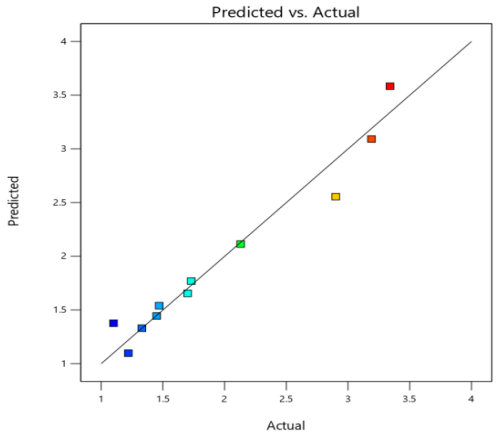

(a)

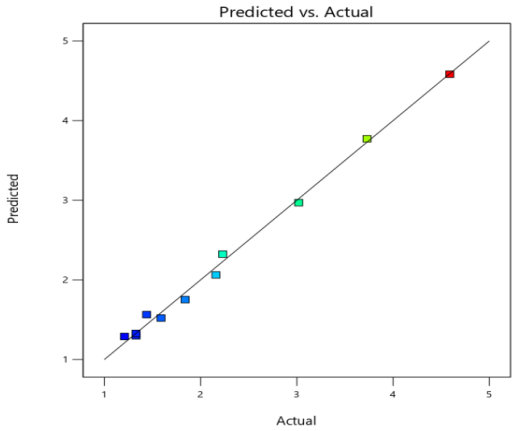

(b)

Figure 4.13: Correlation between Predicted and experimental water absorption of the cement-metakaolin blended concrete using river sand and quarry dust at 750ºC metakaolin production temperature.

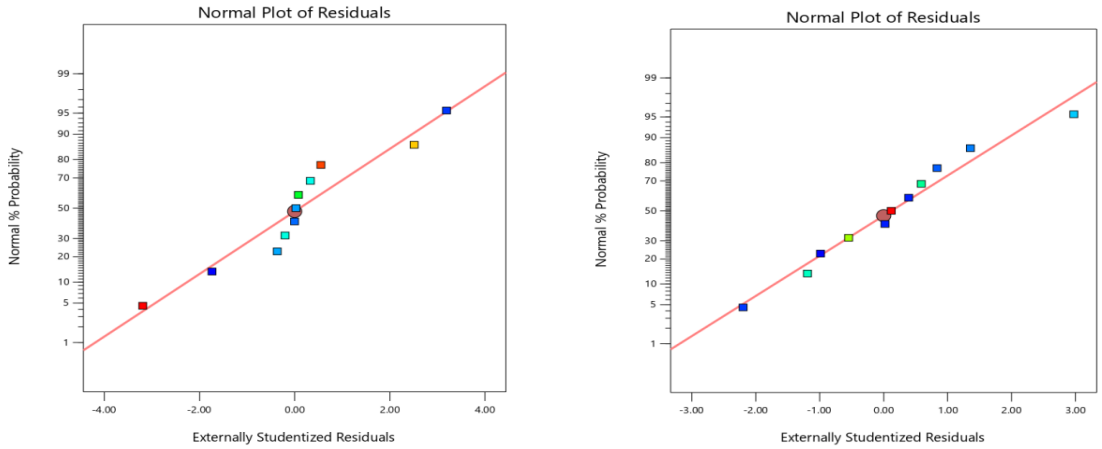

(a) (b)

Figure 4.14: Diagnostic plots of residual against experimental runs for the young modulus of elasticity of the cement-metakaolin blended concrete using river sand and quarry dust at 750ºC metakaolin production temperature.

Figure 4.15a and Figure 4.15b show the contour plots for cement-metakaolin concrete using river sand and quarry dust respectively, while Figure 4.16a and Figure 4.16b presents and 3D plots respectively.

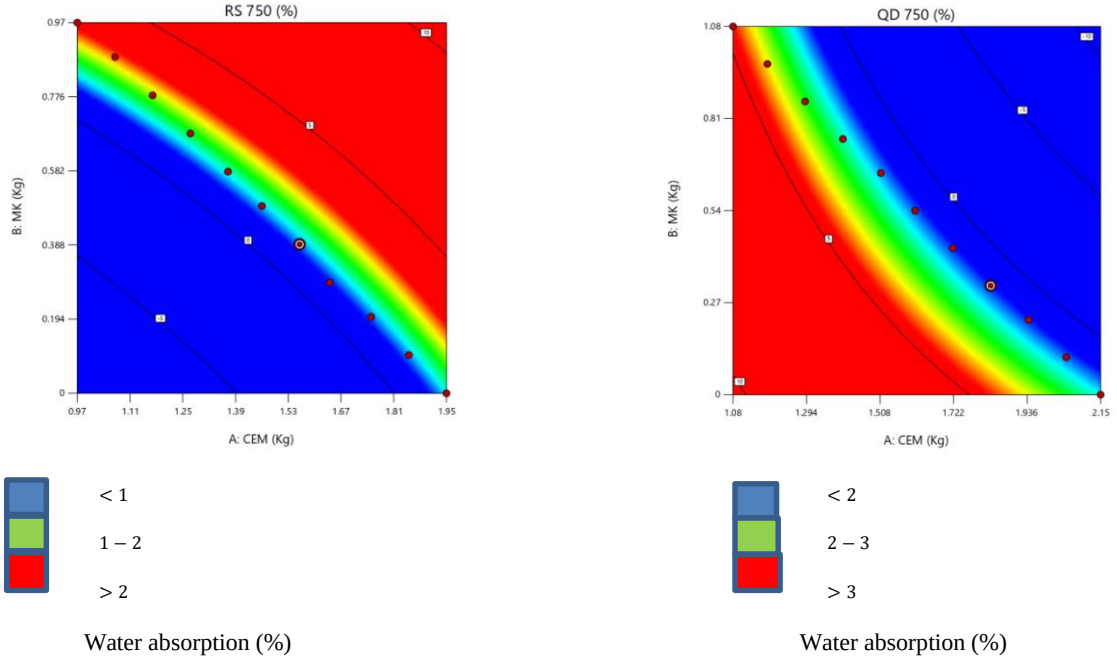

(a) (b)

Figure 4.15: Contour plots for the water absorption of the cement-metakaolin blended concrete using river sand and quarry dust at 750ºC metakaolin production temperature.

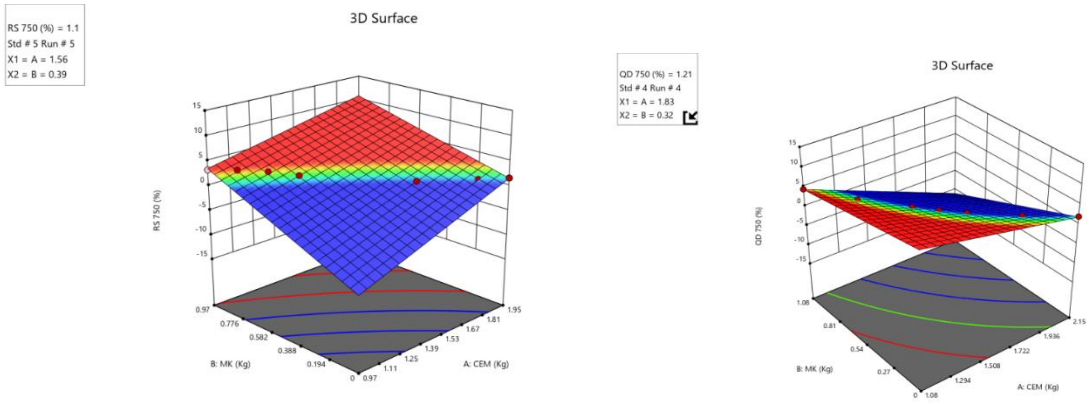

(a) (b)

Figure 4.16: 3D plots for the water absorption of the cement-metakaolin blended concrete using river sand and quarry dust at 750ºC metakaolin production temperature.

4.1.16 Check for the adequacy of model predictions using ANOVA

The results of the analysis of variance (ANOVA) were developed through the RSM models which were analyzed and used to check the adequacy of the models for future use. The results are presented as follow.

4.1.16.1 ANOVA result for compressive strength of the cement-metakaolin blended concrete using river sand and quarry dust at 750ºC metakaolin production

The independent factors and response values shown in Table 4.15 were used for the statistical analysis to obtain the compressive strength models of the cement-metakaolin blended concrete using river sand and quarry dust at 750ºC metakaolin production with the application of analysis

of variance (ANOVA) and the results obtained are depicted in Table 4.24 and Table 4.25 respectively.

Table 4.24: ANOVA result for the compressive strength of cement-metakaolin blended concrete using river sand at 750ºC metakaolin production.

Source	Sum of Squares	df	Mean Square	F-value	p-value	
Model	923.77	3	307.92	26.2	0.0004	Significant
A-CEM	26.81	1	26.81	2.28	0.1747	
B-MK	32.6	1	32.6	2.77	0.1398	
AB	186.9	1	186.9	15.9	0.0053	
Residual	82.27	7	11.75			
Cor Total	1006.04	10				
Std. Dev.	3.43		R^2	0.9182		
Mean	28.85		Adjusted R^2	0.8832		
C.V. %	11.88		Predicted R^2	0.8658		
			Adequate Precision	14.692		

Table 4.25: ANOVA result for the compressive strength of metakaolin blended concrete using quarry dust at 750ºC

Source	Sum of Squares	df	Mean Square	F-value	p-value	
Model	991.19	3	330.4	58.81	< 0.0001	Significant
A-CEM	0.7039	1	0.7039	0.1253	0.7338	
B-MK	0.2101	1	0.2101	0.0374	0.8521	
AB	212.09	1	212.09	37.75	0.0005	
Residual	39.33	7	5.62			
Cor Total	1030.52	10				
Std. Dev.	2.37		R^2	0.9618		
Mean	26.78		Adjusted R^2	0.9455		
C.V. %	8.85		Predicted R^2	0.8935		
			Adequate Precision	20.4903		

4.1.16.2 ANOVA result for young modulus of elasticity of the cement-metakaolin blended concrete using river sand and quarry dust at 750ºC metakaolin production

The independent factors and response values shown in Table 4.16 were used for the statistical analysis to obtain the young modulus of elasticity models of the cement-metakaolin blended concrete using river sand and quarry dust at 750ºC metakaolin production with the

application of analysis of variance (ANOVA) and the results obtained are depicted in Table 4.26 and Table 4.27 respectively.

Table 4.26: ANOVA result for the young modulus of cement-metakaolin blended concrete using river sand at 750ºC metakaolin production

Source	Sum of Squares	df	Mean Square	F-value	p-value	
Model	321.34	3	107.11	48.29	< 0.0001	significant
A-CEM	4.96	1	4.96	2.24	0.1784	
B-MK	6.49	1	6.49	2.93	0.1309	
AB	59.39	1	59.39	26.78	0.0013	
Residual	15.53	7	2.22			
Cor Total	336.86	10				
Std. Dev.	1.49		R^2	0.9539		
Mean	28.15		Adjusted R^2	0.9342		
C.V. %	5.29		Predicted R^2	0.8014		
			Adequate Precision	19.4033		

Table 4.27: ANOVA result for the young modulus of cement-metakaolin blended concrete using quarry dust at 750ºC metakaolin production

Source	Sum of Squares	df	Mean Square	F-value	p-value	
Model	387.59	3	129.2	93.19	< 0.0001	Significant

A-CEM	0.0011	1	0.0011	0.0008	0.9785
B-MK	0.0446	1	0.0446	0.0322	0.8627
AB	66.29	1	66.29	47.82	0.0002
Residual	9.7	7	1.39		
Cor Total	397.3	10			
Std. Dev.	1.18		R^2	0.9756	
Mean	26.76		Adjusted R^2	0.9651	
C.V. %	4.4		Predicted R^2	0.9301	
			Adeq Precision	25.5399	

4.1.16.3 ANOVA result for water absorption of the cement-metakaolin blended concrete using river sand and quarry dust at 750ºC metakaolin production

The independent factors and response values shown in Table 4.17 were used for the statistical analysis to obtain the water absorption models of the cement-metakaolin blended concrete using river sand and quarry dust at 750ºC metakaolin production with the application of analysis of variance (ANOVA) and the results obtained are depicted in Table 4.28 and Table 4.29 respectively.

Table 4.28: ANOVA result for the water absorption of cement-metakaolin blended concrete using river sand at 750ºC metakaolin production

Source	**Sum of Squares**	**df**	**Mean Square**	**F-value**	**p-value**	
Model	6.35	3	2.12	51.38	< 0.0001	Significant
A-CEM	0.0387	1	0.0387	0.9387	0.3649	
B-MK	0.0571	1	0.0571	1.39	0.2774	
AB	1.79	1	1.79	43.45	0.0003	
Residual	0.2882	7	0.0412			
Cor Total	6.63	10				
Std. Dev.	0.10486		**R^2**	0.9566		
Mean	1.96		**Adjusted R^2**	0.9379		

C.V. %	5.35	**Predicted R^2**	0.8299
		Adeq Precision	20.3145

Table 4.29: ANOVA result for the water absorption of cement-metakaolin blended concrete using quarry dust at 750ºC metakaoiln production

Source	**Sum of Squares**	**df**	**Mean Square**	**F-value**	**p-value**	
Model	12.24	3	4.08	494.85	< 0.0001	Significant
A-CEM	0.0299	1	0.0299	3.62	0.0986	
B-MK	0.0182	1	0.0182	2.21	0.1806	
AB	4.49	1	4.49	545.22	< 0.0001	
Residual	0.0577	7	0.0082			
Cor Total	12.29	10				
Std. Dev.	0.0908		**R^2**	0.9953		
Mean	2.22		**Adjusted R^2**	0.9933		
C.V. %	4.08		**Predicted R^2**	0.9809		
			Adeq Precision	60.1564		

4.2 DISCUSSIONS

The results of the properties of materials and properties of the fresh and hardened Mk blended concrete as well as the regression analysis using the RSM are discussed in the following.

4.2.1 Chemical properties of metakaolin (MK)

Table 4.1 presents the chemical composition of metakaolin used for this research. The major oxides detected were SiO_2, Al_2O_3 and Fe_2O_3 with percentage values of 56.5%, 34.5%, 2.82%; 58.62%, 34.9%, 2.95%, and 55.94%, 35.5%, 2.61%, for the 650ºC**,** 750ºC**,** 850ºC MKs respectively. This means that the metakaolin satisfies the chemical requirement for N-class pozzolanic materials in ASTM C 618- (2005) presented in Table 4.2. Generally, metakaolin with $Al_2O_3 + SiO_2 + Fe_2O_3$ greater than or equal to 90% are referred to as high-reactivity metakaolin (HRM) and the loss on ignition (L.O.I) shall not be more than 10. The 650ºC**,** 750ºC**,** 850ºC MKs has $Al_2O_3 + SiO_2 + Fe_2O_3$, Sulfur trioxide (SO_3) and LOI of 93.9% , 96.4%, 94.1%

; 0.07, 0.07, 0.13 and 1.90, 1.50, 1.10 respectively. The 750ºC metakaolin with Al_2O_3 + SiO_2 + Fe_2O_3 of 96.4% will have a higher percentage of reactivity and it is expected to produce a better binder.

The results further indicated that the Al_2SO_3 present in the activated metakaolin at 650ºC, 750ºC and 850ºC were within 34% to 36%. Al_2SO_3 is the major constituents of meatakaolin which determines its ability to exhibit strong pozzolanic activity (Fernandez *et al.* 2011). The values obtained from this study were higher than the value of 32% obtained by Alabi and Omojola (2013). The presence of SiO_2 and Fe_2O_3 were also detected in the metakaolin. According to Hamdy *et al.* (2015), the active form of silica and iron in metakaolin aid in durability enhancement of concretes and thus its characteristics as a microfiller (Frias *et al.* 2000). Metakaolin activated at 750ºC exhibited higher characteristics of pozzolanic activity than 650ºC and 850ºC since the strength gain at 750ºC is higher. Ayininuola and Adekitan (2016), reported that at temperature below 700ºC (973K), calcination of metakaolin produces residual kaolinite clays that makes the products less reactive. However, at temperature above 800ºC (1123K), recrystallization occurs which can result to formation of non-pozzolanic materials (Ayininuola and Adekitan, 2016).

4.2.2 Specific gravity of metakaolin

The results of the specific gravity for the metakaolin at 650^0C, 750^0C and 850^0C were 2.62, 2.74 and 2.66 respectively as shown in Table 4.3. According to Mohammed and Pandey (2015), the specific gravity of concrete materials plays vital role in the quality of the mix and the overall strength of the concrete by correlating the voids and the solid of the cementitious material. The variation in the specific gravities of the metakaolin show that the calcination temperature

influence the chemical composition as well as the content of amorphous compound in the metakaolin which has an effect on the reactivity of the metakaolin (Abduallah *et al.,* 2017). It was observed that the metakaolin treated at 750^0C had the highest value and it is expected to have higher reactivity over 650^0C and 850^0C thereby producing concrete with better strength performance.

4.2.3 Moisture content of the aggregates

Table 4.4 shows the results for moisture content of coarse and fine aggregates. The moisture content value obtained for granite chippings, river sand and quarry dust were 1.8%, 1.9% and 2.5% respectively. They low moisture content of the aggregate ranging from 1.8% - 2.5% suggests that there are less spaces between aggregate materials. This ensures that excess water is avoided between the aggregates and only few air voids will be left after evaporation occurs. With lesser air voids, adequate compaction of the solid could be achieved thereby leading to higher strength of the concrete. Since moisture content of aggregate plays an important role in developing a proper water/cementitious ratio, it is important to determine its quantity so as not to introduce execess mixing water into the concrete mix. This is because too much mixing water will produce a weaker concrete. It therefore follows that the aggregates tested have very low moisture content values and hence are very suitable for concreting works.

4.2.4 Water absorption of the aggregates

In addition to the moisture content and condition of the aggregates, the method used to prepare the concrete, and the composition of the concrete, the rate and amount of the aggregates' water absorption in concrete also depend on these factors. The loss of the mixture's workability might result from a reduction in the water-binder ratio in freshly laid concrete, which is typically

viewed as a bad phenomena (Lucyna, 2015). In many instances, it is advisable to wet the aggregates before using them since doing so protects newly-poured concrete from water-binder reduction and preserves the workability of the mixture. According to Table 4.5, the water absorption for river sand, quarry dust, and granite chippings was 0.16 %, 0.2 %, and 0.3%, respectively. This is all less than 3% for a typical weight aggregate. The low water absorption rate of these aggregates from freshly laid concrete would improve cement paste adhesion to the aggregate and heighten concrete's tightness. As a result, the concrete will be stronger and more durable (Wojciech and Bartlomiej, 2017).

4.2.5 Specific gravity of the aggregate

The specific gravities of the various materials are shown in Table 4.6. The values of the specific gravities for granite chipping, river sand, and quarry dust were 2.95, 2.75, and 2.79 respectively. This demonstrates that the result of specific gravity of aggregates falls within the range of 2.50 to 3.0 respectively as specified by ACI EI 201 (2001). The specific gravity is normally used to calculate the solid volume of aggregates in a concrete mix and along with the water-cement ratio can be used to obtain and evaluate the expected weight, quality and strength of the concrete (Mohammed and Pandey, 2015).

4.2.6 Particle size distribution of the aggregates

The particle size distribution for the river sand and quarry dust as fine aggregates as shown in Table 4.7a and Table 4.7b fell under Zone 1 according to the BS 882:1973, which is in accordance with the percentage limits for the various recommended sieve sizes. The revised BS 882:1992 indicates that both river sand and quarry dust are under grade M. Figure 4.1b shows the grading curves for both river sand and quarry dust with 4.75mm nominal size. The

coefficient of uniformity (C_u) and coefficient of curvature (C_c) values for river sand are 15.56 and 2.93, while that for the quarry dust are 12.31 and 2.25. The granite chippings have coefficient of uniformity and coefficient of curvature values of 2.11 and 1.1 respectively. According to BS EN 933-1 (2012), the river sand and quarry dust were well graded because their C_u are greater than 6 and C_c are greater than 1. While the granite is uniformly graded, this is because the C_u is less than 4.

According to Neville (2003), these types of fine aggregates are suitable for rich mix or where low workability is required in concrete. Adopting proper percentages for the various aggregate sizes will result to an aggregate mix that is thoroughly graded. According to Haque *et al.*, (2012), a properly graded aggregate produces dense concrete and needs smaller quantities of fine aggregate and cement. Table 4.5c summarizes the results for the granite chippings. The gradation of the granite chippings shows that the aggregate had various sizes with maximum size of 20mm. The curve in Figure 4.1a indicates that the coarse aggregate is well graded resulting in lesser voids and minimum paste to fill up the concrete. Mohammed *et al.* (2010) linked particle size distribution of coarse aggregate as one of those parameters

that affects the compressive strength of concrete by ensuring workable concrete mix, higher strength lower shrinkage and greater durability.

4.2.7 Bulk density test on aggregates

Table 4.8 present the results of bulk densities of granite chippings, river sand, quarry dust respectively. The compacted and un-comapacted bulk densities for the granite chippings, river sand and quarry dust were 1310kg/m^3, 1411 kg/m^3, 1695kg/m^3 and 1192kg/m^3 , 1248 kg/m^3, 1491kg/m^3 respectively. The aggregates used gave an un-compacted to compacted ratio of 0.87-

0.91, which is in conformity with the standard ratio of 0.87-0.96 according to BS 812: Part 2 (1995) which also states the range for normal weight aggregates to be between 1180 and 1920 kg/m^3. The compacted specific densities of the aggregates shows values higher than 1100kg/m^3, which is the maximum value for aggregates used for lightweight concrete and a lower value than 2080kg/m^3, which is the minimum value for heavyweight concrete (Mehta and Monteiro, 2013). Therefore, the aggregates can be used to produce normal concrete which usually generates a compressive strength between 20MPa to 40MPa. This type of concrete is used for structural purposes.

4.2.8 Specific gravity of superplasticizer

From Table 4.9, the specific gravity for the superplasticizer was rescorded at 1.2. This material produced high workability of the concrete with variation of the cement content, reduce the water requirement of the concrete and helps in designing a good strength of concrete with less cement content (Muhsen, 2016).

4.2.9 Slump test on the fresh cement-metakaolin blended concrete

Generally, it can be seen from Table 4.10a and Table 4.10b that the variation in the production temperature of metakaolin used in making concrete did not greatly affect the slump values of the concrete produced. However, slump obtained from the 750^{0}C cement-metakaolin blended concrete, gave slightly higher readings than those from 650^{0}C and 850^{0}C for both river sand and quarry dust concrete respectively. Highest slump values of 112 mm and 98 mm at 0%MK were obtained for concrete produced with river sand and quarry dust respectively. A lowest slump value of 18 mm was recorded for the 650^{0}C cement-metakaolin concrete using quarry dust at

50%MK. It was observed that as the % content of metakaokin increased, the workability of the concrete dropped.

Considering the 750^0C cement-metakaolin concrete using river sand, slump values obtained at 0%MK to 25%MK were all higher than 100 mm. This means that replacing portland cement with 0% to 25% of metakaolin in concrete production with river sand as fine aggregate will likely generate a high slump concrete. In addition, 30%MK and 35%MK content in the concrete produced slump values 89 mm and 72 mm correspondingly. These are classified as medium slump concrete according to (Khatib *et al.,* 2018). The 40%MK and 45%MK content concrete resulted in a low slump concrete. While, the 50%MK content generated a very low slump concrete.

The cement-metakaolin concrete using quarry dust did not generate a high slump concrete for all percentage of metakaolin content and production temperature of metakaolin. Rather, its inclusion in making a the concrete ledto the production of medium slump concrete at 0% t0 35%MK content, low slump concrete at 40% and 45%MK , finally very low slump concrete at 50%Mk replacement. According to Khatib *et al.,* (2018), concrete modified by metakaolin requires less high-range water reducing admixture than other cementitious materials to achieve the same workability at the same water/binder ratio. The reduction in high- range water reducing admixture demand will reduce the tendency of surface tearing during finishing operations and consequently lead to an overall finishability.

4.2.10 Bulk density test on the hardened cement-metakaolin blended concrete

Table 4.11 clearly shows the bulk densities for all the cement-metakaolin concretes for both river sand and quarry dust respectively. The result shows that the highest and lowest values for bulk

density of the cement-metakaolin using river sand were 2521.48 kg/m^3 and 2385.19 kg/m^3, while using quarry dust were 2518.5 kg/m^3 and 2293.33 kg/m^3 respectively. According to Shohana (2015), the density of normal weight concrete lies within the range of 2,200 to 2,600 kg/m3, therefore the cement-metakaolin blended concrete for all the percentages of metakaolin replacement for both river sand and quarry dust concrete falls under the normal weight concrete. The higher values obtained with the 750^{0}C metakaolin production temperature for the river sand and quarry concrete across all percentages of replacement is associated with the degree of hydration (Hamdy, Ahmed, Tarek and Samir, 2018). During the hydration process, the hydration products for 750^{0}C temperature fills a greater part of the pore volume because the volume of the hydration products is more than that obtained for the 650^{0}C and 850^{0}C temperatures.

4.2.11 Compressive strength test on the hardened cement-metakaolin blended concrete

The compressive strength of the concrete determines the ability of the concrete to withstand load. Overall, it can be seen from Table 4.12a that the compressive strength obtained from cement-metakaolin blended concrete using river sand generated higher strength values than those produced from cement-metakaolin blended concrete using quarry dust since it has been revealed that addition of quarry dust in the production of concrete reduces the fluidity, consequently reducing the hydration water needed for fully develop the needed strength of the concrete (Luqman, Ifeyinwa, Ahmed, Azikiwe, Alfred and Olugbenga, 2022).

The results of this study further shows that there was a progressive increase in the percentage of early strength development of the binary blended concrete. Addition of metakaolin led to early strength development of the concrete. At 7days, strength readings greater than 20 N/mm^2 were already obtained at replacement levels of metakaolin ranging from 5% to 25% for both concrete under investigation and at the varying metakaolin types as illustrated in Figure 4.2a and Figure

4.2b. At 30% replacement level, 750^0C and 850^0C metakaolin produced concrete with compressive strengths greater than 20 N/mm^2 for the cement-metakaolin blended concrete using river sand. But for the cement-metakaolin blended concrete using quarry dust, only the 750^0C metakaolin produced concrete gave strength values higher than 20 N/mm^2. Replacement levels of metakaolin greater than 30% produced low load strength readings as a result of the dilution of the portland cement, which leads to decreases in the compressive strength of the cement-metakaolin pastes (Hamdy *et al.,* 2018).

The 28days compressive strength results showed that replacing portland cement with metakaolin by up to 20% will produce strength values greater than the control values. Optimum strength for all mix proportion considered and type of concrete was achieved at 20% portland cement replacement with 750^0C metakaolin using river sand as fine aggregate as shown in Figure 4.2c. Value obtained was 42.05 N/mm^2 and this was 30.81% higher than the control value. Maximum compressive values obtained for 650^0C and 850^0C metakaolin using river sand were 38.92 N/mm^2 at 15% replacement and 40.98 N/mm^2 at 20% replacement level respectively. This gave a 20.98% and 27.39% higher strength readings than their various control values respectively.

Considering the cement-metakaolin blended concrete using quarry dust, maximum strength values were obtained at 20% portland cement replacement with metakaolin for all production temperature of the metakaolin as presented in Figure 4.2d. Highest compressive strength value of 38.02 N/mm^2 was obtained from the 750^0C cement-metakaolin concrete using quarry dust as fine aggregate leading to a strength gain of about 22.02% when compared to the control value. The 650^0C cement-metakaolin concrete generated a maximum strength of 36.48 N/mm^2 while the 850^0C cement-metakaolin concrete produced a greater strength of 36.30 N/mm^2.This generated strength boost of about 17.07% and 20.38% when compared to their respective control values.

4.2.12 Young modulus of elasticity test on hardened cement-metakaolin blended concrete

The modulus of elasticity of a concrete shows the relationship between stress and strain within elasticity limit. It is a crucial property used to estimate the extent of deformation when different loads are applied on the concrete. Table 4.13 presents the young modulus of elasticity obtained from cement-metakaolin blended concrete using both river sand and quarry dust. The young modulus values followed the same path with the compressive strength values, having higher values for the cement-metakaolin concrete using river sand than using quarry dust. This is as a result of the relationship between young modulus of elasticity and the compressive strength of concrete stated in Equation (3.9) which is according to ACI building code 318.

Young modulus of elasticity readings greater than 30GPa were obtained at replacement levels of metakaolin ranging from 0% to 20% for both concrete under investigation and at the varying metakaolin types. According to Rafat (2018), the presence of metakaolin in concrete improves the mechanical properties of the concrete and its ability to withstand strains and stress in form of load. The replacement levels of metakaolin greater than 20% produced lower readings as a result of the laminar structure of the metakaolin particles. The increase in the percentage of the metakaolin causes the metakaolin particles to slide under the influence of load and thus increase the strain. The results showed that replacing portland cement with metakaolin by up to 20% will produce young modulus values greater than the control values (Fladr, Bilyand Trtik, 2019). Optimum values for all mix proportion considered and type of concrete was achieved at 20% portland cement replacement with 750^0C metakaolin using river sand as fine aggregate as illustrated in Figure 4.3a. Value obtained was 34.88 GPa and this was 12.95% higher than the control value. Maximum values obtained for 650^0C and 850^0C metakaolin using river sand were

33.55 GPa at 15% replacement and 34.30 GPa at 20% replacement level respectively. This gave 8.65% and 11.08% higher readings than their various control values respectively.

Considering the cement-metakaolin blended concrete using quarry dust, maximum young modulus values were obtained at 20% portland cement replacement with metakaolin for all production temperature of the metakaolin as shown in Figure 4.3b. Highest value of 33.16 GPa was obtained from the 750^0C cement-metakaolin concrete using quarry dust as fine aggregate leading to a gain of about 9.29% when compared to the control value. The 650^0C cement-metakaolin concrete generated a maximum value of 32.45 GPa while the 850^0C cement-metakaolin concrete produced a greater strength of 32.64 GPa.This generated strength boost of about 7.58% and 20.38% when compared to their respective control values.

4.2.13 Water absorption test on hardened cement-metakaolin blended concrete

The volume of water in a concrete matrix has a direct influence on the fresh and hardened concrete, therefore, therer need to control the amount of water present in the cement-meatakaolin concrete. Table 4.14 presents the water aborption capacity values obtained from cement-metakaolin blended concrete using both river sand and quarry dust.

Water absorption values lesser than 3% standard percentage according to BS 6349 (1989) were obtained at replacement levels of cement-metakaolin concrete using river sand ranging from 0% to 35% while 0% t0 30% for both concrete using quarry dust. The code specifies that water absorption should not exceed 3% and 2% in critical conditions such as highly aggressive chloride or freeze-thaw exposure.

The water absorption of the concrete depends on the size and interconnection of the capillary pores in the concrete as well as the moisture gradient within the surface of the concrete (Neil and Dhir, 2006). The replacement levels of metakaolin below 30% produced lower readings as a

result of increase in the percentage of metakaolin in the concrete which reduces the pores in the concrete, this is linked to filler effect and pozzolanic reaction that contributes to the reduction of porosity of the concrete (Dinakar, Pradosh and Sriram,2013). The results showed that replacing portland cement with metakaolin by up to 20% will produce water absorption values lesser than the control values. The lowest values for all mix proportion considered and type of concrete was achieved at 20% portland cement replacement with 750^0C metakaolin using river sand as fine aggregate as illustrated in Figure 4.4a. Value obtained was 1.10% and this was 54.54% lower than the control value. The same values was obtained for 650^0C and 850^0C metakaolin using river sand which was 1.22% at 20% replacement respectively. This gave 39.34% lower reading than their control value.

Considering the cement-metakaolin blended concrete using quarry dust, lowest water absorption values were obtained at 20% portland cement replacement with metakaolin for all production temperature of the metakaolin as shown in Figure 4.4b. Lowest value of 1.33% was obtained from the 750^0C cement-metakaolin concrete using quarry dust as fine aggregate leading to loss of about 62.41% when compared to the control value. The 650^0C cement-metakaolin concrete generated a maximum value of 1.46% while the 850^0C cement-metakaolin concrete produced a greater strength of 1.45%. This led 47.95% and 48.97% reduction when compared to their respective control values. Guneyisi, Gesoglu, and Mermerdas (2008) affirmed that the reduction in water absorption is due to the beneficial effect of the filling effect of MK as well as due to its pozzolanic reaction

4.2.14 Multiple regression analysis for the cement-metakaolin blended concrete

Regression analysis was carried out on the properties of the cement-metakaolin blended concrete with calcination temperature of 750^0C which had the best properties in terms of compressive

strength, young modulus of elasticity and water absorption. The models generated for the properties are discussed below;

4.2.14.1 Regression model for the compressive strength of cement-metakaolin blended concrete at 750ºC metakaolin production temperature

The multiple regression analysis of the experimental data as shown in Table 4.15, for the compressive strength of the cement-metakaolin concrete for both river sand and quarry dust gave a two factor (2FI) equation as seen in Equation (4.1) and Equation (4.2), which were statistically analyzed with the historical data (HD) using response surface methodology (RSM) in design expert software. According to Nambiar and Ramamurthy (2006), RSM allows equal precious of estimates in all directions. It has the ability to predict the results within experimental range with great precision. The statistical model generated have the attraction that once fitted ,it can be used to perform predictions more quicker than other modelling techniques and are correspondingly simpler to implement in software. This is especially true when comparing statistical modeling with artificial intelligence techniques. The statistical analysis can also provide insight into key factors influencing the compressive strength of the concrete at 28 days through correlation analysis (Zain and Abd, 2009). The 2FI model produces an interaction between the compressive strength and the actual values of the independent variables (mass of cement and mass of metakaolin) which are believed to have significant effect on the properties of the produced model.

4.2.14.2 Regression model for the young modulus of elasticity of the cement-metakaolin blended concrete at 750ºC metakaolin production temperature

The modulus of elasticity is an important mechanical property that describes the tendency of a material to deform elastically (Silva *et al.,* 2016). The multiple regression analysis of the experimental data presented in Table 4.16, for the young modulus of elasticity of the cement-metakaolin concrete for both river sand and quarry dust gave a two factor (2FI) equation as seen in Equation (4.3) and Equation (4.4) which were statistically analyzed with the historical data (HD) using response surface methodology (RSM) in design expert software. . A reduction in elastic modulus was observed with the increment in metakaolin solids; this was also reported in a previous research (Nematollahi, 2015).Furthermore, the increase of metakaolin after 20%MK tends to decrease the elastic modulus.

4.2.14.2 Regression model for the water absorption of the cement-metakaolin blended concrete at 750ºC metakaolin production temperature

The multiple regression analysis of the experimental data as shown in Table 4.17, for the water absorption of the cement-metakaolin concrete for both river sand and quarry dust gave a two factor (2FI) equation as seen in Equation (4.5) and Equation (4.6), which were statistically analyzed with the historical data (HD) using response surface methodology (RSM) in design expert software. The pozzolanic reaction provided reduction in the volume of pore space which water absorption values of concrete specimens reduced gradually as the age increases from earlier ages to 28 days. The metakaolin sample having 5%-20% had reduction in the water absorption value both for the river sand and quarry dust concrete. After 20%, the values increased with increase of metakaolin dosage. The presence of metakaolin causes refinement in

pore structure, in that pastes containing metakaolin decreases the threshold diameter and increase the percentage of small pores (Khatib and Clay 2004).

4.2.15 Model prediction and comparison with the experimental results.

The models obtained were used to predict the compressive strength, young modulus and water absorption of the cement-metakaolin blended concrete. Values obtained were compared to those generated experimentally, while the effects of independent parameters and their mutual interactions with the aid of the regression coefficients were used to generate the contour plot and 3-D surface plot from the fitted two factor interaction (2FI) equations. The results are discussed below.

4.2.15.1 Comparison between the experimental and model predicted compressive strength results for the cement-metakaolin blended concrete.

The compressive strength values generated experimentally and the model predicted results for cement-metakaolin blended concrete using river sand and quarry dust are shown in Table 4.18 and Table 4.19 respectively. The actual values for the compressive strength of the concrete using river sand and quarry dust were obtained in the laboratory, these values generated the models in Equation (4.1) and Equation (4.2) used to obtain the predicted values. It was observed that both values were closed based on the low residual values for all level of replacement. Figure 4.5a and Figure 4.5b presented the plot for the predicted-actual values. The plots shows that the points are close to the regression line due to the low residual values. Figure 4.6a and Figure 4.6b illustrated the normal plots of residuals, it shows that the values of the independent variable and the residual errors are approximately distributed in the same manner. This satisfies the assumption that regression model residuals are independent and normally distributed. The contour and 3D plots

demonstrated in Figure 4.7a, Figure4.7b and 4.8a, 4.8b respectively, indicates that combined decrease in cement and increase in metakaolin resulted to an increase of compressive strength up to a particular replacement level 20%MK and decrease of the strength of metakaolin binary concrete using river sand and quarry dust at 750ºC after this level. The decrease in compressive strength could be attributed to the clinker dilution effect of metakaolin on cement (Parande, Ramesh, Aswin, Deepak and Palaniswamy, 2008).

4.2.15.2 Comparison between the experimental and model predicted young modulus results for the cement-metakaolin blended concrete.

The young modulus of elasticity values generated experimentally and the model predicted results for cement-metakaolin blended concrete using river sand and quarry dust are shown in Table 4.20 and Table 4.21 respectively. The actual values for the young modulus of the concrete using river sand and quarry dust were obtained in the laboratory, these values generated the models in Equation (4.3) and Equation (4.4) used to obtain the predicted values. It was observed that both values were closed based on the low residual values for all level of replacement. Figure 4.9a and Figure 4.9b presented the plot for the predicted-actual values. The plots shows that the points are close to the regression line due to the low residual values. Figure 4.10a and Figure 4.10b illustrated the normal plots of residuals, it shows that the values of the independent variable and the residual errors are approximately distributed in the same manner. This satisfies the assumption that regression model residuals are independent and normally distributed. The contour and 3D plots demonstrated in Figure 4.11a, 4.11b and Figure 4.112a, Figure 4.12b indicates that combined decrease in cement and increase in metakaolin resulted to an increase of young modulus up to a particular replacement level 20%MK and decrease of the strength of cement-metakaolin binary concrete using river sand and quarry dust at 750ºC after this level.

4.2.15.3 Comparison between the experimental and model predicted water absorption results for the cement-metakaolin blended concrete.

The water absorption results generated experimentally and the model predicted values for the cement-metakaolin blended concrete using river sand and quarry dust are shown in Table 4.22 and Table 4.23 respectively. The actual values for the water absorption of the concrete using river sand and quarry dust were obtained in the laboratory, these values generated the models in Equation (4.5) and Equation (4.6) used to obtain the predicted values. It was observed that both values were closed based on the low residual values for all level of replacement. Figure 4.13a and Figure 4.13b presented the plot for the predicted-actual values. The plots shows that the points are close to the regression line due to the low residual values. Figure 4.14a and Figure 4.14b illustrated the normal plots of residuals, it shows that the values of the independent variable and the residual errors are approximately distributed in the same manner. This satisfies the assumption that regression model residuals are independent and normally distributed**.** The contour and 3D plots demonstrated in Figure 4.15a, 4.15b and Figure 4.16a, Figure 4.16b indicate that combined decrease in cement and increase in metakaolin resulted to a decrease of water absorption up to a particular replacement level 20%MK and an increase of water ingress of the cement-metakaolin binary concrete using river sand and quarry dust at 750ºC after this level.

4.2.16 Check for the adequacy of model predictions using ANOVA

The results of the analysis of variance (ANOVA) were developed through the Response Surface Method (RSM) models which were analyzed and used to check the adequacy of the models for future use. The results are discussed below.

4.2.16.1 ANOVA result for compressive strength of the cement-metakaolin blended concrete using river sand and quarry dust at 750ºC metakaolin production

The independent factors and response values shown in Table 4.15 were used for the statistical analysis to obtain the compressive strength models of the cement-metakaolin blended concrete using river sand and quarry dust at 750ºC metakaolin production with the application of analysis of variance (ANOVA) and the results obtained are depicted in Table 4.24 and Table 4.25 respectively.

For the compressive strength of the cement-metakaolin blended concrete using river sand at 750°C, the statistical results in Table 4.24 showed a standard deviation of 3.43, mean of 28.85, coefficient of variation (C.V) of 11.88, R2 of 0.9182, adjusted R^2 of 0.8832, and adequate precision of 14.692. The coefficient of determination of R^2 and the coefficient of adjusted R^2, which were calculated as 0.9182 and 0.8832, respectively, served as measures of the model's fitness. According to Goos and Gilmour (2013), these values should be at least 0.80 in order for the model to fit the data well. As a result, the regression model is suitable, as evidenced by the R^2 value of 0.9182 and the adjusted R^2 value of 0.8832. The "Adjusted R Squared" of 0.8832, as indicated in Table 4.24, is reasonably consistent with the expected R-Squared of 0.8658. The significance of the model terms can be inferred from the F-value of 26.2 and the related low probability value of 0.0004, which is less than 0.05. In this instance, the model's signal-to-noise ratio is adequate because the adequate precision value (Adequate precision = 14.692) is larger than 4, which is ideal.

According to Table 4.25, the statistical analysis of the compressive strength of the cement-metakaolin blended concrete using quarry dust at 750°C was determined to have a standard

deviation of 2.37, a mean of 26.78, a coefficient of variation (C.V) of 8.85, an R^2 of 0.9618, an adjusted R^2 of 0.9455, and an adequate precision of 20.4903. The coefficient of determination of R^2 and the coefficient of adjusted R^2 obtained as 0.9618 and 0.9455, respectively, were used to measure the fitness of the 2FI model. The R^2 value of 0.9618 and the adjusted R^2 value of 0.9455 both shows that the regression model is suitable because they are greater than 0.80. The model terms are significant, as shown by the F-value of 58.81 and the related low probability value of 0.0001, which is less than 0.05. This model has an adequate signal-to-noise ratio because the adequate precision value (Adequate precision = 20.4903) is larger than 4, which is preferred.

4.2.16.2 ANOVA result for young modulus of elasticity of the cement-metakaolin blended concrete using river sand and quarry dust at 750ºC metakaolin production

The independent factors and response values shown in Table 4.16 were used for the statistical analysis to obtain the young modulus of elasticity models of the cement-metakaolin blended concrete using river sand and quarry dust at 750ºC metakaolin production with the application of analysis of variance (ANOVA) and the results obtained are depicted in Table 4.26 and Table 4.27 respectively.

The statistical results for the young modulus of the cement-metakaolin binary concrete using river dust at 750ºC are shown in Table 4.26. They show a standard deviation of 1.49, a mean of 28.15, a coefficient of variation (C.V) of 5.29, an R^2 of 0.9539, an adjusted R^2 of 0.9342, and an adequate precision of 19.4033. The coefficient of determination of R^2 and the coefficient of adjusted R^2, which were determined to be 0.9539 and 0.9342, respectively, were used to express the fitness of the 2FI model. The R^2 value of 0.9539 and the adjusted R^2 value of 0.9342 both shows that the regression model is suitable because they are greater than 0.80. The model terms

are significant, as shown by the F-value of 48.29 and the accompanying low probability value of 0.0001, which is less than 0.05. In this instance, the value for acceptable precision (acceptable precision = 19.4033) is more than 4, which is preferable for the model to display an adequate signal-to-noise ratio.

The statistical results for the young modulus of the cement-metakaolin blended concrete using quarry dust at 750ºC are shown in Table 4.27. They show a standard deviation of 1.18, a mean of 26.76, a coefficient of variation (C.V) of 4.4, an R^2 of 0.9756, an adjusted R^2 of 0.9651, and an adequate precision of 25.5399. The coefficient of determination of R^2 and the coefficient of adjusted R^2, which were determined to be 0.9756 and 0.9651, respectively, were used to express the fitness of the 2FI model. The R^2 value of 0.9756 and the adjusted R^2 value of 0.9651 both show that the regression model is suitable because they are greater than 0.80.

The model terms are significant, as shown by the F-value of 93.19 and the accompanying low probability value of 0.0001, which is less than 0.05. As shown by the model's appropriate signal-to-noise ratio of 0.9651, the regression model is suitable in this instance since the adequate precision value (appropriate precision = 25.5399) is more than 4, which is ideal. **4.2.16.3 ANOVA result for water absorption of the cement-metakaolin blended concrete using river sand and quarry dust at 750ºC metakaolin production**

The independent factors and response values shown in Table 4.17 were used for the statistical analysis to obtain the water absorption models of the cement-metakaolin blended concrete using river sand and quarry dust at 750ºC metakaolin production with the application of analysis of variance (ANOVA) and the results obtained are depicted in Table 4.28 and Table 4.29 respectively.

For the water absorption of the cement-metakaolin blended concrete using river sand at 750°C, the statistical results in Table 4.28 showed a standard deviation of 0.10486, mean of 1.96, coefficient of variation (C.V) of 5.35, R^2 of 0.9566, adjusted R^2 of 0.9379, and adequate precision of 20.3145. The coefficient of determination of R^2 and the coefficient of adjusted R^2, which were calculated as 0.9566 and 0.9379, respectively, served as measures of the 2FI model's fitness. According to Goos and Gilmour (2013), the values should be at least 0.80 in order for the model to fit the data well. As a result, the regression model is suitable, as evidenced by the R^2 value of 0.9566 and the adjusted R^2 value of 0.9379. The "Adjusted R^2" of 0.9379, as given in Table 4.28, is reasonably consistent with the expected R-Squared of 0.8299. The significance of the model terms can be inferred from the F-value of 51.38, which corresponds to a low probability value of 0.0001, or less than 0.05. In this instance, the value for acceptable precision (acceptable precision = 20.3145) is more than 4, which is preferable for the model to demonstrate an adequate signal-to-noise ratio.

For the water absorption of the cement-metakaolin binary concrete using quarry dust at 750°C, the statistical results in Table 4.29 showed a standard deviation of 0.0908, mean of 2.22, coefficient of variation (C.V) of 4.08, R^2 of 0.9953, adjusted R^2 of 0.9933, and adequate precision of 60.1564. The coefficient of determination of R^2 and the coefficient of adjusted R^2 obtained as 0.9953 and 0.9933, respectively, were used to quantify the fitness of the 2FI model. According to Goos and Gilmour (2013), these values should be at least 0.80 in order for the model to fit the data well. As a result, the regression model is suitable, as evidenced by the R^2 value of 0.9953 and the adjusted R^2 value of 0.9933. The "Adjusted R^2" of 0.9933, as indicated in Table 4.29, and the expected R-Squared of 0.9809 are reasonably in agreement.The significance of the model terms can be inferred from the F-value of 494.85, which corresponds to

a low probability value of 0.0001, or less than 0.05. In this instance, the value for acceptable precision (acceptable precision = 60.1564) is more than 4, which is preferable for the model to display an adequate signal-to-noise ratio.

CHAPTER FIVE

CONCLUSIONS AND RECOMMENDATIONS

5.1 Conclusion

After a careful study on the evaluation of the properties of concrete made with Metakaolin at 650^0C, 750^0C and 850^0C respectively the following conclusions were drawn:

i. The summation of the oxides $Al_2O_3 + SiO_2 + Fe_2O_3$ for metakaolin treated at 750^0C had a higher percentage of 96.4% followed by that of 850^0C and the 650^0C with 94.1 and 93.9% respectively. They are all high reactive metakaolin but that produced at 750^0C performed better as a supplementary cementitious material (SCM). The properties of the materials such as specific gravity, bulk density and moisture content were found to be satisfactory for the production of a binary concrete for structural use.

ii. The workability of the fresh metakaolin binary concrete with river sand had higher slump values for some replacement levels than that of the quarry dust. The slump values decrease with increase in metakaolin. The properties of the hardened binary concrete samples showed that the compressive strength had a constant and progressive strength growth from 7 days -28days for 5%MK, 10%MK, 15%MK, and 20%MK accordingly. The highest compressive strength for the cement-metakaolin blended concrete using river sand at 750^0C and 850^0C production temperature was obtained at 20%MK, while 650^0C production temperature was obtained at 15%MK. The samples with quarry dust recorded the same progressive growth for all the

treatment temperatures and had the highest at 20%MK. Samples of the binary concrete made with river sand had higher strength than those made with quarry dust. The young modulus investigation showed the same growth path with that of the compressive strength. Water absorption capacity for the river sand samples were within the 0%-5% limit for all replacement levels and treatment temperatures. The quarry dust samples recorded above a 5% limit at 50%MK for both the 650^0C and 850^0C.

iii. The multiple regression analysis of the experimental result for the best cement-metakaolin blended concrete for the compressive strength, young modulus and water absorption was done at 750ºC for both the river sand and quarry dust. The experimental results of the blends at 750ºC generated a two factor interaction (2FI) model, which were statistically analyzed with the historical design (HD) in Response Surface Methodology (RSM) in Design Expert Software version 13.0. The predicted values were compared with the actual values and were discovered to be close based on the low residual values.

iv. The compressive strength , young modulus and water absorption values generated experimentally and the model predicted results for cement-metakaolin blended concrete using river sand and quarry dust were compared. The actual values for the properties of the concrete using river sand and quarry dust were obtained in the laboratory, these values generated the models used to obtain the predicted values. It was observed that both values were closed based on the low residual values for all level of replacement. The plot for the predicted-actual values shows that the points are close to the regression line due to the low residual values. The normal plots of

residuals show that the values of the independent variable and the residual errors are approximately distributed in the same manner which satisfies the assumption that regression model residuals are independent and normally distributed**.** The contour and 3D plots indicate that combined decrease in cement and increase in metakaolin resulted to an increase of compressive strength and the young modulus up to a particular replacement level of 20% MK and a decrease of the water absorption up to same replacement level for the cement- metakaolin produced 750ºC .

v. Using R^2, adjusted R^2 and adequate precision values in the analysis of variance table (ANOVA), the test for adequacy on the regression models showed that they are significant and adequate in predicting the effect of the interaction between cement and metakaolin. The probability values and F-values were further used to confirm the significant of the models

5.2 Recommendations

Based on the findings of this study, the following recommendations are made:

1. Kaolin obtained from Umuariga, Umudike in Abia State can be used as a binder for binary or ternary blended concrete.
2. Concrete produced with metakaolin in this research, can be used as a standard material in Nigerian construction sites and should be included in the Nigerian specification for construction materials when developed.
3. Concrete containing 5%, and up to 20% Umuariaga metakaolin can be used for structural work.
4. Kaolin from different sources in various regions in Nigeria should be explored to produce same or better quality of concrete.

5. Where early strength of concrete is desired, metakaolin can be used as replacement at percentages between 5% and 20%. However, the more the percentage addition of metakaolin, the lesser the 28day strength will be.
6. Artificial intelligence models can be used to explore the effect of metakaolin or other SCMs so as to provide advanced intelligence methodologies.

5.3 Contributions to knowledge

i. This study established that the best performance of cement-metakaolin blended concrete with respect to compressive strength, young modulus of elasticity and water absorption capacity can be obtained using metakaolin produced at calcination temperature of 750ºC as against 650ºC and 850ºC
ii. Optimum replacement level of Portland cement with metakaolin was established at 20%. For the cement-metakaolin concrete using river sand, best values for the compressive strength, young modulus of elasticity and water absorption capacity were 42.05 N/mm2, 34.88 GPa and 1.01% respectively. While, for cement-metakaolin concrete using quarry dust, optimal readings of 38.02 N/mm2 and 33.16 GPa were obtained for compressive strength, young modulus of elasticity respectively. The best value for water absorption of 1.21 was recorded at 15% replacement level.
iii. Six (6) models using the RSM have been developed to predict compressive strength, young modulus of elasticity and water absorption capacity of the cement-metakaolin blended concrete by using only the mass of metakaolin and that of Portland cement.
iv. This study established that Umuariaga metakaolin is a viable supplementary cementitious material that can be used to replace cement in concrete by 20%.

REFERENCES

Abduallah, M.M; Megat, A.M; Zainal, A.A, (2017). Characterization of metakaolin treated at different calcination temperatures. AIP conference Proceedings 1892,020028.

Abdul Aleem, M.T. and Arumairaj, P. (2012).Geopolymer concrete-A review. International Journal of Engineering Sciences and Emerging Technologies. 1(2):118-122.

Abdul Razak. (2005) "Strength Estimation Model for High Strength Concrete incorporating Metakaolin and Silica Fume", Cement & Concrete Research 35,pp 688-695

Abuguo, N. A (2004): "Civil Engineering Materials". RDC Artser Limited, Hong Kong.

Adeyanju E. and Okeke C.A. (2019). Exposure effect to cement dust pollution: A mini review. Sn Appl. Sci. 1:1572. doi: 10.1007/s42452-019-1583-0

Akinoso R., Aboaba S.A. and Olajide W.O. (2011). Optimization of roasting temperature and time during oil extraction from orange (Citrus Sinensis) Seeds. A Response Surface Methodology Approach. *African Journal of Food, Agriculture, Nutrition and Development* 11(6).

Akinoso R., Aboaba S.A. and Olajide W.O. (2011). Optimization of roasting temperature and time during oil extraction from orange (Citrus Sinensis) Seeds. A Response Surface Methodology Approach. African Journal of Food, Agriculture, Nutrition and Development 11(6).

Alaa M. R.; Hosan El-Din H. and Khalid M. (2009).Building Research Journal 57-107.

Alaa, M. R. (2013). Construction and Building Materials Pp 47- 29.

Alaa, M. R. and Sayieda, R. Z. (2011).Construction and Building Materials Pp 25- 3098.

Alabi, F.M. and Omojola, M.O.(2013). Potential of Nigerian calcined kaolin as paint pigment. African Journal of Pure and Applied Chemistry, 7(12),

Ali, M. Saidur, R. and Hossain, M. (2011). "A review on emission analysis in cement industries," Renewable and Sustainable Energy Reviews, 15(5): 2252–2261.

Ambroise, J. Murat, M. and Pera J. (2009). Cement and Concrete Research 15-261.

Annisa, R.; Hariyadi, K. and Jauhar, F. (2019). The Application of Response Surface Methods (RSM) to Study the Effect of Partial Portland cement Replacement Using Silica Fume on the Properties of Mortar. *International Journal of Civil Engineering and Technology* (IJCIET) Volume 10, Issue 04, April 2019, pp. 133-141.

Arthur, A and Peter, C (2011): " Effects of curing and composition on the properties of the outer skin of concrete". Journal of Materials in Civil Engineering, Vol 3, No 4, Pp 252-262.

ASTM C 618-17 (2017). Standard Specification for Coal Fly Ash and Raw or Calcined Natural Pozzolan for Use in Concrete. ASTM International, 100 Barr Harbor Drive, PO Box C700, West Conshohocken, PA 19428-2959. United States.

ASTM C 494/C494-81(2017). Standard specification for chemical admixtures for concrete. American Society for Testing and Materials, Philadelphia, United States, www.astm.org

ASTM D2016-74 (1987)."Method for Laboratory Determination of Water (Moisture) Content of Soil, Rock, and Soil-Aggregate Mixtures." Annual Book of ASTM Standards, Vol. 04–08. American Society for Testing and Materials, Philadelphia, United States, www.astm.org.

ASTM D 4643. 2006. "Test Method for Determination of Water (Moisture) Content of Soils by the Microwave Oven Method." Annual Book of ASTM Standards, Vol. 04–08. American Society for Testing and Materials, Philadelphia, United States, www.astm.org.

ASTM Standard C33, (2003). "Specification for Concrete Aggregates", ASTM International, West Conshohocken, PA

ASTM C 618-94 (1994). Significance of Tests and Properties of Concrete and Concrete-Making Materials, STP-169C, Philadelphia, 610 pp

Asuguo, F. O (2007): " The effect of coarse aggregate grading on strength properties of concrete". B. Eng. Project, Federal University of Technology, Owerri (unpublished).

Ayininuola, G.M.;Adekitan, O.A. (2016). Charaterization of Ajebo kaolinite clay for production of natural pozzolan. Int'l J Civ. Environ. Struct. Constr. Arch Eng, Vol 10,Issue 9, pp 1212-9.

Ayobami Busari1, Bamidele Dahunsi, Joseph Akinmusuru1, Tolulope Loto, Samuel Ajayi, (2019). Response Surface Analysis of the Compressive Strength of Self-Compacting Concrete Incorporating Metakaolin. Volume 13, Issue 2, pages 7–13.

Baba, S.U. and Usman, B. (2011). Thermal treatment of Kankara kaolin clay to produce metakaolin as partial replacement of cement in concrete production. Unpublished undergraduate project , submitted to the department of building, Faculty of Environmental Design, Ahmadu Bello University, Zaria.

Berugo, O.Y (2010): " strength and plasticity of concrete:" Doklady academic Nuak, No 4, pp 617-620.

Bignozzi, M.C.; Manzi, S.; Natali, M.E.; Rickard, W.D.; van Riessen, A. (2014). Room temperature alkali activation of fly ash: The effect of Na_2 O/SiO_2 ratio. Constr. Build. Mater. 69, 262–270.

Biljana R, Alexandra A. and Ljiljana R. (2010). “Thermal Treatment of Kaoilin Clay to obtain MK”, Institute for Testing of Materials, Belgrade, Serbia, Scientific Paper, Hem. ind. 64 (4) 351356 (2010), UDC 553.612:66.094.32

Bogue R.H. Calculation of the Compounds in Portland cement. Ind. Eng. Chem. 1929;1:1207–1214. doi: 10.1021/ac50068a006

Bondar Dali (2013). Geo-polymer concrete as a new type of sustainable construction materials.. 3rd International Conference on Sustainable Construction Materials and Technologies. http//www.claisse.info/Proceedings. Htm

Bristish Standard Institution, BS EN 197-1 (2011). Cement. Composition, specifications and conformity criteria for common cements. 389 Chiswick high road London BSI UK.

British Standard BS 882, (1992). “Specification for aggregates from natural sources for concrete”, British Standards Institute, London, United Kingdom

British Standard Institutes, BS 882: (1992). Specification for aggregates from natural sources for concrete.

British Standards Institution (2011). Testing Concrete: Method for Determination of Water Absorption.BS1881-122.

British Standards Institution, BS 1881-125 (1986). Methods for mixing and sampling fresh concrete in the laboratory. London, UK.

British Standards Institution, BS 1881-102 (1983). Method for determination of slump. London , UK.

British Standards Institution, BS 1881-108 (1983). Method for making test cubes from fresh concrete. London , UK.

British standards Institution, BS 877 (1967): “Foamed or expanded blast furnace slag lightweight aggregate for concrete” London Pp 8.

Browne, M. W. (1975). A comparison of single sample and cross-validation methods for estimating the mean squared error of prediction in multiple linear regression. British Journal of Mathematical and Statistical Psychology, 28, 112-120.

BS 8110-3 (1985). Design charts for singly reinforced beams, doubly reinforced beams and rectangular columns.

BS 812-109 (1990) BS 1377: 1990—Methods of Test for Soils for Civil Engineering Purposes. British Standards Institute, Milton Keynes.

Bucher, R.,Diederich, P., Escadeillas, G., Cyr, M. (2017). Service life of metakaolin based concrete exposed to carbonation comparison with blended cement containing fly ash,

blast furnace slag and limestone filler. Cement and concrete research journa, Vol. 99, PP 18-29.

Busari, A., Dahunsi, B., Akinmusuru, J., Loto, T. and Ajayi, S. (2019). Response Surface Analysis of the Compressive Strength of Self-Compacting Concrete Incorporating Metakaolin. Advances in Science and Technology Research Journal, 13(2): 7 – 13

Cai, J., Wu, H., Ren, Q., Lin, L., Zhou, T. and Lyu, Q. (2020). Innovative NOx reduction from cement kiln and pilot-scale experimental verification. Fuel Processing Technology, 199:

Cara, S., Gianfranco, G., Luigi, M., Paola, M., Ulrico, S., and Massimo, T., (2006). Applied Clay Science (33) 66.

Cement Admixtures Association (2009). Concrete Admixtures: Use and Application, Construction Press, New York.

Chabrelie, A., Müler, U., Skrivener, K.L. (2011). Mechanism of degradation of concrete by external sulfate ions under laboratory and field conditions. The 13th International Congress on the Chemistry of Cement, Madrid (3rd- 8th July 2011).

Chitlange, M.R.; Pajgade, P.S.(2010). Strength appraisal of artificial sand as fine aggregate in SFRC. J. Eng. Appl. Sci. 5, 34–38.

Ciobanu, C. Istrate, I. A., Tudor, P. and Voicu, G. (2021). Dust Emission Monitoring in Cement Plant Mills: A Case Study in Romania. International Journal of Environmental Res Public Health. 18(17): 9096

Composition of Cement. (2017). http://www.engr.psu.edu/ce/courses/ce584/concrete/library/construction/curing/Composition%20of%20cement.htm.

Courtland Robert (2011).Concrete planet: The strange and fascinating story of world most common man-made materials, Amherst. N.Y.

Davidovits J., (2013). Global Warming Impact on the Cement and Aggregates Industries. *World Resource Review*.6: 263.

Devi, M.; Kannan, K.(2011). Analysis of strength and corrosion resistance behavior of inhibitors in concrete containing quarry dust as fine aggregate. J. Eng. Appl. Sci. 6, 124–135.

Dinakar, P., Pradosh, K. S. and Sriram, G. (2013). Effect of Metakaolin Content on the Properties of High Strength Concrete. International Journal of Concrete Structures and Materials. 7(3): 215–223

Ding, Z and Zongjin, L (2004): " Effect of aggregates and water contents on the properties of magnesium phospho- silicate cement". Cement and Concrete Composite, 27, Pp 11-18.

Duggal, S. K. (2008). Building Materials. 3rd Revised Edition, New Age International Publishers, New Delhi, India – 110002.

Elimbi, A. Tchakoute, H. and Njopwouo, D. (2011).“Effects of calcination temperature of kaolinite clays on the properties of geopolymer cements,” Construction and Building Materials, vol. 25, no. 6, pp. 2805–2812.

Ephraim, M.E.; Akobo, I.Z.S.; Ukpata, J.O.; Akeke, G.A. (2012). Structural properties of concrete containing lateritic sand and quarry dust as fine aggregates. Adv. Civ. Eng. Build. Mater. 325–328

Etim, M. (2021). Cement Production in Nigeria. Encyclopedia. Available online: https://encyclopedia.pub/entry/14248 (accessed on 25 August 2023).

Faridah, A. S. (2009). Influence of Maximum Particulate Size of Aggregate on the Properties of Concrete. *Unpublished Undergraduate Project,* Department of Building, Ahmadu Bello University, Zaria.

Febin, G.K.; Abhirami, A.; Vineetha, A.K.; Manisha, V.; Ramkrishnan, R.; Sathyan, D.; Mini, K.M. (2019). Strength and durability properties of quarry dust powder incorporated concrete blocks. Constr. Build. Mater.228, 116793.

Felipe MA, Xiao Y, Kubicki JD (2001) Molecular orbital modeling and transition state theory in geochemistry. Rev Miner Geochem 42:485-531

Fernandez, R.;Martirena F.; Scrivener, K.I. (2011). The origin of the pozzolanic activity of calcined clay minerals: A comparison between kaolinite, illite and montmorillonite. Cement and concrete research journal,Vol.41,Issue 1, pp 113-122.

Ferraris, C.F, David, F.L and Clinton J.R (2007): “Absorption of Alkali Silica Reaction in concrete matrix. Journal of American Concrete Institute, Vol 4, No 3, Pp 101- 108.

Ferraris, C.F, Garboczi, E.J, David F.L and Clinton, J.R (2007). “The effect of stress relaxation, self-desiccation and water Absorption on the Alkali- Silica reaction in low water- cement ratio mortar”. National institute of standard and technology, building materials division 226/B350, Gaithersburg, M.D 20899.

Fladr, J., Bily, P., and Trtik, T. (2019). Analysis of the influence of supplementary cementitious materials used in UHPC on modulus of elasticity. JOP conference Series:Materials Science and Engineering, pp. 012010

Franklin associate. (2009). Characterization of building-related construction and demolition debris in the United States, Report No.EPA530-R-98-010. USA.

Frias, M.;Sanchez de Rojas;Cabrera, J. (2000). The effect that the pozzolanic reaction of metakaolin on the heat evolution in metakaolin-cement mortars. Cement and concrete research journal, Vol.30,Issue 2, pp 209-216.

Fries, M. (2000). “Pore Size Distribution and Degree of Hydration of Metakaolin Cement Pastes” Cement & Concrete Research Vol. 30,pp 561-569.

Gamble, W. (2016). "Cement, Mortar and Concrete," in Mark's Handbook for Mechanical Engineers, T. Baumeister and A.Avallone, Eds., p.177,McGraw Hill,NewYork, NY, USA, 8th edition.

Ghrici, M.; Kenai, S.; Said-Mansour, M. (2007). Mechanical Properties and Durability of Mortar and Concrete Containing Natural Pozzolana and Limestone Blended Cements. *Cement & Concrete Composites.29*, 542-549.

Gonçalves, J. Tavares, L., Toledo Filho, R. D. and Fairbairn, E. (2009). "Performance evaluation of cement mortars modified with metakaolin or ground brick," Construction and Building Materials, vol. 23, pp. 1971-1979.

Goos, P. and Gilmour, S. G. (2013). Testing for Lack of Fit of Blocking and Split Plot Response Design; 1–19. http://www.google.com.ng/url?q=https://eprints.soton.ac.uk/ 341926/1/ REMLLackofFitWorkingPaperSot

Guneyisi, E., Gesoglu, M., & Mermerdas, K. (2008). Improving strength, drying shrinkage, and pore structure of concrete using metakaolin. Materials and Structures, 41, 937–949.

Guseva, T. V., Potapova, E. N., Tichonova, I. O. and Shchelchkov, K. A. (2021). Nitrogen oxide emissions reducing in cement production. IOP Conf. Series: Materials Science and Engineering 1083 (2021) 012083

Hahn, T.F. and Emory, L.K. (1997). Cement mills along the Potomac river. Morgantown West Virginia University press.

Hale, M.W.; Freyne, S.F.; Bush, T.D.; Russell, B.W. (2008). Properties of Concrete Mixtures Containing Slag Cement and Fly Ash for use in Transportation Structures. *Construction and Building Materials.22*, 1990-2000.

Hamdy, E., Ahmed, A.A., Tarek, M.S. and Samir, E. (2018). Hydration and characteristics of metakaolin pozzolanic cement pastes. HBRC Journal, Volume 14(2), pp.150-158

Hamilton, L. C. (2012). Regression with graphics. Belmont, CA: Duxbury Press.

Haque, M.B., Tuhin, I.A and Farid, M.S., (2012). Effect of aggregate size distribution on concrete compressive strength. SUST journal of science and Technology, Vol. 19, No.5;P:35-39.

Hardjito, D.; Wallah, S.E.; Sumajouw, D.M.J. (2014).On the Development of Fly Ash Based Geopolymer Concrete. *ACI Mater. J.* 101, 467–472.

Hendriks, C. A., Worrell, E., de Jager, D., Blok, K. and Riemer, P. (2004). Emission Reduction of Greenhouse Gases from the Cement Industry. *Greenhouse gas control technologies conference paper,* 1-11.

Holland, T. C. (2005). Silica Fume User's Manual, Technical Report FHWA-IF-05-016,Silica Fume Association and United States Department of Transportation Federal Highway Administration, Washington, DC, USA.

Huat, O.C., (2006). Performance of concrete containing metakaolin as cement replacement material (Master thesis, Faculty of Civil Engineering, University Technology Malaysia,.

Hudson, B. (2009). 'Concrete Workability with High Fines Content Sands', Quarry, vol. 7, February 1999, pp. 22-25b.

Ibrahim, A.G.; Okoli, O.G.; and Dahiru, D. (2016). Comparative study of the properties of ordinary Portland cement concrete and binary concrete containing metakaolin made from Kankara kaolin in Nigeria . ATBU journal of environmental technology, Vol. 9, Issue 2, PP 53-59.

International Energy Agency (2010).World energy outlook.Online on https://www.iea.org/reports/world-energy-outlook-2010.Accessed on November, 2010.

IS 2386(Part 3):1963 Methods of test for Aggregates for Concrete: Determination of Specific Gravity. Reaffirmed- Dec 2016

Jackson, N (2011). "Civil Engineering Materials" .RDC ArtserLtd Hong Kong.

Jackson, N and Dhir, R.K (2006)."Civil Engineering Materials". Macmillan press Co- Ltd London.

Jadhao Pradip D, and Shelorkar Ajay P. (2013). "Determination of durability of Metakaolin Blend High Grade Concrete by using Water Permeability Test". *Journal of Mechanical and Civil Engineering* (IOSR-JMCE) e-ISSN: 2278-1684 Volume 5, PP 35-39.

Jani, Y. and Hogland, W. (2014).Waste Glass in the Production of Cement and Concrete. A Review: Journal of Environmental Chemical Engineering, 2(8): 1767-1775.

Jyothi, C. N. and Chaitanya, J. D. (2015). Partial replacement of cement with metakaolin in high strength concrete. Int. J. Engg. Res. & Sci. & Tech. 4(4):339 - 349

Kamalanathan, G and Sivakumar, A (2008). Study of self compacting properties of quarry dust cement mortar using marsh cone flow studies, Proceedings, International Conference on Advances in Concrete and Construction, ICACC-2008, 7-9 February 2008, Hyderabad, India, pp. 7278.

Karakurt, C., Topçu, I.B. (2011). Effect of blended cements produced with natural zeolite and industrialby-products on alkali-silica reaction and sulfate resistance of concrete. Construct Build Mater 25: 1789-1795.

Kathleen M. Carley, Natalia Y. Kamneva, Jeff Reminga, 2004. Response surface methodology-CASOS technical report. Institute for Software Research International-04-136.

Khater, H.M. (2014). “Preparation and Characterization of MK-Blended Cement Mortar Having Various Water/Binder Ratios” *Housing and Building National Research Centre* (HBNRC) 87 P.O. Box 1770 Cairo.

Khatib, J.M. and Clay, R. (2004). Absorption chacracteristics of metakaolin concrete. Cement and concrete research journal, Vol. 34, No. 1, 2004,PP 19-29.

Khatib, J.M.; Baalbaki, O.; ElKordi, A.A. (2018). Metakaolin. Online at :https://www.researchgate.net/publication/325801270. Accessed on 01/2018

Khatib, J.M.; Hibbert, J.J. (2005).Selected Engineering Properties of Concrete Incorporating Slag and Metakaolin. *Construction and Building Materials*.,*19*, 460-472.

Kong D.L.Y. and Sanjayan J.G.(2008). Cem.Concr.Compos.30 : 986.

Kosmatka, S. and Panarese, W. (2008). Design and Control of Concrete Mixtures, Portland Cement Association, Skokie,IL,USA.

Kosmatka, S.; Kerkhoff, B. and Panerese, W. (2002).Design and Control of Concrete Mixtures, Portland Cement Association, Skokie, IL, USA, 14th edition.

Kurtins, K.E. (2011). Benefits of metakaolin in HPC. HPC bridge views, issue

Lea, F. (2018). The Chemistry of Cemen andConcrete .https://ci.nii.ac.jp/naid/10003996296/.

Lee, S. T., Moon H.Y., Swamy, R. N. (2005). Sulfate attack and role of silica fume in resisting strength los. Cement & Concrete Composites 27: 65-76.

Liew, Y .M.; Kamarudin, H.; Mustafa, A.M.; Luqman, M.; KhairulNizar, I.; and Heah, C.Y (2011). *Australian Journal of Basic and Applied Sciences* 5-441.

Lim, C.; Jung, E.; Lee, S.; Jang, C.; Oh, C.; Shin, K. (2020). Global trend of cement production and utilization of circular resources. Journal of energy engineering, Vol. 29, Issue 3,pp 57-63.

Luqman, A.T., Ifeyinwa, I.O., Ahmed, O.O., Peter, O., Alfred, B.O., Olugbenga, O.A. (2022). Mechanical behavior of composite produced with quarry dust and rice husk ash for sustainable building applications. Case Studies in Construction Materials, Volume 17,e01157.

Mahajan, B. (2020). Density of Cement, Sand, Aggregate & Steel | Density of Steel. https://civiconcepts.com/blog/density-of-cement

Malhotra V. M. (2002). “High-performance high volume fly ash concrete,” ACI Concrete International, vol. 24, pp. 1–5.

Malhotra V. M. (2002). “Introduction: sustainable development and concrete technology,” ACI Concrete International, vol. 2, pp. 4.

Malhotra, V. M., (2009). "Correlation between particle shape and surface texture of fine aggregates and their water requirement", Materials Research & Standard, December, pp.656-658.

Mamlouk, M. and Zaniewski, J. (2009). Materials for Civil and Construction Engineers, Addison Wesley Longman, Inc, Menlo Park, CA, USA.

Manu, S., Menashi, C., Olek Jan, D. (2002). Mechanism of sulfate attack: A fresh look Part1: Summary of experimental results. Cem Concr Res 32: 915-921.

Marquez, S.; Tikalsky, P.J.; Hanson, S. (2009). *Environmental Advantages of Ternary Cement Combinations*, Proceedings of the Second International Symposium on UltraHigh Performance Concrete, Kassel, Germany, March 5-7, 2008; Fehling, E; Schmidt, M.; Sturwalt, S. Eds.; University of Kassel: Germany. 135-141.

Matar, W. and Elshurafa, A.M. (2017). Striking a balance between profit and carbon dioxide emissions in the Saudi cement industry. International journal of greenhouse gas control, Vol. 61, pp 111-123

Mehta, P.K. (2009). Advancements in Concrete Technology. Concrete International.21, 69-76.

Mehta, P.K. (1999). Concrete technology for sustainable development. Concr. Int., 21(11): 47-52.

Mehta, P.K; Monteiro, A. (2013). Concrete structure, properties and materials. Edition: fourth edition. Publisher: McGraw-Hill ISBN: 978-0-07-179787-0. Prentice Hall, Inc., Englewood cliffs,NJ.

Melis, L. M (2015): "An evaluation of tensile strength testing". Center for transportation research report 432-1F, University of Texas.

Menendez, G.; Bonavetti, V.; Irassar, E.F. (2002).Strength Development of Ternary Blended Cement with Limestone Filler and Blast-Furnace Slag.Ce*ment & Concrete Composites*, *25*, 61-67.

Mindess, S.and Young, J. F. (2008). Concrete, Prentice-Hall, Inc., Englewood Cliffs, NJ, USA.

Mir, A.H. (2015).Improved Concrete Properties Using Quarry Dust as Replacement for Natural Sand. Int. J.Eng. Res. Dev. 11, 46–52.

Misnikov, O.S. (2014). "A study of the properties of Portland cement modified using peat-based hydrophobic admixtures," Polymer Science Series D, vol. 7, no. 3, pp. 252–259.

Mohammed S. I., Collette C. and Sean M. (2013). Trends and Developments in Green Cement and Concrete Technology. *International Journal of Sustainable Built Environment*, 194 – 216.

Mohammed, A.A. and Pandey, R.K.,(2015).Influence of specific gravity on weight of proportions of concrete. International journal of Engineering Research and Technology (IJERT), Vol.4 Issue 02.

Mohammed, M.A., Gomathi, D. (2017). Strength properties of concrete using metakaolin. International journal of Engineering Research and Technology (IJERT). Vol. 6, Issue 11, 149-152.

Mohammed, M.S.,Salim, Z., and Said, B.(2010). Effect of content and particle size distribution of coarse aggregate on compressive strength of concrete construction and building materials, 24,505-512.

Morsy, M.S, Rashed, A.M and El-nouhy, H.A (2009). Effect of Elevated Temperature on the Physico-Mechanical Properties of Metakaolin Blended Cement Mortar. Structural Engineering Mechanics 3(6): 1-10.

Morsy, M.S, Shebi.S.S and Rashad, A. M. (2010). Effect of Fire on Micro structure and Mechanical Properties of Blended Cement Paste Containing Metakaolin and Silica Fumes, Sillic Ind. 56(23): 173-185.

Mosteller, F., &Tukey, J. W. (1977). Data analysis and regression. Reading, MA: Addison-Wesley.

Muhsen, S.; Salahaldein, A.; Megat, J. (2016). Effect of Superplasticizer Dosage on Workability and Strength Characteristics of Concrete. IOSR Journal of Mechanical and Civil Engineering (IOSR-JMCE),Volume 13, Issue 4 Ver. VII, pages 153-158.

Mukherjee, S. P. and Vesmawala, G. (2013). Literature Review on Technical Aspect of Sustainable Concrete. *International Journal of Engineering Science Invention.* 2(8)1-9.

Murat, M. and Sorrentino, F. (2006). "Effect of large additions of Cd, Pb, Cr, Zn, to cement raw meal on the composition and the properties of the clinker and the cement," Cement and Concrete Research, vol. 26, no. 3, pp. 377–385.

Murat, M., (1983). "Hydration Reaction and Hardening of Calcined Clays and Related Minerals", Cement and Concrete Research, 13(2), 259- 266.

Myers R.H. and Montgomery D.C. (2005). Response surface methodology; Process and product optimization using designed experiments. John Wiley and Sons, Canada.

Myers Raymond H. & Montgomery, D.C., (2002). "Response Surface Methodology: process and product optimization using designed experiment,." A Wiley-Interscience Publication.

Nambiar, E.K. and Ramamurthy, K. (2006). Models relating mixture composition to the density and strength of foam concrete using responses surface methodology. Cement concrete composition journal, Vol., pp 752-760.

Natesan , M.;Steve, S.; Kenneth, H.(2003). The cement industry and global climate change: Current and potential future cement industry CO^2. Proceedings of the 6th international conference on greenhouse gas control technologies, Volume II, 2003, pages 995-1000

Neil, J. and Dhir, R.K. (2006) Civil Engineering Materials. 5th Edition, Macmillan Education, Basingstoke. Khatib, J.M. and Clay, R.M. (2003) Absorption Characteristics of Metakaolin Concrete. Cement and Concrete Research.

Nematollahi, B.; Sanjayan, J.; Shaikh, F.U.A. (2015).Matrix design of strain hardening fiber reinforced geopolymer composite. Compos. Part B Eng.,27,PP 253-265.

Neville, A. M (2009): " Properties of concrete". Longman publishing Co- Ltd, London.

Neville, A. M (2013): "Properties of Concrete". English language Book society and pitman publishing, London.

Neville, A.M. and J.J. Brooks (2010). Concrete Technology, 2nd Edition, Pearson Education Canada, 464pp.

Okeke O.C and Iwuoha S.C (2005). Strength and durability characteristics of crushed – rock aggregates from Oban Massif, Southeastern Nigeria. Journal of Science Engineering and Technology 12(3), p,6259-6269.

Omopariola, S.S. and Jimoh, A.A. (2017). An evaluation of the physical and mechanical properties of coarse aggregates produced in Ogun state, Nigeria. International journal of scientific & engineering research, Vol.8, Issue 11,pp 1238-1245.

Onyenuga, V.O (2009). "Reinforced concrete design".Asros Limited, Lagos.

Parande, A.K.; Ramesh Babu, B.; Aswin Karthik, M.; Deepak Kumaar, K.K.; Palaniswamy, N (2008). Study on strength and corrosion performance for steel embedded in metakaolin blended mortar. Constr. Build. Mater., 22, 127–134

Patentsgoogle.com, (2018). "Portland cement manufacture," Patent No. US4081285A. https://patents.google.com/patent/ US4081285A/en.

Patricija, K., Aleksandrs, K. and Valdemars, S. (2013). Evaluation of Properties of Concrete Incorporating Ash as Mineral Admixture. *Construction Science*, 17-25.

Pedhazur, E. J. (2012). Multiple regression in behavioral research: Explanation and Prediction (2nd ed.). New York, NY: Holt, Rinehart and Winston.

Portland Cement Clinker: (2017). The Bogue Calculation. http://www.understanding-cement.com/bogue.html#.

Portland Cement Association (2012). Retrieved: December, 28,2012 Website: http:// www.cement.org/basics/concrecelibasicsaggregate.asp

Potgieter, J.H. (2012). An overview of cement production: How green and sustainable is the industry?

Powers, T. C. and Brownyard, T. L. (2009). "Studies of the physical properties of hardened Portland cement paste," ACI Journal Proceedings, vol. 43, no. 9, pp. 101–132.

Priya, R. and Partheeban, P. (2013). Durability Study of Low Calcium Flyash Based Geopolymer Concrete. *Indian Journal of Applied Research (IJAR),Volume 3,Issue 6,pages 180-182*

Rafat Siddique, and Juvas Klaus, (2008). "Influence of Meatakaolin on the Properties of Mortar and Concrete", An International Journal on the Application and Technology of Clays and Clay Minerals, ISSN NO:0169-1317, volume 43, issues 3-4, march 2009, Year 2008.

Rashad A. M. (2013). Metakaolin as Cementitious Material: History, Scours, Production and Composition: A Compressive Overview. Construction and Building Materials, 4(1): 308-318.

Ruben, S., Gilles, M. and Jan, E. (2012). Supplementary Cementitious Materials. Reviews in Mineralogy & Geochemistry,Vol. 74 pp. 211-278.

Sabir, B.B.; Bai, S. and Wild, J. (2001). Cement & Concrete Composites 23 - 441.

Sanjay, N. P., Anil, K. G. and Subhash, S. D. (2013). Metakaolin- Pozzolanic Material for Cement in High Strength concrete. In: *Proceeding of the 2nd international Conference on Emerging Trends in Engineering* (SICETE' 13), 46-49.

Schneider, A., Hommel, G. and Blettner, M. (2010). Linear regression analysis. Dtsch Arztebl Int. 107(44): 776–782

Schneider, M. Romer, M. Tschudin, M. and Bolio, H. (2011)."Sustainable cement production—present and future," Cement and Concrete Research, vol. 41, no. 7, pp. 642–650.

Shehata, M.H.; Thomas, M.D.A. (2011). Use of Ternary Blends Containing Silica Fume and Fly Ash to Suppress Expansion due to Alkali-Silica Reaction in Concrete. *Cement and Concrete Research*, *32*, 341-349.

Shetty M.S. (2005). Concrete Technology Theory and Practice S. Chand & Company Ltd. Ram Nagar, New Delhi - 110 055.

Shetty, M.S (2000): " Construction technology". Pitman publishing company London.

Shetty, M.S (2004). "Concrete Technology". Pitman publishing company, London.

Shetty, M.S. (2012). "Concrete Technology". Schand publishers, India.

Siddique, R. and Klaus, J. (2009).Applied Clay Science 43-392.

Silva, R. V.; De Brito, J.;Dhir,R.K. (2016).Establishing a relationship between modulus of elasticity and compressive strength of recycled aggregate concrete. J clean. Prod.,112, PP 2171-2186

Srinivasan, R., Sathiya, K. and Palanisamy, M. (2010). Experimental Investigation in Developing Low Cost Concrete from Paper Industry Waste. *Buletinul Institutului Politehnic Din Iaşi,* 56(1), 43.

Stoiber W. (2003). Communition technology and energy consumption, part 1. Cement International 1(2), pp. 45 - 52

Subasi, A.;Sahin, B.; Kaymaz, I.(2016). Multi-objective optimization of honeycomb heat sinkusing the Response Surface Method.Int. J. Heat Mass Transf.,101,295-302.

Sundaralingam, K., Peiris, A., Anburuvel, A. and Sathiparan, N. (2022). Quarry dust as river sand replacement in cement masonry blocks: Effect on mechanical and durability characteristics. Materialia, 21: 101324

Thai, T.; Kučera, P.; Bernatik, A. Noise Pollution and Its Correlations with Occupational Noise-Induced Hearing Loss in Cement Plants in Vietnam. Int. J. Environ. Res. Public Health 2021, 18, 4229

Thiery, M; Villain, G.; Dangla, P.; and Platret, G. (2018).“Investigation of the carbonation front shape on cementitious materials: effects of the chemical kinetics,” Cement and Concrete Research, vol. 37, no. 7, pp. 1047–1058.

Thomas, M.; Hopkins, D.S.; Perreault, M.; Cail, K. (2012).Ternary cement in Canada. *Concrete International*, *29*, 59-65.

Tian, B., Cohen, M.D. (2000). Does gypsum formation during sulfate attack on concrete lead to expansion?. Cem Concr Res 30:117-123.

Venkatarama Reddy, B. V (2004). Sustainable building technologies: Application of Science &Technology to Rural Areas (ASTRA), Special Section, Current Science, 87(7): 899-907.

Viswanadha Varma D., Rama Rao G.V., Sindhu J., (2014). “Effect of Temperature on Metakaolin Blended High Strength Concrete”. *International Journal of Engineering Research and Development.* e-ISSN: 2278-067X, p-ISSN: 2278-800X, www.ijerd.com Volume 10, Issue 5 PP.57-67.

Walker, D and Bloem R (2009): “Free and restrained shrinkage of Normal and High strength concrete”. ACI Materials Journal, Vol 92, No 2, pp 211- 217.

Wild, S.; Khatib J.M. and Jones, A., (1996). “Relative Strength, Pozzolanic Activity and Cement Hydration in Superplasticised Metakaolin Concrete”, Cement and Concrete Research, 26(10), 1537-44.

Wojciech, P. and Bartlomiej Z. (2017). The effect of cement paste volume and w/c ratio on shrinkage strain, water absorption and compressive strength of high performance concrete. Construction and Building Materials, Volume 140 (1), pp 395-402.

www.hpcbridgeviews.com/i67/Article 3.asp.

Yassar M.H (2006): " Composition Action of foamed and lightweight aggregate concrete". Journal of Materials in Civil Engineering , Vol 8, No 3, pp 111-113.

Zahid, M.; Shafiq, N.; Jalal, A.,(2018). Investigating the effects of solarcure curing method on the compressive strength, microstructure and polymeric reaction fly ash based geopolymer. Construction Building Materials.181, 227-237.

Zain, M.F.M and Abd, S.M. (2009). Multiple regression model for compressive strength prediction of high performance concrete journal of applied sciences, Vol. 9, Issue 1,pp 155-160

Zongjin, Li. (2011). *Advanced Concrete Technology*. Hoboken, New Jersey: John wiley and sons. Inc.

APPENDICES

Appendix A1

MIX DESIGN (River Sand)

Compressive Strength (28 days) = $30N/mm^2$

- Aggregate type – Crushed (Coarse)
- Aggregate type – Uncrushed (Fine)
- Cement type – 42.5 Class (O.P.C) plan
- Particle density on SSD for Fine – 2.75
- Particle density on SSD for Coarse – 2.95
- Maximum size of aggregate – 20mm
- Percentage passing through 600µm = 25%

STEP 1: Selection of target mean strength

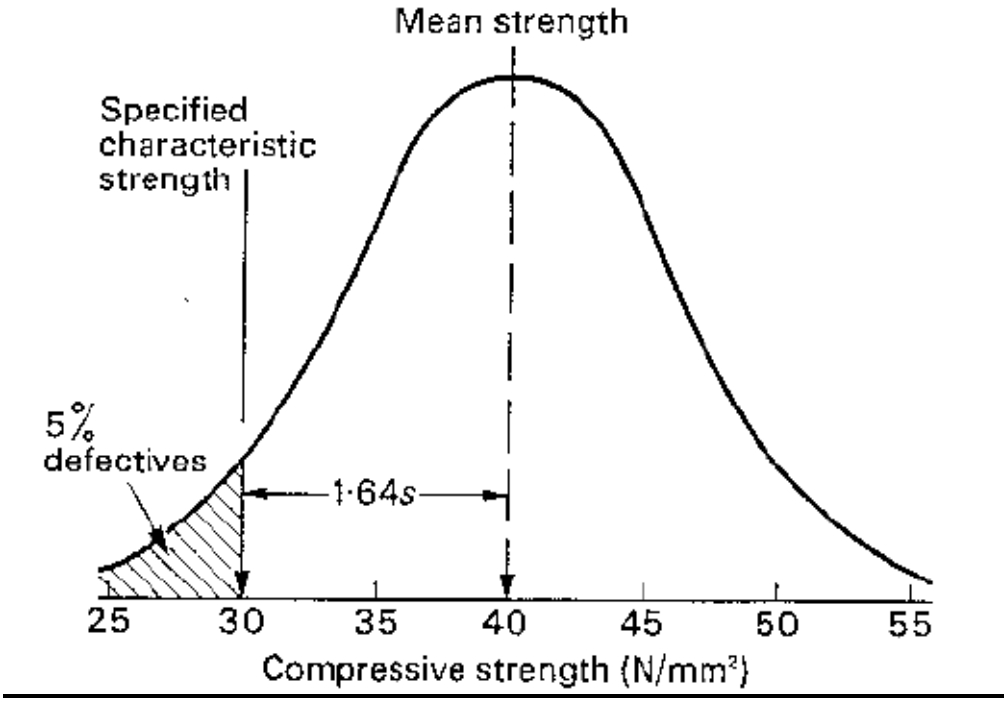

Figure A1.1: Normal distribution of concrete strength (source: Building Research Establishment, 1997)

Table A1.1: K factor table

Percentage	K
10	1.28
5	1.64
2.5	1.96

1	2.33

(source: Building Research Establishment, 1997)

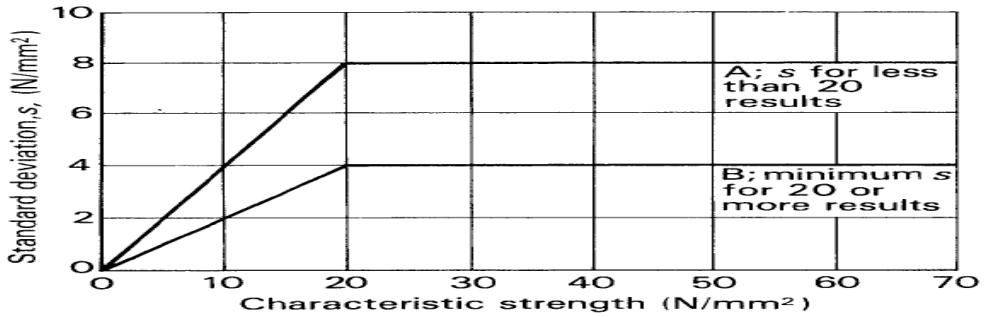

Figure A1.2: Characteristic Strength Versus Standard Deviation Relationship (source: Building Research Establishment, 1997)

Computation of Mean target strength

Fm = Fc + Ks

From Figure 1

For 5% defective

K = 1.64

From Figure 3

S = 4 N/mm^2

Fc = 30 N/mm^2

Fm = 30 + (1.64×4)

Fm = 36.56 N/mm^2

STEP 2: Selection of water/cement ratio

Table A1.2: Approximate compressive strength of concrete mixes made with free water/cement ratio of 0.5

Cement Strength Class	**Type of coarse aggregate**	**Compressive strengths(N/mm2) Age (days)**			
		3	7	28	91
42.5	Uncrushed	22	30	42	49
	Crushed	27	36	49	56
52.5	Uncrushed	29	37	48	54
	Crushed	34	43	55	61

(source: Building Research Establishment, 1997)

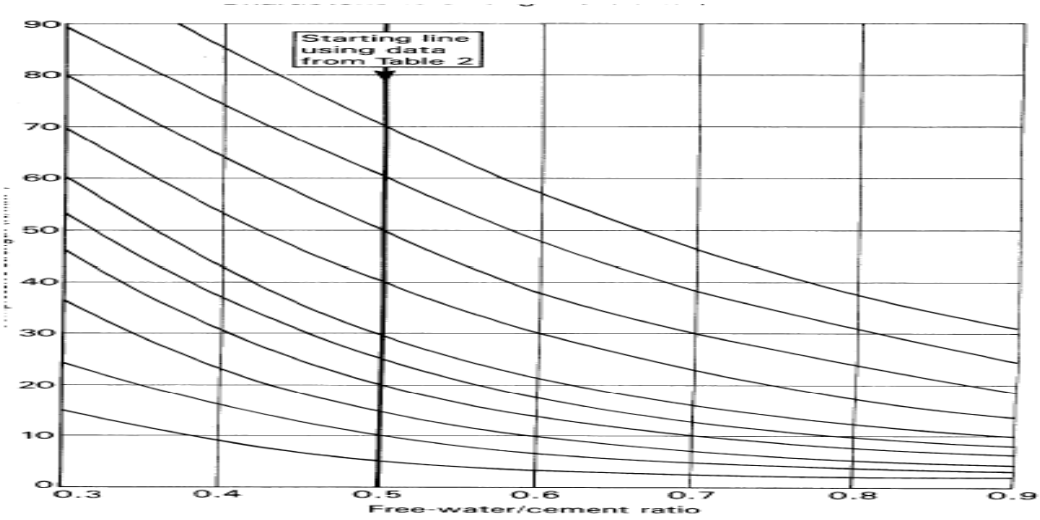

Figure A1.3: Relationship between compressive strength and free/water ration (source: Building Research Establishment, 1997)

Table A1.3: Maximum water cement ratio for reasonable durability

Condition of Exposure	**Maximum Water Cement Ratio**	
	Plain Concrete	**Reinforced Concrete**
Internal, Subject to heavy condensation	-	0.60
Alternate wetting and drying	0.60	0.60
Freezing and Thawing	0.55	0.50
Seawater or salt spray	0.50	0.45
Water retaining structure	-	0.50

(source: Building Research Establishment, 1997)

Determination of the required water-cement ratio involves using 42.5 grade of cement, crushed coarse aggregate and 28 days in Table A1.2 to get the approximate compressive strength ($49N/mm^2$). Using Figure A1.3, we first trace out the Fm and approximate compressive strength curves gotten from (Table A1.2), parallel to the existing curves. Then, we trace a

horizontal line from where the Fm curve intercept with the starting line towards the approximate compressive strength curve. At the point of interception, trace vertically downwards to get its corresponding value on the horizontal or x axis (water/cement ratio) which was gotten as 0.64.

According to Table A1.3, for alternate wetting and drying condition and concrete being plain, which has its maximum as 0.6 , then adopt **0.4** to produce a concrete with better strength.

STEP 3: Selection of slump range

Table A1.4: Workability, Slump and Compacting factor of concrete with 19mm or 38mm size of aggregate

Degree of workability	Slump		Compacting factor	Use for which concrete is suitable
	mm	in.		
Very low	0–25	0–1	0.78	Roads vibrated by power-operated machines. At the more workable end of this group, concrete may be compacted in certain cases with hand-operated machines.
Low	25–50	1–2	0.85	Roads vibrated by hand-operated machines. At the more workable end of this group, concrete may be manually compacted in roads using aggregate of rounded or irregular shape. Mass concrete foundations without vibration or lightly reinforced sections with vibration.
Medium	25–100	2–4	0.92	At the less workable end of this group, manually compacted flat slabs using crushed aggregates. Normal reinforced concrete manually compacted and heavily reinforced sections with vibration.
High	100–175	4–7	0.95	For sections with congested reinforcement. Not normally suitable for vibration.

(Building Research Establishment, Crown copyright)

(Source: Building Research Establishment, 1997)

Adopt range of 25mm-100mm slumps for medium degree of workability

STEP 4: Selection of free water content

Table A1.5: Approximate Free-Water Content (kg/m^3) Required to Give Various Levels of Workability.

Slump (mm)		**0-10**	**10-3**	**30-60**	**60-180**
Vebe time (s)		**>12**	**6-12**	**3-6**	**0-3**
Max. size of aggregate (mm)	**Type of Aggregate**				
10	Uncrushed	150	180	205	225
	Crushed	180	205	230	250
20	Uncrushed	135	160	180	195

	Crushed	170	190	210	225
40	Uncrushed	115	140	160	175
	Crushed	155	175	190	205

(Source: Building Research Establishment, 1997)

Selection of free water content kg/m^3 from Table A1.5 considering the workability, size of aggregate and type of aggregate and using the formula(since the fine and coarse are of different types);

$\frac{2}{3}W_f + \frac{1}{3}W_c$

$= \frac{2}{3} \times 180 + \frac{1}{3} \times 210$

$= 120 + 70$

$= 190kg/m^3$

STEP 5: Selection of the cement content

Determination of cement content

$\frac{Water}{Cement} = 0.4$

$\frac{190}{Cement} = 0.4$

Cement = $\frac{190}{0.4}$

Cement = $475kg/m^3$

STEP 6: Confirmation of the calculated cement content

Table 6.1: Maximum Cement Content for Concretes with 20mm Maximum Aggregate Size under

Table A1.6: Different Condition of Exposure

Exposure Conditions	**Minimum Cement Content for Concrete (Kg/m3)**		
	Plain	**Reinforced**	**Pre-stressed**
Non-corrosive	220	250	300
buried or sheltered from rain	250	290	300

Exposed to alternate wetting and drying or seawater	310	360	360
subject to de-icing salt	280	390	300

(source: Building Research Establishment, 1997)

Comparing the amount of the cement content calculated and the minimum allowable cement content for durability, since the minimum for alternate wetting and drying condition for plain concrete is $310kg/m^3$

$475kg/m^3$ is okay.

STEP 7: Selection total aggregate content

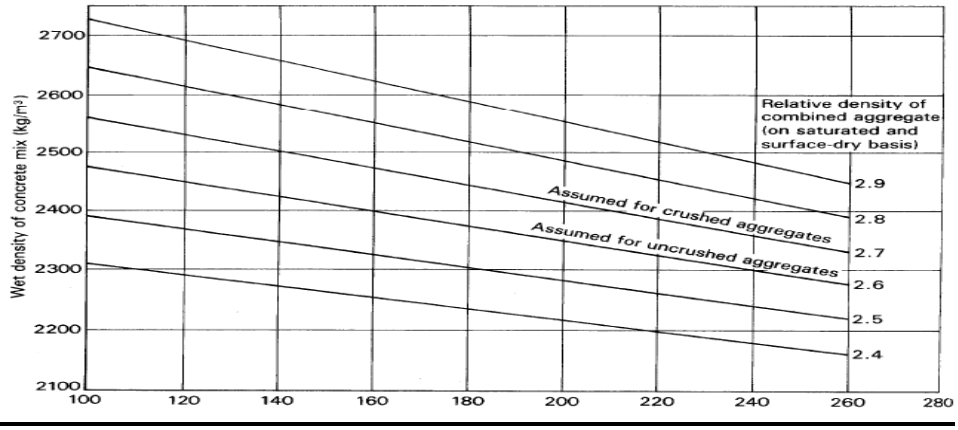

Figure A1.4: Relationship between free-water content and Estimated wet density of fully compacted concrete (source: Building Research Establishment, 1997)

Determination of total aggregate content

Using Figure 7.1 ;

Particle density for Coarse = 2.95

Particle density for Fine = 2.75

Combined = 2.90

Using the value for water content gotten as $190kg/m^3$

We trace the value vertically upward to touch 2.9 line. From the point of interception, draw a line to touch the y axis and read off the value (which is the wet density of concrete)

D = 2565kg/m^3, C= 475kg/m^3, W= 190kg/m^3

D = 2565 – 475 – 190

D = 1900kg/m^3

STEP 8: Selection of fine and coarse aggregate contents

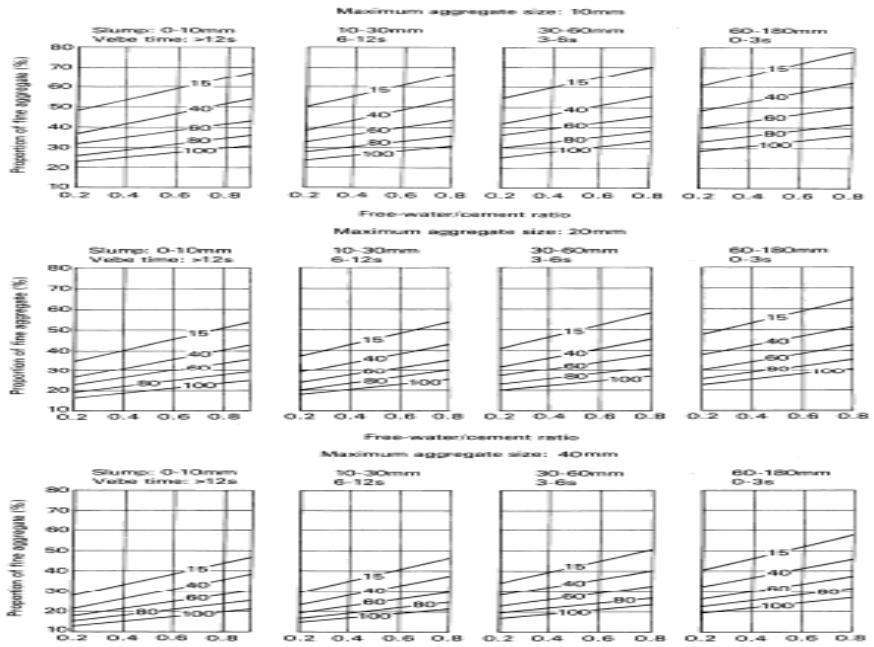

Figure A1.5: Recommended Percentages of fine aggregate in total aggregate as a function of free-water/cement ratio for values of workability and maximum size of aggregate

Selection of Fine and Coarse aggregate contents:

From the sieve analysis for aggregate, we use % passing 600μm sieve size which is 24.49%

From figure A1.5

Slump = 30 – 60 mm

Maximum size of aggregate = 20mm

Proportion of the fine aggregate = 42%

Fine aggregate Content

$= \frac{42}{100} \times 1900$

$= 798 kg/m^3$

Coarse aggregate Content

= 1900 – 798

$= 1102 kg/m^3$

STEP 9: Selection of the mix proportion of materials by weight

Estimating the mix proportion by weight

Water Content	Cement	Fine Aggregate	Coarse Aggregate
$\mathbf{190 kg/m^3}$	$475 kg/m^3$	$798 kg/m^3$	$1102 kg/m^3$

Divide through by the content of cement to get the mix ratio, using 0.4 water/cement ratio.

STEP 10: Selection of the laboratory quatities of materials in (kg)

Quantity of materials in kg

Volume of concrete in a cube (150m × 150m × 150m)

$V = 0.15 \times 0.15 \times 0.15$

$V = 0.0034 m^3$

Adding 20% waste of total volume

$= (\frac{20}{100} \times 0.0034) + 0.0034$

$= 0.0041 m^3$

Quantity of Water $= 190 \times 0.0041 = 0.78 kg$

Quantity of Cement = $475 \times 0.0041 = 1.9475kg$

Quantity of FA = $798 \times 0.0041 = 3.3kg$

Quantity of CA = $1102 \times 0.0041 = 4.52kg$

Quantity of superplasticizer = 0.03kg (1.3% of cement content)

For Metakaolin treated at 650^{oC}, 750^{oC} and 850^{oC}

100% Cement- 0% Metakaolin

Water Content kg/m^3	**Cement** kg/m^3	**Fine Aggregate** kg/m^3	**Coarse Aggregate** kg/m^3
0.78	1.95	3.3	4.52

95% Cement- 5% Metakaolin

Water Content kg/m^3	**Cement** kg/m^3	**Metakaolin** kg/m^3	**Fine Aggregate** kg/m^3	**Coarse Aggregate** kg/m^3
0.78	1.85	0.10	3.3	4.52

90% Cement- 10% Metakaolin

Water Content kg/m^3	**Cement** kg/m^3	**Metakaolin** kg/m^3	**Fine Aggregate** kg/m^3	**Coarse Aggregate** kg/m^3
0.78	1.755	0.195	3.3	4.52

85% Cement- 15% Metakaolin

Water Content kg/m^3	**Cement** kg/m^3	**Metakaolin** kg/m^3	**Fine Aggregate** kg/m^3	**Coarse Aggregate** kg/m^3
0.78	1.6575	0.2925	3.3	4.52

80% Cement-20% Metakaolin

Water Content kg/m^3	**Cement** kg/m^3	**Metakaolin** kg/m^3	**Fine Aggregate** kg/m^3	**Coarse Aggregate** kg/m^3
0.78	1.56	0.39	3.3	4.52

75% Cement- 25% Metakaolin

Water Content kg/m^3	**Cement** kg/m^3	**Metakaolin** kg/m^3	**Fine Aggregate** kg/m^3	**Coarse Aggregate** kg/m^3
0.78	1.4625	0.4875	3.3	4.52

70% Cement-30% Metakaolin

Water Content kg/m^3	**Cement** kg/m^3	**Metakaolin** kg/m^3	**Fine Aggregate** kg/m^3	**Coarse Aggregate** kg/m^3
0.78	1.365	0.585	3.3	4.52

65% Cement-35% Metakaolin

Water Content kg/m^3	**Cement** kg/m^3	**Metakaolin** kg/m^3	**Fine Aggregate** kg/m^3	**Coarse Aggregate** kg/m^3
0.78	1.2675	0.6825	3.3	4.52

60% Cement-40% Metakaolin

Water Content kg/m^3	**Cement** kg/m^3	**Metakaolin** kg/m^3	**Fine Aggregate** kg/m^3	**Coarse Aggregate** kg/m^3
0.78	1.17	0.78	3.3	4.52

55% Cement-45% Metakaolin

Water Content kg/m^3	**Cement** kg/m^3	**Metakaolin** kg/m^3	**Fine Aggregate** kg/m^3	**Coarse Aggregate** kg/m^3
0.78	1.0725	0.8775	3.3	4.52

50% Cement-50% Metakaolin

Water Content kg/m^3	**Cement** kg/m^3	**Metakaolin** kg/m^3	**Fine Aggregate** kg/m^3	**Coarse Aggregate** kg/m^3
0.78	0.975	0.975	3.3	4.52

Appendix A2

MIX DESIGN (Quarry Dust)

Compressive Strength (28 days) = $30N/mm^2$

- Aggregate type – Crushed (Coarse)
- Aggregate type – Crushed (Fine)
- Cement type – 42.5 Class (O.P.C) plain
- Particle density on SSD for Fine – 2.79
- Particle density on SSD for Coarse – 2.95
- Maximum size of aggregate – 20mm
- Percentage passing through 600µm = 30.55%

STEP 1: Selection of target mean strength

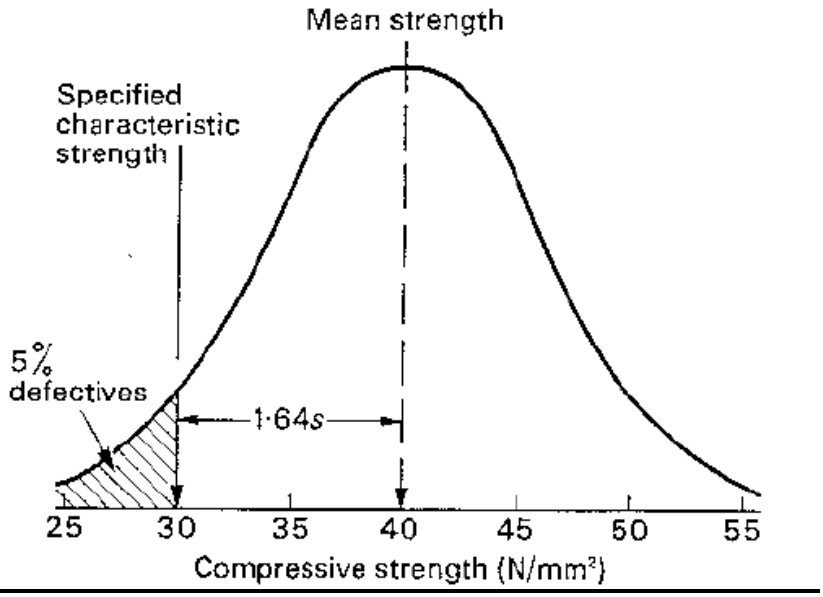

Figure A2.1: Normal distribution of concrete strength (source: Building Research Establishment, 1997)

Table A2.1: K factor table

Percentage	K
10	1.28
5	1.64
2.5	1.96
1	2.33

(source: Building Research Establishment, 1997)

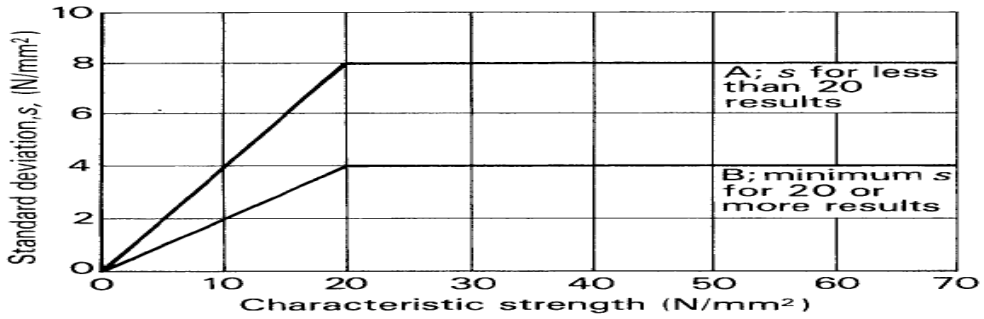

Figure A2.2: Characteristic Strength Versus Standard Deviation Relationship (source: Building Research Establishment, 1997)

Computation of Mean target strength

Fm = Fc + Ks

From Figure 1

For 5% defective

K = 1.64

From Figure 3

S = 4 N/mm^2

Fc = 30N/mm^2

Fm = 30 + (1.64×4)

Fm = 36.56N/mm^2

STEP 2: Selection of water/cement ratio

Table A2.2: Approximate compressive strength of concrete mixes made with free water/cement ratio of 0.5

Cement Strength Class	**Type of coarse aggregate**	**Compressive strengths(N/mm2) Age (days)**			
		3	7	28	91
42.5	Uncrushed	22	30	42	49
	Crushed	27	36	49	56
52.5	Uncrushed	29	37	48	54
	Crushed	34	43	55	61

(source: Building Research Establishment, 1997)

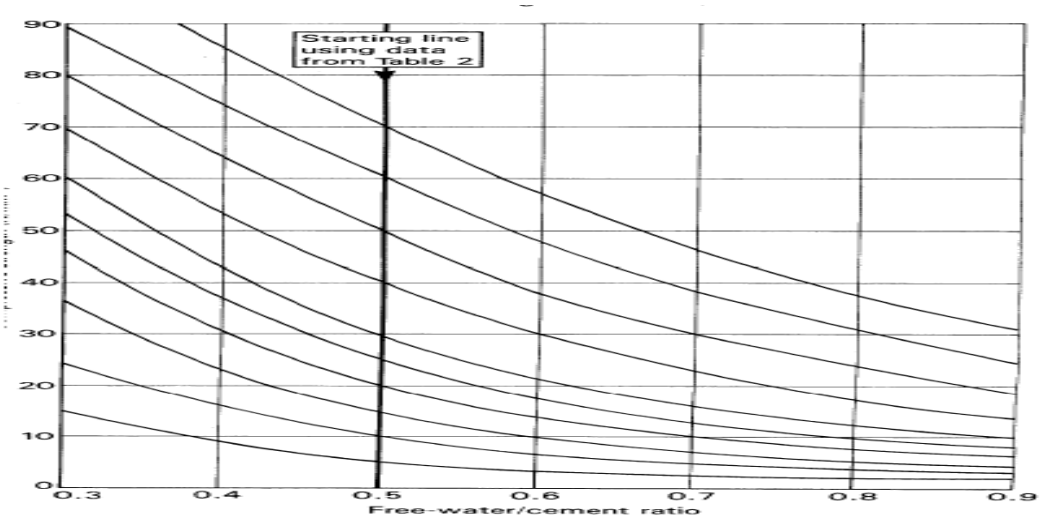

Figure A2.3: Relationship between compressive strength and free/water ration (source: Building Research Establishment, 1997)

Table A2.3: Maximum water cement ratio for reasonable durability

Condition of Exposure	**Maximum Water Cement Ratio**	
	Plain Concrete	**Reinforced Concrete**
Internal, Subject to heavy condensation	-	0.60
Alternate wetting and drying	0.60	0.60
Freezing and Thawing	0.55	0.50
Seawater or salt spray	0.50	0.45
Water retaining structure	-	0.50

(Source: Building Research Establishment, 1997)

Determination of the required water-cement ratio involves using 42.5 grade of cement, crushed coarse aggregate and 28 days in Table A2.2 to get the approximate compressive strength ($49N/mm^2$). Using Figure A2.3, we first trace out the Fm and approximate compressive strength curves gotten from (Table A2.2), parallel to the existing curves. Then, we trace a horizontal line from where the Fm curve intercept with the starting line towards the approximate compressive strength curve. At the point of interception, trace vertically downwards to get its corresponding value on the horizontal or x axis (water/cement ratio) which was gotten as 0.64.

According to Table A2.3, for alternate wetting and drying condition and concrete being plain, which has its maximum as 0.6 , then adopt **0.4** to produce a concrete with better strength.

STEP 3: Selection of slump range

Table A2.4: Workability, Slump and Compacting factor of concrete with 19mm or 38mm size of aggregate

Degree of workability	Slump		Compacting factor	Use for which concrete is suitable
	mm	in.		
Very low	0–25	0–1	0.78	Roads vibrated by power-operated machines. At the more workable end of this group, concrete may be compacted in certain cases with hand-operated machines.
Low	25–50	1–2	0.85	Roads vibrated by hand-operated machines. At the more workable end of this group, concrete may be manually compacted in roads using aggregate of rounded or irregular shape. Mass concrete foundations without vibration or lightly reinforced sections with vibration.
Medium	25–100	2–4	0.92	At the less workable end of this group, manually compacted flat slabs using crushed aggregates. Normal reinforced concrete manually compacted and heavily reinforced sections with vibration.
High	100–175	4–7	0.95	For sections with congested reinforcement. Not normally suitable for vibration.

(Building Research Establishment, Crown copyright)

(Source: Building Research Establishment, 1997)

Adopt range of 25mm-100mm slumps for medium degree of workability

STEP 4: Selection of free water content

Table A2.5: Approximate Free-Water Content (kg/m^3) Required to Give Various Levels of Workability.

Slump (mm)			**0-10**	**10-3**	**30-60**	**60-180**
Vebe time (s)			**>12**	**6-12**	**3-6**	**0-3**
Max. size of aggregate (mm)	**Type of Aggregate**					
10		Uncrushed	150	180	205	225
		Crushed	180	205	230	250
20		Uncrushed	135	160	180	195
		Crushed	170	190	210	225
40		Uncrushed	115	140	160	175

	Crushed	155	175	190	205

(Source: Building Research Establishment, 1997)

Selection of free water content kg/m^3 from Table A2.5 considering the workability, size of aggregate and type of aggregate; adopt $210kg/m^3$.

STEP 5: Selection of the cement content

Determination of cement content

$\frac{Water}{Cement}$ = 0.4

$\frac{210}{Cement}$ = 0.4

Cement = $\frac{210}{0.4}$

Cement = $525kg/m^3$

STEP 6: Confirmation of the calculated cement content

Table 6.1: Maximum Cement Content for Concretes with 20mm Maximum Aggregate Size under

Table A2.6: Different Condition of Exposure

Exposure Conditions	**Minimum Cement Content for Concrete (Kg/m3)**		
	Plain	**Reinforced**	**Pre-stressed**
Non-corrosive	220	250	300
buried or sheltered from rain	250	290	300
Exposed to alternate wetting and drying or seawater	310	360	360
subject to de-icing salt	280	390	300

(source: Building Research Establishment, 1997)

Comparing the amount of the cement content calculated and the minimum allowable cement content for durability, since the minimum for alternate wetting and drying condition for plain concrete is $310kg/m^3$

$525kg/m^3$ is okay.

STEP 7: Selection total aggregate content

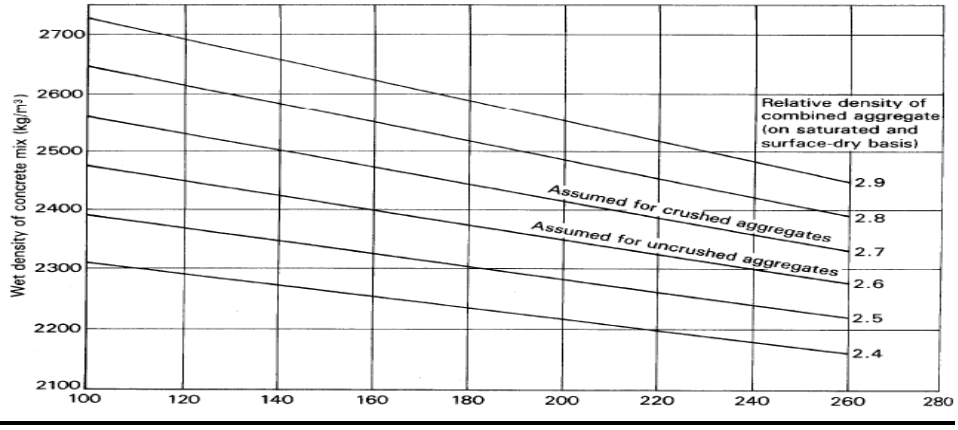

Figure A2.4: Relationship between free-water content and Estimated wet density of fully compacted concrete (source: Building Research Establishment, 1997)

Determination of total aggregate content

Using Figure A2.4 ;

Particle density for Coarse = 2.95

Particle density for Fine = 2.79

Combined = 2.90

Using the value for water content gotten as $210kg/m^3$

We trace the value vertically upward to touch 2.9 line. From the point of interception, draw a line to touch the y axis and read off the value (which is the wet density of concrete)

D = $2550kg/m^3$, C= $525kg/m^3$, W= $210kg/m^3$

D = 2550 – 525 – 210

D = $1815kg/m^3$

STEP 8: Selection of fine and coarse aggregate contents

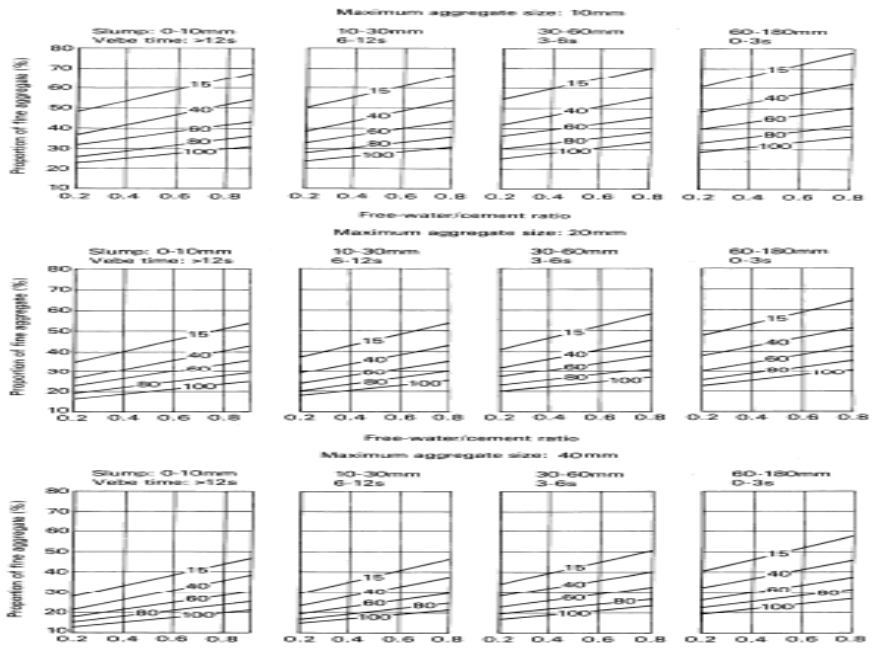

Figure A2.5: Recommended Percentages of fine aggregate in total aggregate as a function of free-water/cement ratio for values of workability and maximum size of aggregate

Selection of Fine and Coarse aggregate contents:

From the sieve analysis for aggregate, we use % passing 600µm sieve size which is 30.55%

From figure 8.1

Slump = 30 – 60 mm

Maximum size of aggregate = 20mm

Proportion of the fine aggregate = 41%

Fine aggregate Content

$= \frac{41}{100} \times 1815$

$= 744.15 kg/m^3$

Coarse aggregate Content

= 1815 – 744.15

$= 1070.85 kg/m^3$

STEP 9: Selection of the mix proportion of materials by weight

Estimating the mix proportion by weight

Water Content	Cement	Fine Aggregate	Coarse Aggregate
$210kg/m^3$	$525kg/m^3$	$744.15kg/m^3$	$1070.85kg/m^3$

Divide through by the content of cement to get the mix ratio, using 0.55 water/cement ratio.

STEP 10

Quantity of materials in kg

Volume of concrete in a cube (150m × 150m × 150m)

V = $0.15 \times 0.15 \times 0.15$

V = $0.0034m^3$

Adding 20% waste of total volume

= $(\frac{20}{100} \times 0.0034) + 0.0034$

= $0.0041m^3$

Quantity of Water = $210 \times 0.0041 = 0.86kg$

Quantity of Cement = $525 \times 0.0041 = 2.153kg$

Quantity of FA = $744.15 \times 0.0041 = 3.05kg$

Quantity of CA = $1070.85 \times 0.0041 = 4.394kg$

Quantity of superplasticizer = 0.03kg (1.3% of cement content)

For Metakaolin treated at 650^{oC}, 750^{oC} and 850^{oC}

100% Cement- 0% Metakaolin

Water Content kg/m^3	Cement kg/m^3	Fine Aggregate kg/m^3	Coarse Aggregate kg/m^3
0.86	2.153	3.05	4.39

95% Cement- 5% Metakaolin

Water Content	Cement	Metakaolin	Fine Aggregate	Coarse

kg/m^3	kg/m^3	kg/m^3	kg/m^3	Aggregate kg/m^3
0.86	2.0454	0.1077	3.05	4.39

90% Cement- 10% Metakaolin

Water Content kg/m^3	Cement kg/m^3	Metakaolin kg/m^3	Fine Aggregate kg/m^3	Coarse Aggregate kg/m^3
0.86	1.9377	0.2153	3.05	4.39

85% Cement- 15% Metakaolin

Water Content kg/m^3	Cement kg/m^3	Metakaolin kg/m^3	Fine Aggregate kg/m^3	Coarse Aggregate kg/m^3
0.86	1.8301	0.3230	3.05	4.39

80% Cement-20% Metakaolin

Water Content kg/m^3	Cement kg/m^3	Metakaolin kg/m^3	Fine Aggregate kg/m^3	Coarse Aggregate kg/m^3
0.86	1.7224	0.4306	3.05	4.39

75% Cement- 25% Metakaolin

Water Content kg/m^3	Cement kg/m^3	Metakaolin kg/m^3	Fine Aggregate kg/m^3	Coarse Aggregate kg/m^3
0.86	1.6148	0.5383	3.05	4.39

70% Cement-30% Metakaolin

Water Content kg/m^3	Cement kg/m^3	Metakaolin kg/m^3	Fine Aggregate kg/m^3	Coarse Aggregate kg/m^3
0.86	1.5071	0.6459	3.05	4.39

65% Cement-35% Metakaolin

Water Content kg/m^3	Cement kg/m^3	Metakaolin kg/m^3	Fine Aggregate kg/m^3	Coarse Aggregate

				kg/m^3
0.86	1.3995	0.7536	3.05	4.39

60% Cement-40% Metakaolin

Water Content kg/m^3	**Cement** kg/m^3	**Metakaolin** kg/m^3	**Fine Aggregate** kg/m^3	**Coarse Aggregate** kg/m^3
0.86	1.2918	0.8612	3.05	4.39

55% Cement-45% Metakaolin

Water Content kg/m^3	**Cement** kg/m^3	**Metakaolin** kg/m^3	**Fine Aggregate** kg/m^3	**Coarse Aggregate** kg/m^3
0.86	1.1842	0.9689	3.05	4.39

50% Cement-50% Metakaolin

Water Content kg/m^3	**Cement** kg/m^3	**Metakaolin** kg/m^3	**Fine Aggregate** kg/m^3	**Coarse Aggregate** kg/m^3
0.86	1.0765	1.0765	3.05	4.39

Appendix A3

Table A3.1: Number of cement-metakaolin concrete cubes to be produced (650°C)

Samples		**Curing Days**	**Tests**		
River Sand	**Quarry Dust**	**7days**	**Compressive strength**	**Young modulus test**	**Absorption capacity**
$0\%MK_{RS}$	$0\%MK_{QD}$		3	-	-
$5\%MK_{RS}$	$5\%MK_{QD}$		3	-	-
$10\%MK_{RS}$	$10\%MK_{QD}$		3	-	-
$15\%MK_{RS}$	$15\%MK_{QD}$		3	-	-
$20\%MK_{RS}$	$20\%MK_{QD}$		3	-	-
$25\%MK_{RS}$	$25\%MK_{QD}$		3	-	-
$30\%MK_{RS}$	$30\%MK_{QD}$		3	-	-
$35\%MK_{RS}$	$35\%MK_{QD}$		3	-	-
$40\%MK_{RS}$	$40\%MK_{QD}$		3	-	-
$45\%MK_{RS}$	$45\%MK_{QD}$		3	-	-
$50\%MK_{RS}$	$50\%MK_{QD}$		3	-	-
SUB-TOTAL			**33*2=66**		
		28days			
$0\%MK_{RS}$	$0\%MK_{QD}$		3		3
$5\%MK_{RS}$	$5\%MK_{QD}$		3		3
$10\%MK_{RS}$	$10\%MK_{QD}$		3		3
$15\%MK_{RS}$	$15\%MK_{QD}$		3		3
$20\%MK_{RS}$	$20\%MK_{QD}$		3		3
$25\%MK_{RS}$	$25\%MK_{QD}$		3		3
$30\%MK_{RS}$	$30\%MK_{QD}$		3		3
$35\%MK_{RS}$	$35\%MK_{QD}$		3		3
$40\%MK_{RS}$	$40\%MK_{QD}$		3		3

45%MK_{RS}	45%MK_{QD}	3	3
50%MK_{RS}	50%MK_{QD}	3	3
SUB-TOTAL		**66**	**66**

Table A3.2: Number of cement-metakaolin concrete cubes to be produced (750°C)`

Samples		**Curing Days**	**Tests**		
River Sand	**Quarry Dust**	**7days**	**Compressive strength**	**Young modulus test**	**Absorption capacity**
0%MK_{RS}	0%MK_{QD}		3	-	-
5%MK_{RS}	5%MK_{QD}		3	-	-
10%MK_{RS}	10%MK_{QD}		3	-	-
15%MK_{RS}	15%MK_{QD}		3	-	-
20%MK_{RS}	20%MK_{QD}		3	-	-
25%MK_{RS}	25%MK_{QD}		3	-	-
30%MK_{RS}	30%MK_{QD}		3	-	-
35%MK_{RS}	35%MK_{QD}		3	-	-
40%MK_{RS}	40%MK_{QD}		3	-	-
45%MK_{RS}	45%MK_{QD}		3	-	-
50%MK_{RS}	50%MK_{QD}		3	-	-
SUB-TOTAL			**66**		
		28days			
0%MK_{RS}	0%MK_{QD}		3	-	3
5%MK_{RS}	5%MK_{QD}		3	-	3
10%MK_{RS}	10%MK_{QD}		3	-	3
15%MK_{RS}	15%MK_{QD}		3	-	3
20%MK_{RS}	20%MK_{QD}		3	-	3
25%MK_{RS}	25%MK_{QD}		3	-	3
30%MK_{RS}	30%MK_{QD}		3	-	3
35%MK_{RS}	35%MK_{QD}		3	-	3

40%MK_{RS}	40%MK_{QD}	3	-	3
45%MK_{RS}	45%MK_{QD}	3	-	3
50%MK_{RS}	50%MK_{QD}	3	-	3
SUB-TOTAL		**66**		**66**

Table A3.3:Number of cement-metakaolin concrete cubes to be produced (850°C)

Samples		**Curing Days**	**Tests**		
River Sand	**Quarry Dust**	**7days**	**Compressive strength**	**Young modulus test**	**Absorption capacity**
0%MK_{RS}	0%MK_{QD}		3	-	-
5%MK_{RS}	5%MK_{QD}		3	-	-
10%MK_{RS}	10%MK_{QD}		3	-	-
15%MK_{RS}	15%MK_{QD}		3	-	-
20%MK_{RS}	20%MK_{QD}		3	-	-
25%MK_{RS}	25%MK_{QD}		3	-	-
30%MK_{RS}	30%MK_{QD}		3	-	-
35%MK_{RS}	35%MK_{QD}		3	-	-
40%MK_{RS}	40%MK_{QD}		3	-	-
45%MK_{RS}	45%MK_{QD}		3	-	-
50%MK_{RS}	50%MK_{QD}		3	-	-
SUB-TOTAL			**66**		
		28days			
0%MK_{RS}	0%MK_{QD}		3	-	3
5%MK_{RS}	5%MK_{QD}		3	-	3
10%MK_{RS}	10%MK_{QD}		3	-	3
15%MK_{RS}	15%MK_{QD}		3	-	3
20%MK_{RS}	20%MK_{QD}		3	-	3
25%MK_{RS}	25%MK_{QD}		3	-	3

30%MK_{RS}	30%MK_{QD}	3	-	3
35%MK_{RS}	35%MK_{QD}	3	-	3
40%MK_{RS}	40%MK_{QD}	3	-	3
45%MK_{RS}	45%MK_{QD}	3	-	3
50%MK_{RS}	50%MK_{QD}	3	-	3
SUB-TOTAL		**66**		**66**

Appendix A4

Table A4.1: Specific Gravity of Metakaolin at 650^0C

Description	**Sample**
Mass of vessel (M_1)	63.8g
Mass of vessel + sample (M_2)	460.8g
Mass of vessel + sample + water (M_3)	1199.0g
Mass of vessel + water (M_4)	983.1g
Mass of water ($M_3 - M_2$)	768.2g
Mass of sample used ($M_2 - M_1$)	397g
Volume of sample used ($M_4 - M_1$)	919.3
S.G = $\frac{(\boldsymbol{M2} - \boldsymbol{M1})}{(\boldsymbol{M4} - \boldsymbol{M1}) - (\boldsymbol{M3} - \boldsymbol{M2})}$	S.G = $\frac{397}{919.3-768.2}$
	S.G = 2.62
Specific gravity	**2.62**

Table A4.2: Specific Gravity of Metakaolin at 750^0C

Description	**Sample**
Mass of vessel (M_1)	63.8g
Mass of vessel + sample (M_2)	621.6g
Mass of vessel + sample + water (M_3)	1237.6g
Mass of vessel + water (M_4)	983.1g
Mass of water ($M_3 - M_2$)	716g
Mass of sample used ($M_2 - M_1$)	557.8g
Volume of sample used ($M_4 - M_1$)	919.3g
S.G = $\frac{(\boldsymbol{M2} - \boldsymbol{M1})}{(\boldsymbol{M4} - \boldsymbol{M1}) - (\boldsymbol{M3} - \boldsymbol{M2})}$	S.G = $\frac{557.8}{919.3-716}$
	S.G = 2.74
Specific gravity	**2.74**

Table A4.3: Specific Gravity of Metakaolin at 850^0C

Description	**Sample**
Mass of vessel (M_1)	63.8g
Mass of vessel + sample (M_2)	567.6g
Mass of vessel + sample + water (M_3)	1227.5g
Mass of vessel + water (M_4)	983.1g
Mass of water ($M_3 - M_2$)	729.9g
Mass of sample used ($M_2 - M_1$)	503.8g
Volume of sample used ($M_4 - M_1$)	919.3g
S.G = $\frac{(\boldsymbol{M2 - M1})}{(\boldsymbol{M4 - M1}) - (\boldsymbol{M3 - M2})}$	S.G = $\frac{503.8}{919.3-729.9}$ S.G = 2.66
Specific gravity	**2.66**

Table A4.4: Specific Gravity of Super-plasticizer

Description	**Sample A**	**Sample B**
Mass of vessel (M_1)	25.48g	8.85g
Mass of vessel + sample (M_2)	86.01g	68.39g
Mass of sample (M_3) ($M_2 - M_1$)	60.53g	59.54g
Volume of bottle	50cm^3	50cm^3
S.G= $\frac{M3}{50}$	$\frac{60.53}{50}$= $\frac{1.2106}{1.003}$ **= 1.20698**	$\frac{59.54}{50}$= $\frac{1.1908}{1.007}$ **= 1.1872**
Average specific gravity = $\frac{1.20698\ X\ 1.1872}{2}$	**1.2**	

Table A4.5: Specific Gravity of Quarry Dust

Description	**Sample**
Mass of vessel (M_1)	620g
Mass of vessel + sample (M_2)	1077g
Mass of vessel + sample + water (M_3)	1717g
Mass of vessel + water (M_4)	1424g
Mass of water ($M_3 - M_2$)	640g
Mass of sample used ($M_2 - M_1$)	457g
Volume of sample used ($M_4 - M_1$)	804g
S.G = $\frac{(\boldsymbol{M2 - M1})}{(\boldsymbol{M4 - M1}) - (\boldsymbol{M3 - M2})}$	S.G = $\frac{457}{804-640}$

	S.G = 2.79
Specific gravity	**2.79**

Table A4.6: Specific Gravity of Coarse Aggregate

Description	**Sample A**	**Sample B**
Mass of vessel (M_1)	620g	620g
Mass of vessel + sample (M_2)	1178g	1167g
Mass of vessel + sample + water (M_3)	1793g	1783g
Mass of vessel + water (M_4)	1424g	1424g
Mass of water ($M_3 - M_2$)	617g	616g
Mass of sample used ($M_2 - M_1$)	558g	547g
Volume of sample used ($M_4 - M_1$)	804g	804g
S.G = $\frac{(\boldsymbol{M2 - M1})}{(\boldsymbol{M4 - M1}) - (\boldsymbol{M3 - M2})}$	$\frac{558}{804-617}$ **= 2.98**	$\frac{547}{804-616}$ **= 2.91**
Average specific gravity = $\frac{2.98\ X\ 2.91}{2}$		**2.95**

Table A4.7: Specific Gravity of River Sand

Description	**Sample**
Mass of vessel (M_1)	620g
Mass of vessel + sample (M_2)	1013g
Mass of vessel + sample + water (M_3)	1674g
Mass of vessel + water (M_4)	1424g
Mass of water ($M_3 - M_2$)	661g
Mass of sample used ($M_2 - M_1$)	393g
Volume of sample used ($M_4 - M_1$)	804g
S.G = $\frac{(\boldsymbol{M2 - M1})}{(\boldsymbol{M4 - M1}) - (\boldsymbol{M3 - M2})}$	S.G = $\frac{393}{804-661}$
	S.G = 2.75
Specific gravity	**2.75**

Appendix A5

Table A5.1: Compressive Strength Result of Specimen at 7days (River Sand)

Sample	**650^{0}C (MPa)**	**750^{0}C (MPa)**	**850^{0}C (MPa)**
0%MK_{RS}	19.63	19.63	19.63
5%MK_{RS}	21.75	22.30	21.89
10%MK_{RS}	22.47	24.02	22.80
15%MK_{RS}	27.21	27.56	27.37
20%MK_{RS}	27.29	27.91	27.72
25%MK_{RS}	24.74	26.71	25.68
30%MK_{RS}	19.56	23.88	20.66
35%MK_{RS}	16.83	19.12	17.76
40%MK_{RS}	11.70	16.59	16.03
45%MK_{RS}	8.22	10.42	9.29
50%MK_{RS}	6.78	8.10	6.91

Table A5.2: Compressive Strength Result of Specimen at 7days (Quarry Dust)

Sample	**650^{0}C (MPa)**	**750^{0}C (MPa)**	**850^{0}C (MPa)**
0%MK_{QD}	19.42	19.42	19.42
5%MK_{QD}	21.28	21.60	21.34
10%MK_{QD}	22.39	23.67	22.62
15%MK_{QD}	26.68	27.33	26.76
20%MK_{QD}	26.93	27.83	27.04
25%MK_{QD}	22.59	26.61	22.70
30%MK_{QD}	19.24	22.80	19.53
35%MK_{QD}	15.60	18.31	16.12
40%MK_{QD}	10.65	15.15	14.67
45%MK_{QD}	8.01	9.66	9.03

50%MK_{QD}	6.02	7.53	6.75

Table A5.3: Compressive Strength Result of Specimen at 28days (River Sand) 650^{0}C

Sample	**W_1 (kg)**	**W_2 (kg)**	**W_3 (kg)**	**Strength (Mpa)**			**S_{Av} (MPa)**
0%MK_{RS}	8.48	8.54	8.51	32.09	32.2	32.27	32.17
5%MK_{RS}	8.46	8.48	8.50	33.09	33.19	33.03	33.10
10%MK_{RS}	8.52	8.45	8.37	35.2	35.31	35.46	35.32
15%MK_{RS}	8.49	8.44	8.38	38.85	39.01	38.10	38.92
20%MK_{RS}	8.48	8.40	8.41	37.79	37.92	38.01	37.97
25%MK_{RS}	8.35	8.37	8.33	28.95	28.87	28.77	28.86
30%MK_{RS}	8.31	8.30	8.36	25.84	25.65	25.72	25.74
35%MK_{RS}	8.31	8.27	8.24	21.40	21.26	21.18	21.28
40%MK_{RS}	8.22	8.19	8.18	14.78	14.16	13.78	14.24
45%MK_{RS}	8.10	8.09	8.13	12.15	11.14	11.33	11.54
50%MK_{RS}	8.03	8.04	8.07	8.81	8.44	8.01	8.42

Table A5.4: Compressive Strength Result of Specimen at 28days (River Sand) 650^{0}C

Sample	**W_1 (kg)**	**W_2 (kg)**	**W_3 (kg)**	**Strength (Mpa)**			**S_{Av} (MPa)**
0%MK_{RS}	8.48	8.54	8.51	32.09	32.2	32.27	32.17
5%MK_{RS}	8.46	8.48	8.50	33.09	33.19	33.03	33.10
10%MK_{RS}	8.52	8.45	8.37	35.2	35.31	35.46	35.32
15%MK_{RS}	8.49	8.44	8.38	38.85	39.01	38.10	38.92
20%MK_{RS}	8.48	8.40	8.41	37.79	37.92	38.01	37.97
25%MK_{RS}	8.35	8.37	8.33	28.95	28.87	28.77	28.86
30%MK_{RS}	8.31	8.30	8.36	25.84	25.65	25.72	25.74
35%MK_{RS}	8.31	8.27	8.24	21.40	21.26	21.18	21.28
40%MK_{RS}	8.22	8.19	8.18	14.78	14.16	13.78	14.24

45%MK_{RS}	8.10	8.09	8.13	12.15	11.14	11.33	11.54
50%MK_{RS}	8.03	8.04	8.07	8.81	8.44	8.01	8.42

Table A5.5: Compressive Strength Result of Specimen at 28days (River Sand) 750^0C

Sample	**W_1 (kg)**	**W_2 (kg)**	**W_3 (kg)**	**Strength (Mpa)**			**S_{Av} (MPa)**
0%MK_{RS}	8.48	8.54	8.51	32.09	32.2	32.22	32.17
5%MK_{RS}	8.49	8.48	8.52	35.26	36.00	35.47	35.58
10%MK_{RS}	8.51	8.50	8.46	37.93	37.33	38.23	37.83
15%MK_{RS}	8.47	8.45	8.49	40.24	40.68	39.98	40.08
20%MK_{RS}	8.45	8.44	8.42	42.16	41.78	42.31	42.05
25%MK_{RS}	8.40	8.42	8.38	29.56	30.45	30.13	30.05
30%MK_{RS}	8.37	8.34	8.35	27.80	27.37	28.06	27.74
35%MK_{RS}	8.29	8.27	8.32	25.08	25.36	24.47	24.97
40%MK_{RS}	8.27	8.21	8.28	18.67	17.80	18.42	18.30
45%MK_{RS}	8.22	8.17	8.20	15.76	15.12	15.05	15.31
50%MK_{RS}	8.12	8.16	8.09	13.44	13.13	12.48	13.02

Table A5.6 Compressive Strength Result of Specimen at 28days (River Sand) 850^0C

Sample	**W_1 (kg)**	**W_2 (kg)**	**W_3 (kg)**	**Strength (Mpa)**			**S_{Av} (MPa)**
0%MK_{RS}	8.48	8.54	8.51	32.09	32.2	32.22	32.17
5%MK_{RS}	8.47	8.51	8.50	34.07	34.48	33.69	34.08
10%MK_{RS}	8.45	8.48	8.48	37.4	36.7	36.97	37.02
15%MK_{RS}	8.41	8.45	8.43	39.89	40.05	39.48	39.79
20%MK_{RS}	8.43	8.45	8.44	41.13	40.47	41.34	40.98

25%MK_{RS}	8.41	8.40	8.36	29.9	29.70	30.33	29.94
30%MK_{RS}	8.38	8.34	8.30	27.69	27.03	27.92	27.55
35%MK_{RS}	8.32	8.27	8.25	24.72	24.98	24.38	24.69
40%MK_{RS}	8.24	8.22	8.26	18.60	18.24	17.6	18.15
45%MK_{RS}	8.17	8.14	8.10	15.49	15.21	15.14	15.28
50%MK_{RS}	8.08	8.05	8.09	12.91	12.52	12.22	12.55

Table A5.7: Compressive Strength Result of Specimen at 28days (Quarry Dust) 650^0C

Sample	**W_1 (kg)**	**W_2 (kg)**	**W_3 (kg)**	**Strength (Mpa)**			**S_{Av} (MPa)**
0%MK_{QD}	8.55	8.45	8.50	31.80	30.68	30.99	31.16
5%MK_{QD}	8.40	8.48	8.45	32.64	32.36	32.98	32.66
10%MK_{QD}	8.40	8.30	8.40	34.16	35.04	34.33	34.51
15%MK_{QD}	8.35	8.43	8.46	35.39	36.37	36.67	36.14
20%MK_{QD}	8.40	8.43	8.37	37.00	36.82	35.61	36.48
25%MK_{QD}	8.30	8.25	8.29	28.37	29.23	28.67	28.76
30%MK_{QD}	8.15	8.20	8.10	26.31	25.88	27.17	26.45
35%MK_{QD}	8.10	8.08	8.14	18.73	18.24	17.42	18.18
40%MK_{QD}	8.02	8.01	8.00	12.89	12.67	11.56	12.37
45%MK_{QD}	7.58	7.75	7.72	9.78	9.24	8.56	9.19
50%MK_{QD}	7.60	7.70	7.65	7.12	6.68	6.51	6.77

Table A5.8: Compressive Strength Result of Specimen at 28days (Quarry Dust) 750^0C

Sample	**W_1 (kg)**	**W_2 (kg)**	**W_3 (kg)**	**Strength (Mpa)**			**S_{Av} (MPa)**
0%MK_{QD}	8.55	8.45	8.50	31.80	30.68	30.99	31.16
5%MK_{QD}	8.49	8.52	8.52	31.89	33.16	33.8	33.95
10%MK_{QD}	8.45	8.48	8.49	35.12	35.84	35.04	35.33

15%MK_{QD}	8.40	8.45	8.48	36.49	37.33	37.75	37.19
20%MK_{QD}	8.47	8.44	8.41	38.62	38.24	37.20	38.02
25%MK_{QD}	8.38	8.26	8.25	29.10	28.91	28.80	28.94
30%MK_{QD}	8.15	8.35	8.20	28.00	27.64	27.78	27.81
35%MK_{QD}	8.17	8.10	8.21	24.36	24	23.8	24.05
40%MK_{QD}	8.05	8.15	8.20	18.00	17.42	17.24	17.55
45%MK_{QD}	8.00	8.05	8.10	12.00	12.84	12.44	12.43
50%MK_{QD}	7.89	7.85	7.94	8.47	8.00	7.73	8.13

Table A5.9: Compressive Strength Result of Specimen at 28days (Quarry Dust) 850^0C

Sample	**W_1 (kg)**	**W_2 (kg)**	**W_3 (kg)**	**Strength (Mpa)**			**S_{AV} (MPa)**
0%MK_{QD}	8.55	8.45	8.50	31.80	30.68	30.99	31.16
5%MK_{QD}	8.47	8.45	8.44	32.88	33.25	33.11	33.08
10%MK_{QD}	8.41	8.42	8.45	34.96	35.21	34.74	34.97
15%MK_{QD}	8.40	8.35	8.43	35.82	36.47	36.61	36.30
20%MK_{QD}	8.38	8.41	8.40	37.11	37.82	37.61	36.30
25%MK_{QD}	8.35	8.22	8.24	28.26	29.35	28.89	28.83
30%MK_{QD}	8.18	8.19	8.21	26.93	27.49	26.76	27.06
35%MK_{QD}	8.14	8.12	8.15	19.32	19.71	19.02	19.35
40%MK_{QD}	8.02	8.04	8.00	15.18	15.73	16.00	15.64
45%MK_{QD}	7.96	7.91	8.00	10.44	11.02	11.16	10.87
50%MK_{QD}	7.87	7.90	7.87	7.33	7.07	6.71	7.64

Table A5.10: Elastic Young Modulus of Concrete at 28days River Sand (650^0C)

Sample	**W_1 (kg)**	**W_2 (kg)**	**W_3 (kg)**	**Average weight (kg)**	**Unit weight of Concrete (kg/m^3)**	**F_C (MPa)**	**E_C (GPa)**
0%MK_{RS}	8.48	8.54	8.51	8.51	2521.48	32.17	30.88

5%MK_{RS}	8.46	8.48	8.50	8.5	2518.52	33.10	31.27
10%MK_{RS}	8.52	8.45	8.37	8.45	2503.70	35.32	32.01
15%MK_{RS}	8.49	8.44	8.38	8.44	2500.74	38.92	33.55
20%MK_{RS}	8.48	8.40	8.41	8.43	2497.78	37.97	33.08
25%MK_{RS}	8.35	8.37	8.33	8.35	2474.07	28.86	28.43
30%MK_{RS}	8.31	8.30	8.36	8.33	2468.15	25.74	26.75
35%MK_{RS}	8.31	8.27	8.24	8.27	2450.37	21.28	24.06
40%MK_{RS}	8.22	8.19	8.18	8.19	2426.67	14.24	19.39
45%MK_{RS}	8.10	8.09	8.13	8.12	2405.93	11.54	18.04
50%MK_{RS}	8.03	8.04	8.07	8.05	2385.19	8.42	14.53

Table A5.11: Elastic Young Modulus of Concrete at 28days River Sand (750^0C MK)

Sample	**W_1 (kg)**	**W_2 (kg)**	**W_3 (kg)**	**Average weight (kg)**	**Unit weight of Concrete (kg/m^3)**	**F_C (MPa)**	**E_C (GPa)**
0%MK_{RS}	8.48	8.54	8.51	8.51	2521.48	32.17	30.88
5%MK_{RS}	8.49	8.48	8.52	8.5	2518.52	35.58	32.42
10%MK_{RS}	8.44	8.50	8.46	8.47	2509.63	37.83	33.25
15%MK_{RS}	8.47	8.45	8.49	8.47	2509.63	40.08	34.32
20%MK_{RS}	8.45	8.44	8.42	8.44	2500.74	42.05	34.88
25%MK_{RS}	8.40	8.42	8.38	8.4	2488.89	30.05	29.27
30%MK_{RS}	8.37	8.34	8.35	8.35	2474.07	27.74	27.87
35%MK_{RS}	8.29	8.27	8.32	8.29	2456.29	24.97	26.16
40%MK_{RS}	8.27	8.21	8.28	8.25	2444.4	18.30	22.23
45%MK_{RS}	8.22	8.17	8.20	8.19	2426.67	15.31	20.11
50%MK_{RS}	8.12	8.16	8.09	8.12	2405.93	13.02	18.31

Table A5.12: Elastic Young Modulus of Concrete at 28days River Sand (850^0C MK)

Sample	**W_1 (kg)**	**W_2 (kg)**	**W_3 (kg)**	**Average weight (kg)**	**Unit weight of concrete (kg/m^3)**	**F_C (MPa)**	**E_C (GPa)**
0%MK_{RS}	8.48	8.54	8.51	8.51	2521.48	32.17	30.88
5%MK_{RS}	8.47	8.51	8.50	8.49	2515.56	34.08	31.67
10%MK_{RS}	8.45	8.48	8.48	8.47	2509.63	37.02	32.89
15%MK_{RS}	8.41	8.45	8.43	8.43	2497.78	39.79	33.86
20%MK_{RS}	8.43	8.45	8.44	8.42	2494.81	40.98	34.30
25%MK_{RS}	8.41	8.40	8.36	8.39	2485.93	29.94	29.16
30%MK_{RS}	8.38	8.34	8.30	8.34	2471.1	27.55	27.72
35%MK_{RS}	8.32	8.27	8.25	8.28	2453.33	24.69	25.96
40%MK_{RS}	8.24	8.22	8.26	8.24	2441.48	18.15	28.09
45%MK_{RS}	8.17	8.14	8.10	8.14	2411.85	15.28	19.91
50%MK_{RS}	8.08	8.05	8.09	8.07	2391.1	12.55	17.81

Table A5.13: Elastic Young Modulus of Concrete at 28days Quarry Dust (650^0C MK)

Sample	**W_1 (kg)**	**W_2 (kg)**	**W_3 (kg)**	**Average weight (kg)**	**Unit weight of Concrete (kg/m^3)**	**F_C (MPa)**	**E_C (GPa)**
0%MK_{QD}	8.55	8.45	8.50	8.5	2518.5	31.16	30.34
5%MK_{QD}	8.40	8.48	8.45	8.44	2500.74	32.66	30.73
10%MK_{QD}	8.40	8.30	8.40	8.37	2480	34.51	31.19
15%MK_{QD}	8.35	8.43	8.46	8.41	2491.85	36.14	32.15
20%MK_{QD}	8.40	8.43	8.37	8.40	2482.96	36.48	32.45
25%MK_{QD}	8.30	8.25	8.29	8.28	2453.33	28.76	28.02
30%MK_{QD}	8.15	8.20	8.10	8.15	2414.81	26.45	26.24
35%MK_{QD}	8.10	8.08	8.14	8.12	2405.93	18.18	21.61
40%MK_{QD}	8.02	8.01	8.00	8.01	2373.33	12.37	17.49
45%MK_{QD}	7.58	7.75	7.72	7.74	2293.33	9.19	14.32
50%MK_{QD}	7.60	7.70	7.65	7.65	2266.67	6.77	12.07

Table A5.14: Elastic Young Modulus of Concrete at 28days Quarry Dust (750^0C)

Sample	**W_1 (kg)**	**W_2 (kg)**	**W_3 (kg)**	**Average weight (kg)**	**Unit weight of concrete kg/m^3**	**F_C (MPa)**	**E_C (GPa)**
0%MK_{QD}	8.55	8.45	8.50	8.5	2518.5	31.16	30.34
5%MK_{QD}	8.49	8.52	8.52	8.51	2521.48	33.95	31.72
10%MK_{QD}	8.45	8.48	8.49	8.47	2509.63	35.33	32.13
15%MK_{QD}	8.40	8.45	8.48	8.45	2503.70	37.19	32.85
20%MK_{QD}	8.47	8.44	8.41	8.44	2500.74	38.02	33.16
25%MK_{QD}	8.38	8.26	8.25	8.29	2456.29	28.94	28.16
30%MK_{QD}	8.15	8.35	8.20	8.13	2408.9	27.81	26.81
35%MK_{QD}	8.17	8.10	8.21	8.16	2417.8	24.05	25.07
40%MK_{QD}	8.05	8.15	8.20	8.13	2408.9	17.55	21.29
45%MK_{QD}	8.00	8.05	8.10	8.05	2420.7	12.43	18.06
50%MK_{QD}	7.89	7.85	7.94	7.89	2444.4	8.13	14.82

Table A5.15: Elastic Young Modulus of Concrete at 28days Quarry Dust (850^0C)

Sample	**W_1 (kg)**	**W_2 (kg)**	**W_3 (kg)**	**Average weight (kg)**	**Unit weight of concrete kg/m^3**	**F_C (MPa)**	**E_C (GPa)**
0%MK_{QD}	8.55	8.45	8.50	8.5	2518.5	31.16	30.34
5%MK_{QD}	8.47	8.45	8.44	8.45	2503.70	33.08	30.98
10%MK_{QD}	8.41	8.42	8.45	8.42	2494.81	34.97	31.69
15%MK_{QD}	8.40	8.35	8.43	8.39	2483.93	36.30	32.07
20%MK_{QD}	8.38	8.41	8.40	8.39	2485.93	36.30	32.64
25%MK_{QD}	8.35	8.22	8.24	8.27	2450.37	28.83	28.01
30%MK_{QD}	8.18	8.19	8.21	8.19	2426.67	27.06	26.74
35%MK_{QD}	8.14	8.12	8.15	8.14	2411.86	19.35	22.40
40%MK_{QD}	8.02	8.04	8.00	8.02	2376.29	15.64	19.69
45%MK_{QD}	7.96	7.91	8.00	7.96	2358.52	10.87	16.24

50%MK_{QD}	7.87	7.90	7.84	7.87	2331.85	7.64	12.85

Table A5.16: Water Absorption of Concrete after Curing for 28day for River sand (650^0C)

Samples	**Dried Cubes (W_D)**			**Average Mean**	**Wet Cubes (W_W)**			**Average Mean**	**Water Absorption**
	W1 (kg)	**W2 (kg)**	**W3 (kg)**	**(kg)**	**W1 (kg)**	**W2 (kg)**	**W3 (kg)**	**(kg)**	**(%)**
0%MK_{RS}	8.25	8.22	8.22	8.40	8.34	8.38	8.23	8.37	1.70
5%MK_{RS}	8.26	8.26	8.19	8.45	8.35	8.32	8.24	8.37	1.58
10%MK_{RS}	8.27	8.24	8.20	8.39	8.36	8.36	8.24	8.36	1.46
15%MK_{RS}	8.22	8.19	8.29	8.32	8.31	8.39	8.23	8.34	1.34
20%MK_{RS}	8.20	8.26	8.21	8.30	8.34	8.31	8.22	8.32	1.22
25%MK_{RS}	8.15	8.10	8.13	8.26	8.22	8.30	8.13	8.26	1.60
30%MK_{RS}	8.08	8.11	8.03	8.24	8.27	8.18	8.07	8.23	1.98
35%MK_{RS}	7.97	8.00	8.06	8.14	8.19	8.25	8.01	8.19	2.25
40%MK_{RS}	8.01	7.88	7.90	8.20	8.10	8.15	7.93	8.15	2.77
45%MK_{RS}	8.03	7.87	7.82	8.21	8.11	8.10	7.91	8.14	2.91
50%MK_{RS}	7.84	7.79	7.88	8.12	8.08	8.15	7.84	8.12	3.57

Table A5.17:Water Absorption of Concrete after Curing for 28day for River sand (750^0C)

Samples	**Dried Cubes (W_D)**			**Average Mean**	**Wet Cubes (W_W)**			**Average Mean**	**Water Absorption (%)**
	W1 (kg)	**W2 (kg)**	**W3 (kg)**	**(kg)**	**W1 (kg)**	**W2 (kg)**	**W3 (kg)**	**(kg)**	**(%)**
0%MK_{RS}	8.25	8.22	8.22	8.40	8.34	8.38	8.23	8.37	1.70
5%MK_{RS}	8.27	8.28	8.22	8.39	8.43	8.22	8.26	8.38	1.45
10%MK_{RS}	8.20	8.29	8.27	8.34	8.37	8.36	8.25	8.36	1.33
15%MK_{RS}	8.16	8.18	8.23	8.27	8.30	8.31	8.19	8.29	1.22
20%MK_{RS}	8.19	8.16	8.17	8.29	8.23	8.27	8.17	8.26	1.10

25%MK_{RS}	8.11	8.17	8.14	8.20	8.30	8.27	8.14	8.26	1.47
30%MK_{RS}	8.09	8.05	8.07	8.23	8.18	8.21	8.07	8.21	1.73
35%MK_{RS}	7.97	7.99	8.03	8.17	8.18	8.15	8.00	8.17	2.12
40%MK_{RS}	7.91	7.89	7.98	8.16	8.13	8.19	7.93	8.16	2.90
45%MK_{RS}	7.84	7.87	7.81	8.09	8.11	8.06	7.84	8.09	3.19
50%MK_{RS}	7.77	7.82	7.76	8.04	8.07	8.01	7.78	8.04	3.34

Table A5.18: Water Absorption of Concrete after Curing for 28day for River sand (850^0C)

Samples	**Dried Cubes (W_D)**			**Average Mean**	**Wet Cubes (W_W)**			**Average Mean**	**Water Absorption**
	W1 (kg)	**W2 (kg)**	**W3 (kg)**	**(kg)**	**W1 (kg)**	**W2 (kg)**	**W3 (kg)**	**(kg)**	**(%)**
0%MK_{RS}	6.25	8.22	8.22	8.40	8.34	8.38	8.23	8.37	1.70
5%MK_{RS}	8.27	8.25	8.27	8.43	8.35	8.40	8.26	8.39	1.57
10%MK_{RS}	8.24	8.26	8.19	8.35	8.37	8.33	8.23	8.35	1.46
15%MK_{RS}	8.19	8.25	8.28	8.29	8.35	8.40	8.24	8.35	1.33
20%MK_{RS}	8.22	8.18	8.20	8.32	8.29	8.30	8.20	8.30	1.22
25%MK_{RS}	8.15	8.17	8.13	8.23	8.31	8.25	8.15	8.27	1.47
30%MK_{RS}	8.06	8.04	8.08	8.21	8.17	8.25	8.06	8.21	1.86
35%MK_{RS}	7.96	8.07	7.96	8.10	8.12	8.21	8.00	8.18	2.25
40%MK_{RS}	7.95	7.91	7.96	8.15	8.13	8.18	7.94	8.15	2.64
45%MK_{RS}	7.88	7.84	7.08	8.16	8.08	8.13	7.86	8.12	3.31
50%MK_{RS}	7.79	7.84	7.80	8.07	8.10	8.08	7.81	8.08	3.46

Table A5.19:Water Absorption of Concrete after Curing for 28day for Quarry Dust (650^0C)

Samples	**Dried Cubes (W_D)**			**Average Mean**	**Wet Cubes (W_W)**			**Average Mean**	**Water Absorption**
	W1 (kg)	**W2 (kg)**	**W3 (kg)**	**(kg)**	**W1 (kg)**	**W2 (kg)**	**W3 (kg)**	**(kg)**	**(%)**
0%MK_{QD}	8.38	8.30	8.33	8.56	8.47	8.52	8.34	8.52	2.16
5%MK_{QD}	8.29	8.34	8.35	8.50	8.46	8.44	8.33	8.47	1.68
10%MK_{QD}	8.27	8.30	8.28	8.38	8.44	8.41	8.28	8.41	1.57
15%MK_{QD}	8.25	8.22	8.28	8.32	8.40	8.38	8.25	8.37	1.46

20%MK_{QD}	8.26	8.24	8.23	8.35	8.38	8.34	8.24	8.36	1.46
25%MK_{QD}	8.12	8.16	8.18	8.32	8.25	8.30	8.15	8.29	2.72
30%MK_{QD}	8.01	7.97	7.94	8.17	8.24	8.13	7.97	8.18	2.63
35%MK_{QD}	7.85	7.89	7.91	8.11	8.10	8.15	7.88	8.12	3.05
40%MK_{QD}	7.80	7.74	7.76	8.03	8.01	8.01	7.77	8.02	3.22
45%MK_{QD}	7.50	7.39	7.42	7.89	7.74	7.76	7.44	7.80	4.84
50%MK_{QD}	7.33	7.42	7.29	7.74	7.82	7.72	7.35	7.76	5.58

Table A5.20: Water Absorption of Concrete after Curing for 28day for Quarry Dust at 750^0C

Samples	**Dried Cubes (W_D)**			**Average Mean**	**Wet Cubes (W_W)**			**Average Mean**	**Water Absorption**
	W1 (kg)	**W2 (kg)**	**W3 (kg)**	**(kg)**	**W1 (kg)**	**W2 (kg)**	**W3 (kg)**	**(kg)**	**(%)**
0%MK_{QD}	8.38	8.30	8.33	8.56	8.47	8.52	8.34	8.52	2.16
5%MK_{QD}	8.30	8.37	8.34	8.44	8.48	8.45	8.34	8.46	1.44
10%MK_{QD}	8.27	8.34	8.29	8.39	8.43	8.40	8.30	8.41	1.33
15%MK_{QD}	8.28	8.35	8.24	8.40	8.41	8.35	8.29	8.39	1.21
20%MK_{QD}	8.30	8.27	8.21	8.42	8.35	8.33	8.26	8.37	1.33
25%MK_{QD}	8.20	8.22	8.18	8.32	8.36	8.30	8.20	8.33	1.59
30%MK_{QD}	8.17	8.15	8.16	8.33	8.29	8.30	8.16	8.31	1.84
35%MK_{QD}	8.04	8.08	8.11	8.24	8.26	8.29	8.08	8.26	2.20
40%MK_{QD}	7.97	7.91	7.95	8.21	8.16	8.17	7.94	8.18	3.02
45%MK_{QD}	7.81	7.76	7.78	8.05	8.08	8.08	7.78	8.07	3.73
50%MK_{QD}	7.59	7.68	7.63	8.01	8.01	7.98	7.63	7.78	4.59

Table A5.21: Water Absorption of Concrete after Curing for 28day for Quarry Dust at 850^0C

Samples	Dried Cubes (W_D)			Average Mean	Wet Cubes (W_W)			Average Mean	Water Absorption
	W1 (kg)	W2 (kg)	W3 (kg)	(kg)	W1 (kg)	W2 (kg)	W3 (kg)	(kg)	(%)
0%MK_{QD}	8.38	8.30	8.33	8.56	8.47	8.52	8.34	8.52	2.16
5%MK_{QD}	8.35	8.34	8.29	8.47	8.47	8.43	8.33	8.46	1.56
10%MK_{QD}	8.31	8.33	8.26	8.43	8.46	8.36	8.30	8.42	1.46
15%MK_{QD}	8.27	8.30	8.24	8.38	8.43	8.34	8.27	8.38	1.33
20%MK_{QD}	8.25	8.21	8.29	8.36	8.34	8.40	8.25	8.37	1.45
25%MK_{QD}	8.20	8.15	8.18	8.33	8.29	8.31	8.17	8.31	1.71
30%MK_{QD}	8.05	8.11	8.10	8.21	8.27	8.24	8.09	8.24	1.85
35%MK_{QD}	7.93	7.98	8.00	8.14	8.19	8.22	7.97	8.18	2.63
40%MK_{QD}	7.88	7.81	7.84	8.09	8.04	8.06	7.84	8.06	2.81
45%MK_{QD}	7.71	7.53	7.57	7.93	7.88	7.91	7.60	7.91	4.08
50%MK_{QD}	7.33	7.42	7.29	7.85	7.92	7.84	7.46	7.87	5.50

Appendix A6

Statistical report

Table A6.1: Statistical report on the compressive strength of the metakaolin binary concrete with river sand (750^{oC})

Run Order	Actual Value	Predicted Value	Residual	Leverage	Internally Studentized Residuals	Externally Studentized Residuals	Cook's Distance	Influence on Fitted Value DFFITS	Standard Order
1	32.17	33.99	-1.82	0.605	-0.846	-0.827	0.275	-1.024	1
2	35.58	35.64	-0.0575	0.293	-0.02	-0.018	0	-0.012	2
3	37.83	36.3	1.53	0.186	0.493	0.465	0.014	0.223	3
4	40.3	41.33	-1.03	0.918(1)	-1.051	-1.06	3.097(2)	-3.551(2)	4
5	42.08	34.87	7.21	0.205	2.357	4.808(3)	0.359	2.442(2)	5
6	30.05	32.7	-2.65	0.219	-0.876	-0.859	0.054	-0.455	6
7	27.74	29.91	-2.17	0.209	-0.713	-0.685	0.034	-0.352	7
8	24.97	25.88	-0.9114	0.187	-0.295	-0.275	0.005	-0.132	8
9	18.3	20.87	-2.57	0.196	-0.836	-0.816	0.043	-0.402	9
10	15.31	14.88	0.4258	0.309	0.149	0.139	0.002	0.093	10
11	13.02	10.96	2.06	0.672	1.051	1.06	0.567	1.519	11

(1) Observation with leverage > 2.00 × (average leverage).
(2) Exceeds limits.
(3) Observation with |External Stud. Residuals| > 4.40

Table A6.2: Statistical report on the compressive strength of the metakaolin binary concrete with quarry dust (750^{oC})

Run Order	Actual Value	Predicted Value	Residual	Leverage	Internally Studentized Residuals	Externally Studentized Residuals	Cook's Distance	Influence on Fitted Value DFFITS	Standard Order
1	31.16	32.18	-1.02	0.727	-0.828	-0.807	0.457	-1.318	1
2	33.95	34.52	-0.5725	0.394	-0.31	-0.289	0.016	-0.233	2
3	35.33	35.49	-0.1581	0.335	-0.082	-0.076	0.001	-0.054	3
4	37.19	34.99	2.2	0.208	1.041	1.048	0.071	0.537	4
5	38.02	33.87	4.15	0.222	1.985	2.779	0.281	1.486	5
6	28.94	31.68	-2.74	0.231	-1.317	-1.406	0.13	-0.77	6
7	27.81	29.01	-1.2	0.437	-0.674	-0.645	0.088	-0.568	7
8	24.05	24.53	-0.4773	0.2	-0.225	-0.209	0.003	-0.104	8
9	17.55	19.23	-1.68	0.217	-0.8	-0.777	0.044	-0.409	9
10	12.43	12.86	-0.4276	0.35	-0.224	-0.208	0.007	-0.153	10
11	8.13	6.2	1.93	0.678	1.435	1.582	1.086(1)	2.297(1)	11

(1) Exceeds limits

Table A6.3: Statistical report on the young modulus of the metakaolin binary concrete with river sand (750^{oC})

Run Order	Actual Value	Predicted Value	Residual	Leverage	Internally Studentized Residuals	Externally Studentized Residuals	Cook's Distance	Influence on Fitted Value DFFITS	Standard Order
1	30.88	31.61	-0.7261	0.605	-0.776	-0.752	0.231	-0.931	1
2	32.42	32.44	-0.0190	0.293	-0.015	-0.014	0.000	-0.009	2
3	33.25	32.72	0.5297	0.186	0.394	0.369	0.009	0.177	3
4	34.32	34.79	-0.4720	0.918(1)	-1.108	-1.129	3.438(2)	-3.781(2)	4
5	34.88	31.73	3.15	0.205	2.369	4.922(3)	0.362	2.500(2)	5
6	29.27	30.42	-1.15	0.219	-0.871	-0.854	0.053	-0.452	6
7	27.87	28.76	-0.8880	0.209	-0.671	-0.642	0.030	-0.330	7
8	26.16	26.39	-0.2313	0.187	-0.172	-0.160	0.002	-0.077	8
9	22.23	23.47	-1.24	0.196	-0.931	-0.920	0.053	-0.454	9
10	20.11	20.00	0.1070	0.309	0.086	0.080	0.001	0.054	10
11	18.31	17.37	0.9440	0.672	1.108	1.129	0.630	1.618	11

(1) Observation with leverage > 2.00 × (average leverage).
(2) Exceeds limits.
(3) Observation with |External Stud. Residuals| > 4.40

Table A6.4: Statistical report on the young modulus of the metakaolin binary concrete with quarry dust (750^{oC})

Run Order	Actual Value	Predicted Value	Residual	Leverage	Internally Studentized Residuals	Externally Studentized Residuals	Cook's Distance	Influence on Fitted Value DFFITS	Standard Order
1	30.34	30.99	-0.6528	0.727	-1.062	-1.073	0.751	-1.752	1
2	31.72	31.79	-0.0729	0.394	-0.08	-0.074	0.001	-0.059	2
3	32.13	32.11	0.0224	0.335	0.023	0.022	0	0.015	3
4	32.85	31.91	0.9416	0.208	0.899	0.885	0.053	0.453	4
5	33.16	31.06	2.1	0.222	2.027	2.919	0.293	1.56	5
6	28.16	29.61	-1.45	0.231	-1.399	-1.526	0.147	-0.836	6
7	26.81	27.61	-0.7955	0.437	-0.9	-0.886	0.157	-0.78	7
8	25.07	25.18	-0.107	0.2	-0.102	-0.094	0.001	-0.047	8
9	21.29	21.99	-0.6986	0.217	-0.671	-0.642	0.031	-0.338	9
10	18.06	18.2	-0.1427	0.35	-0.15	-0.139	0.003	-0.102	10
11	14.82	13.97	0.8461	0.678	1.267	1.336	0.846	1.940(1)	11

(1) Exceeds limits.

Table A6.5: Statistical report on the water absorption of the metakaolin binary concrete with river sand (750^{oC})

Run Order	Actual Value	Predicted Value	Residual	Leverage	Internally Studentized Residuals	Externally Studentized Residuals	Cook's Distance	Influence on Fitted Value DFFITS	Standard Order
1	1.7	1.65	0.0451	0.605	0.354	0.33	0.048	0.409	1
2	1.45	1.44	0.0052	0.293	0.03	0.028	0	0.018	2
3	1.33	1.33	-0.0005	0.186	-0.003	-0.002	0	-0.001	3
4	1.22	1.1	0.1219	0.918(1)	2.099	3.193	12.351(2)	10.691(2)	4
5	1.1	1.38	-0.277	0.205	-1.531	-1.738	0.151	-0.883	5
6	1.47	1.54	-0.0703	0.219	-0.392	-0.367	0.011	-0.194	6
7	1.73	1.77	-0.0391	0.209	-0.217	-0.201	0.003	-0.104	7
8	2.13	2.11	0.0157	0.187	0.086	0.079	0	0.038	8
9	2.9	2.56	0.3447	0.196	1.894	2.512	0.218	1.238	9
10	3.19	3.09	0.098	0.309	0.581	0.551	0.038	0.369	10
11	3.34	3.58	-0.2438	0.672	-2.099	-3.193	2.262(2)	-4.575(2)	11

(1) Observation with leverage > 2.00 × (average leverage).

(2) Exceeds limits.

Table A6.6: Statistical report on the water absorption of the metakaolin binary concrete with quarry dust (750^{oC})

Run Order	Actual Value	Predicted Value	Residual	Leverage	Internally Studentized Residuals	Externally Studentized Residuals	Cook's Distance	Influence on Fitted Value DFFITS	Standard Order
1	2.16	2.06	0.0968	0.727	2.043	2.975	2.781(1)	4.858(1)	1
2	1.44	1.56	-0.1249	0.394	-1.767	-2.198	0.508	-1.774	2
3	1.33	1.3	0.0309	0.335	0.418	0.392	0.022	0.278	3
4	1.21	1.29	-0.0799	0.208	-0.989	-0.988	0.064	-0.506	4
5	1.33	1.33	0.0018	0.222	0.022	0.021	0	0.011	5
6	1.59	1.52	0.068	0.231	0.854	0.835	0.055	0.457	6
7	1.84	1.75	0.0873	0.437	1.281	1.356	0.318	1.194	7
8	2.23	2.32	-0.094	0.2	-1.157	-1.192	0.084	-0.595	8
9	3.02	2.97	0.0496	0.217	0.618	0.588	0.027	0.31	9
10	3.73	3.77	-0.0423	0.35	-0.578	-0.548	0.045	-0.403	10
11	4.59	4.58	0.0066	0.678	0.128	0.119	0.009	0.172	11

(1) Exceeds limits.